AN ABSTRACT OF THE THESIS OF

David K. Nicholson for the degree of Master of Science in Geology presented on November 10, 1988

Title: Geology, Geochemistry, and Mineralization of the Yellowbottom -Boulder Creek Area, Linn County, Oregon

Redacted for Privacy

Abstract approved: Cyrus W. Field

The Yellowbottom-Boulder Creek area is immediately west of the Quartzville Mining District in the Western Cascades of Oregon. Volcanic rocks comprise a series of basaltic to rhyodacitic flows and volcaniclastic deposits which are believed to correlate with the Sardine Formation (mid-Miocene). These volcanic rocks dip to the southeast (5° to 25°), presumably into the hinge zone of the Sardine Syncline located immediately to the east.

Intrusive rocks consist of small stocks of intermediate composition (quartz diorite, quartz monzodiorite, quartz monzonite, granodiorite, and tonalite), and dikes and plugs of basaltic to rhyolitic composition. The largest intrusion is a quartz monzodiorite stock that covers approximately 1 km^2, for which the name Yellowbottom Stock is proposed here.

Pliocene flows of diktytaxitic basalt and porphyritic andesite of High Cascade origin are preserved on the crests of Galena Ridge and Packers Divide. A Quaternary flow of trachybasalt partly fills the valley of Canal Creek and is associated with two cinder cones: they presumably represent the last pulse of volcanic activity in the Quartzville area.

Major-oxide concentrations in the volcanic and plutonic rocks display systematic trends (decreasing Al_2O_3, TiO_2, FeO_T, MgO, CaO, and P_2O_5, and increasing BaO and K_2O, with increasing SiO_2 content) on Harker variation diagrams. These trends may suggest differentiation from a single batch of magma. The chemistry of plutonic rocks from the study area, and from the Western Cascades in general (calc-alkaline, low K_2O content), is similar to that of some island-arc terranes, including the Southern California batholith, Caribbean, southwestern Pacific, and Pacific Northwest areas, and largely suggests that the magma was derived from the mantle with little if any crustal contamination.

Hydrothermal alteration has affected all rocks of Miocene age. Propylitic alteration is widespread in areal extent and is thought to have been produced by the interaction of magmatic fluids with the host rocks. In contrast, argillic-phyllic alteration is structurally controlled, and may have resulted from hydrolysis reactions between the hosts and meteoric waters that invaded the structures subsequent to propylization. Zones of brecciated and silicified rock range from linear to cylindrical in shape, and are commonly mineralized.

Comparisons of the concentrations of trace metals (Ag, Cu, Pb, Zn, and Mo) with those in average granodiorite, Caribbean intrusions associated with porphyry-copper deposits, and rocks of the Western

Cascades, indicate that samples of the Yellowbottom-Boulder Creek area are depleted in Cu, Pb, and Zn and enriched in Ag. Strong correlations are observed (Mo-Ag; Cu-Zn), whereas Pb has an antipathetic relationship to both Cu and Zn. Trends derived from data plotted on a Cu-Pb-Zn ternary diagram suggest that Pb and Zn metallization are associated with vein-type deposition, whereas a one-sample Cu anomaly may be related to porphyry-type mineralization. Mineralized districts to the north in the Western Cascades are more enriched in copper than the Yellowbottom-Boulder Creek area, whereas those to the south contain more zinc. This change in the abundances of trace metals may be related to the depth of erosion that has exposed deeper levels of the hydrothermal systems in districts to the north.

Sulfur-isotope data suggest a magmatic source of sulfur. Depositional temperatures (157 to 260° C) obtained from sulfur-isotope fractionation and fluid-inclusion data derived from a quartz-calcite-galena-sphalerite veinlet suggest mineralization during late-stage gradual cooling of the hydrothermal system.

Several geologic features, including mineralized breccia pipes and zones, quartz-bearing porphyritic intrusions, and anomalous metal concentrations, suggest the presence of a porphyry-type hydrothermal system at depth in the Boulder Creek area. Additionally, linear zones of intense silicification may be associated with shallower mineral deposition in the epithermal environment. The future mineral resource potential of the area is therefore largely, but not completely, dependent on the discovery of porphyry-type mineralization that might be enhanced by association with anomalously high gold and silver concentrations.

Geology, Geochemistry, and Mineralization of the Yellowbottom-Boulder Creek Area, Linn County, Oregon

by

David K. Nicholson

A THESIS

submitted to

Oregon State University

in partial fulfillment of
the requirements for the
degree of

Master of Science

Completed November 10, 1988
Commencement June 1989

APPROVED:

Redacted for Privacy

Professor of Geology in charge of major

Redacted for Privacy

Head of Department of Geology

Redacted for Privacy

Dean of Graduate School

Date thesis is presented November 10, 1988

Acknowledgements

First and foremost, I would like to thank Cy Field for suggesting this project, for his direction and generous financial support, and for his careful editing of the manuscript. I would also like to thank Committee members Ed Taylor, Allen Agnew, and Jon Kimerling. John Curless (graduate student in geology) provided the first review of the manuscript, accompanied me in the field on several occasions, and suggested solutions to many problems encountered. Others who made helpful comments include faculty members Anita Grunder and John Dilles, and graduate student Dana Willis. Ian Thomson and Cole Carter of Orvana Resources Corporation provided geochemical analyses, fluid inclusion data, and field discussions. Jeff Dawley (undergraduate student in geology) served as field assistant for several weeks during the late summer of 1987. Jay Grant of the U.S. Forest Service provided financial support in the form of reduced fees for camping. Russell Anderson of Champion International provided access to closed sections of land. Ruth Lightfoot prepared the thin sections for use in this study. Thanks also to the various Yellowbottom Campground hosts who provided moral support and verified my return from the field each evening, especially Babe and Harry Willis. Above all, I would like to thank my wife Pamela for her patience (and financial and moral support !) during the preparation of this thesis.

TABLE OF CONTENTS

LIST OF FIGURES

LIST OF TABLES

Geology, Geochemistry, and Mineralization of the Yellowbottom-Boulder Creek Area, Linn County, Oregon

INTRODUCTION

The Yellowbottom-Boulder Creek area is adjacent to the Quartzville Mining District in the Western Cascades of Oregon, as depicted in Figure 1. The Quartzville District produced gold for a short period of time in the late 1800's. Recent increases in the prices of gold and silver, coupled with the fall of base metal prices, have made the exploration for near-surface, disseminated deposits of precious metals attractive. The Western Cascade Range is largely unmapped at scales useful for exploration purposes, and, because of its past history as a gold-producing region, there is renewed interest in exploration of this area. The area I have selected for study is immediately west of the Quartzville district, and exposures locally exhibit evidence of intense hydrothermal alteration and metallization. Features suggestive of porphyry-style Cu-Mo mineralization at depth, including a breccia zone cemented by tourmaline, breccia pipes, extensive propylitic and local argillic-phyllic alteration, and parallel stockworks of fractures and veinlets, are present in several parts of the study area. The Boulder Creek area appears to be particularly interesting in this regard, because several rock samples contain anomalous concentrations of copper, molybdenum, gold, and silver.

The purposes of this thesis were to: 1) construct a detailed geologic map at a scale of 1:12,000 (Plate 1) that shows the distribution of the various volcanic and intrusive units, zones of alteration and mineralization, and general structure of the Yellowbottom-Boulder Creek

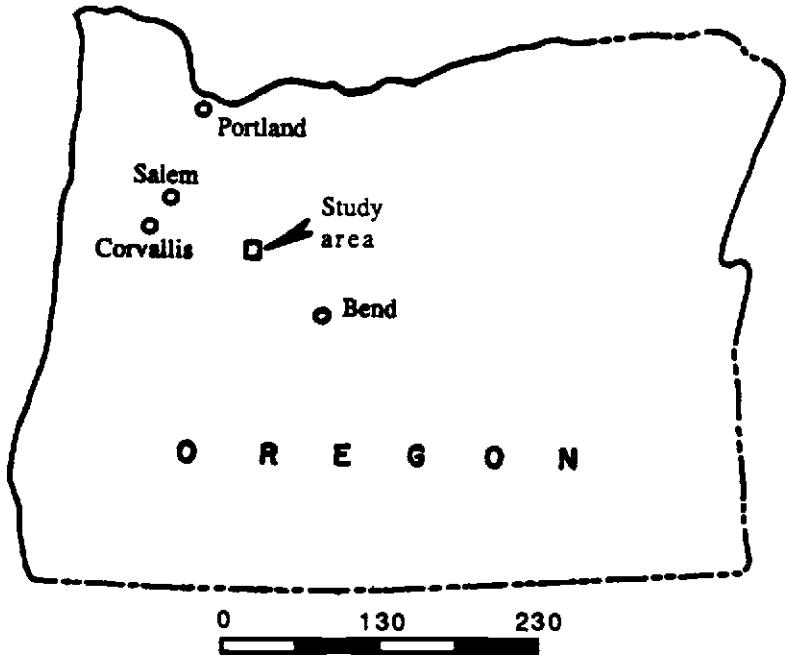

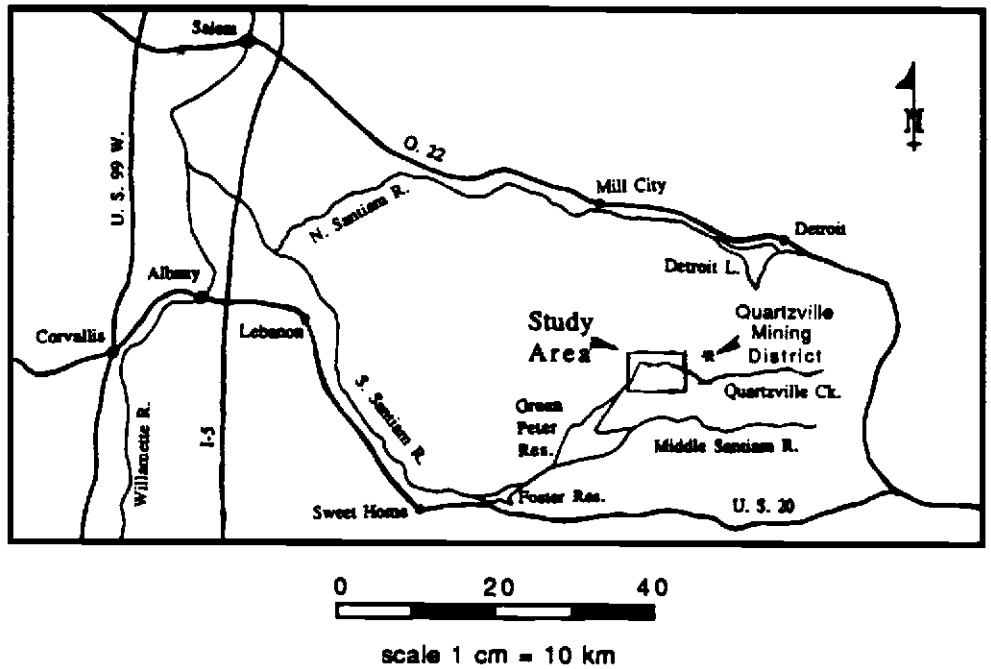

Figure 1- Index maps showing location of study area, nearby towns, major rivers, and principal access.

area; 2) determine the general volcanic stratigraphy and compare and attempt to correlate it with that described in reports dealing with other areas of the Western Cascades; 3) evaluate the gold-silver potential; 4) compare the alteration-mineralization patterns to those of other mineralized districts of the Western Cascades; and 5) summarize the results and conclusions in a formal report.

Geographic Setting

The western slopes of the Cascade Range are characterized by deeply dissected topography and temperate climate. Annual precipitation averages about 45 inches, most falling as rain during the period October-June. Summers are dry and warm. Steep slopes commonly exceeding 40 degrees, sharp ridges, and narrow V-shaped valleys are common landforms of the range. The study area is located in rugged terrain along Quartzville Creek in Linn County. Major drainages and geographic features are depicted in Figure 2. Elevation ranges from 1200 feet (365 meters) along the southwest end of Quartzville Creek to more than 4000 feet (1220 meters) atop Galena Ridge in the southeastern corner. The area is drained by a dendritic pattern of streams that feeds Quartzville Creek, which in turn flows into Green Peter Reservoir (Figure 1). Major tributaries are Boulder Creek, Yellowstone Creek, Packers Gulch, Yellowbottom Creek, and an unnamed creek which I have called Temple Creek in this report (Figure 2).

The segment of Quartzville Creek within the Yellowbottom-Boulder Creek area has been designated a Recreational Mining Corridor by the U.S.

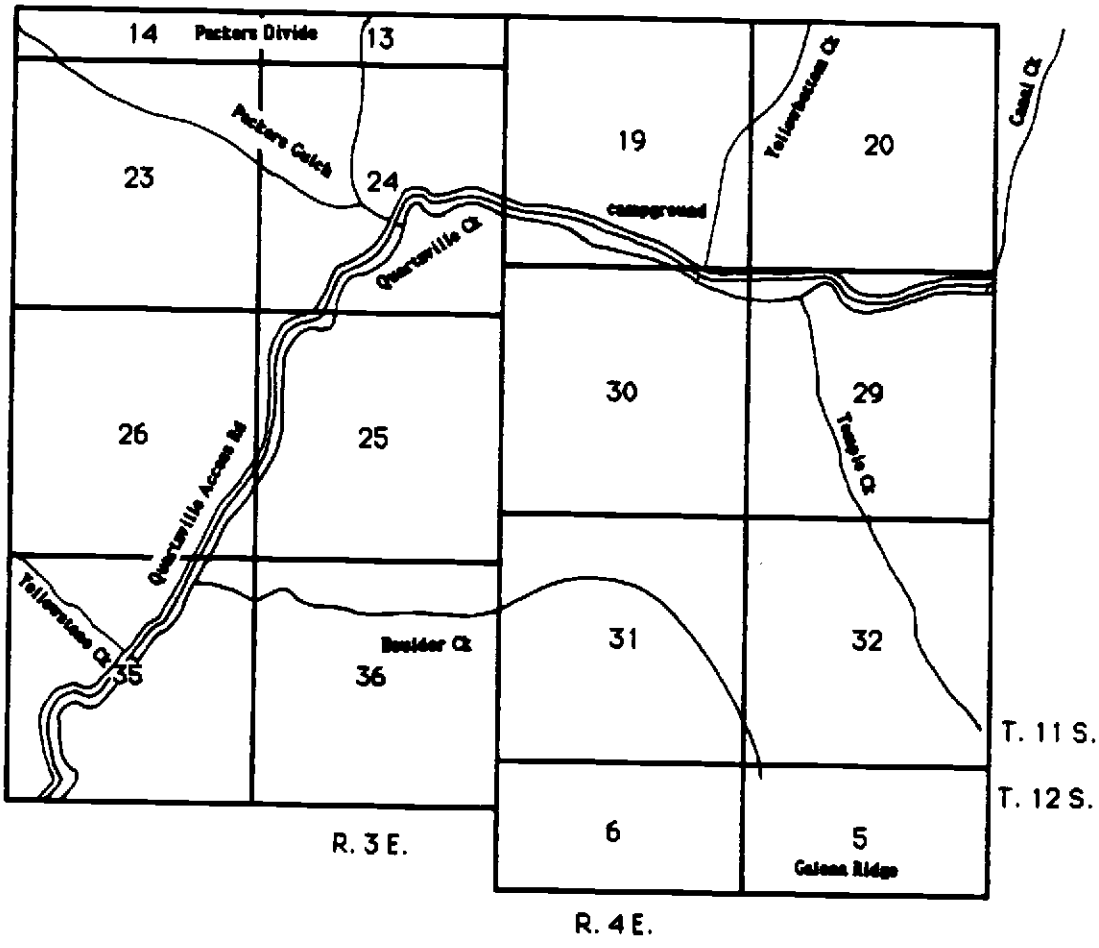

Figure 2- Location map of the study area showing the principal access, major drainages, and geographic features.

Bureau of Land Management on land donated by Champion International Timber Company. It is used for gold-panning and dredging by scores of people each year. Dredges with intake hoses up to 5" in diameter are permitted, and these provide the best method for recovering gold from the creek sediments. Gold can be found all along the creek, from east of McQuade Creek, 7 kilometers east of the study area, to Green Peter Reservoir, as flakes, wires, dust, and rare nuggets up to 1/2 ounce in weight. The best locations for finding gold are bedrock traps in the stream channel and on adjacent bare rock, or associated with organic material such as moss and small roots along the banks. Total production from the river has been estimated to be about 50 ounces yearly (Munts, 1978). Free camping is permitted anywhere along the river within the Recreational Corridor, the best site being the former Boy Scout camp now known as Optimist's Park, located 0.3 kilometers west of the confluence of Canal and Quartzville Creeks. A well-kept U.S. Forest Service campground, built within a grove of old-growth timber at Yellowbottom Recreation Site, also accommodates campers for a reasonable fee. Other recreational opportunities in the area include trout fishing; picnicking; hunting for deer, elk, and grouse in season; and swimming at any of the numerous natural pools along Quartzville Creek. Accordingly, these varied activities render the Yellowbottom-Boulder Creek area a pleasant, yet not well-known, recreation spot.

The area is heavily timbered, primarily by Douglas fir that is being actively logged at present. Other species of trees include western cedar, sugar pine, hemlock, and other varieties of fir and pine. Underbrush

includes rhododendron, manzanita, dogwood, mountain blueberry, Oregon grape, vine maple, and ferns and mosses.

History of the Quartzville Mining District

The Quartzville Mining District was organized in 1864 after the initial discovery of gold in 1863. Gold was derived from the oxidized parts of gold-quartz veins in a sequence of andesitic to rhyodacitic volcanic rocks of mid-Miocene age. Several mines were operated during the period 1864-1871 and yielded about 3900 oz of gold. Production was mostly from the Albany and Lawler Mines. The town of Quartzville, accessible only by a foot trail from Mill City (Figure 1), had a population of about 1,000 during this period. Between 1890 and 1900, additional activity, largely from the Lawler Mine, produced another 12,000 oz of gold and 3000 oz of silver (Callaghan and Buddington, 1938). The total value of recorded metal production from the District has been estimated at $365,000 (at $20.80/oz. Au), although an additional $500,000 in unrecorded gold may have been produced from the Lawler Mine (Munts, 1978). Details of past mining activity in the district have been reviewed by Brooks and Ramp (1968). The central part of the District is currently being reevaluated for disseminated gold mineralization by a joint venture between Utah International and the newly-formed Orvana Resources Corporation of Vancouver, British Columbia, Canada.

Location and Accessibility

The area of study (Figure 2) covers approximately 13 1/4 square miles (35 km^2) west of the main Quartzville District along Quartzville Creek. Access to the area is readily obtained from the south along the Quartzville Access Road off U.S. 20, at the east end of Foster Reservoir (Figure 1). Logging roads in the area are numerous, well maintained, and provide access as well as some of the best bedrock exposures. Offroad travel is difficult because of steep slopes and dense underbrush, making detailed mapping a tedious and largely uncertain endeavor.

Previous Investigations

Pioneering papers on the general geology of the Western Cascades are chiefly those by Thayer (1936), Callaghan and Buddington (1938), and Peck et al. (1964). Topical studies of the region include those by McBirney (1968, 1978), McBirney et al. (1974), Buddington and Callaghan (1936), Mason et al. (1977), and H.P. Taylor (1971). Stowell (1921) provided the first geologic study of the area and assays of many veins from the Quartzville District. Berg (1961) completed for the Burlington Northern Railroad an unpublished preliminary map (scale 1:31,680) of the District that overlaps one-half of the thesis area. Gray (1977) published a field trip guide to the District. In addition, Munts completed a M. S. Thesis on the Quartzville District in 1978, which was later summarized in a published report (Munts, 1981). His work includes a map of the District (scale 1:12,000), as well as detailed descriptions of

the rock units in the area. Power (1984) and Field et al. (1987) have recently summarized the geology and mineralization of mining districts of the Western Cascades of Oregon and Washington, including the Quartzville District. Priest et al. (1983) published an overview of the geology of the central Cascade Range, including the Western Cascades sub-province, and provided detailed descriptions and whole-rock analyses of the various volcanic rock types.

Methods of Study

Reconnaissance study was conducted during the summer of 1986, and detailed mapping was undertaken during the summer of 1987 using a base map prepared from standard 71/2 minute U.S.G.S. Quadrangles, at a scale of 1:12,000. Aerial photograph coverage (scale = 1:12,000) of the area was used to plan traverses and for the recognition of lineaments. Traverses were conducted along all roads, as well as the major stream drainages. The nature of the terrain makes traversing in the woods very difficult and generally unprofitable, as natural exposures in the entire Western Cascades province are limited, being only 1 percent on the average (Priest et al., 1983). Because of this limitation, contacts between the various volcanic units should be treated as only approximate, while the location of intrusive bodies, breccia zones, and local alteration features are generally more precise.

Standard thin sections were prepared from hand samples and examined on a Nikon research-model petrographic scope. Plagioclase compositions were determined using the Michel-Levy method (Kerr, 1977;

Nesse, 1986). Point counts were conducted on sections representative of the various lithologies, with a minimum of 1000 points for each section. Finely crystalline volcanic rocks were point-counted to determine the proportions of phenocrysts to matrix, and the groundmass mineralogy was simply estimated. Normative mineralogy was calculated for some samples using CIPW rules from the major oxide data (Cross et al., 1903) and by means of the PetCalc program for the Macintosh computer. Metal analyses were obtained for 60 samples, representative of the spectrum of rock types present in the area, from Chemical and Mineralogical Services, Inc., of Salt Lake City, Utah, and from Silver Valley Laboratories of Kellogg, Idaho. All samples were assayed for Cu, Ag, Mo, Pb, and Zn. Some were also analyzed for Au, and some for a selection of indicator elements including As, Sb, Co, Ni, Ba, and Bi. Major-element analyses were performed on 17 samples of volcanic flow units, intrusive rocks, and associated alteration types by Chemex Labs, Inc., of Sparks, Nevada. One coeval galena-sphalerite pair was obtained from a breccia zone in the Boulder Creek area; pure samples of the two phases were separated and analyzed for sulfur isotope compositions by Dr. I. R. Kaplan at Global Geochemistry Corporation of Canoga Park, California and were used to determine the temperature of deposition and source of sulfur. Fluid inclusion data were obtained from KRTA limited of Newmarket, New Zealand (courtesy of Orvana Resources Corporation), and by use of the Chaixmeca heating stage at Oregon State University's Department of Geology.

GEOLOGIC SETTING

The Cascade Range of Oregon is a north-trending volcanic arc produced by the subduction of the Juan de Fuca Plate beneath the North American Plate beginning about 40 Ma. The Range, 50 to 110 kilometers wide and 400 kilometers long in Oregon, can be divided into two parallel subprovinces on the basis of the volcanic stratigraphy: the younger High Cascades to the east and the older Western Cascades to the west (Baldwin, 1964).

Volcanic rocks of the Cascade Range have been divided into four groups according to their relative ages: the Early Western Cascade (40-18 Ma), Late Western Cascade (18-9 Ma), Early High Cascade (9-4 Ma), and Late High Cascade (4 m.y. to present) episodes (see Priest et al., 1983). The generalized distribution of these rock types within the Western Cascades subprovince is shown in Figure 3. This figure was constructed after the map by Wells and Peck (1964), by grouping formations of Eocene and Oligocene age as the Early Western Cascades episode and Miocene formations as the Late Western Cascades episode. This time-dependent designation greatly simplifies the stratigraphic correlation of rocks within the subprovince. Formerly, investigators gave various stratigraphic names to these volcanic rocks and mapped them accordingly, especially in the Western Cascades. These names are applicable locally, but correlation between different areas is uncertain.

The Early Western Cascade episode is dominated by voluminous amounts of intermediate-silicic tuffs and lesser iron-rich basaltic to silicic flows (Priest et al., 1983). These rocks have been called the Little Butte

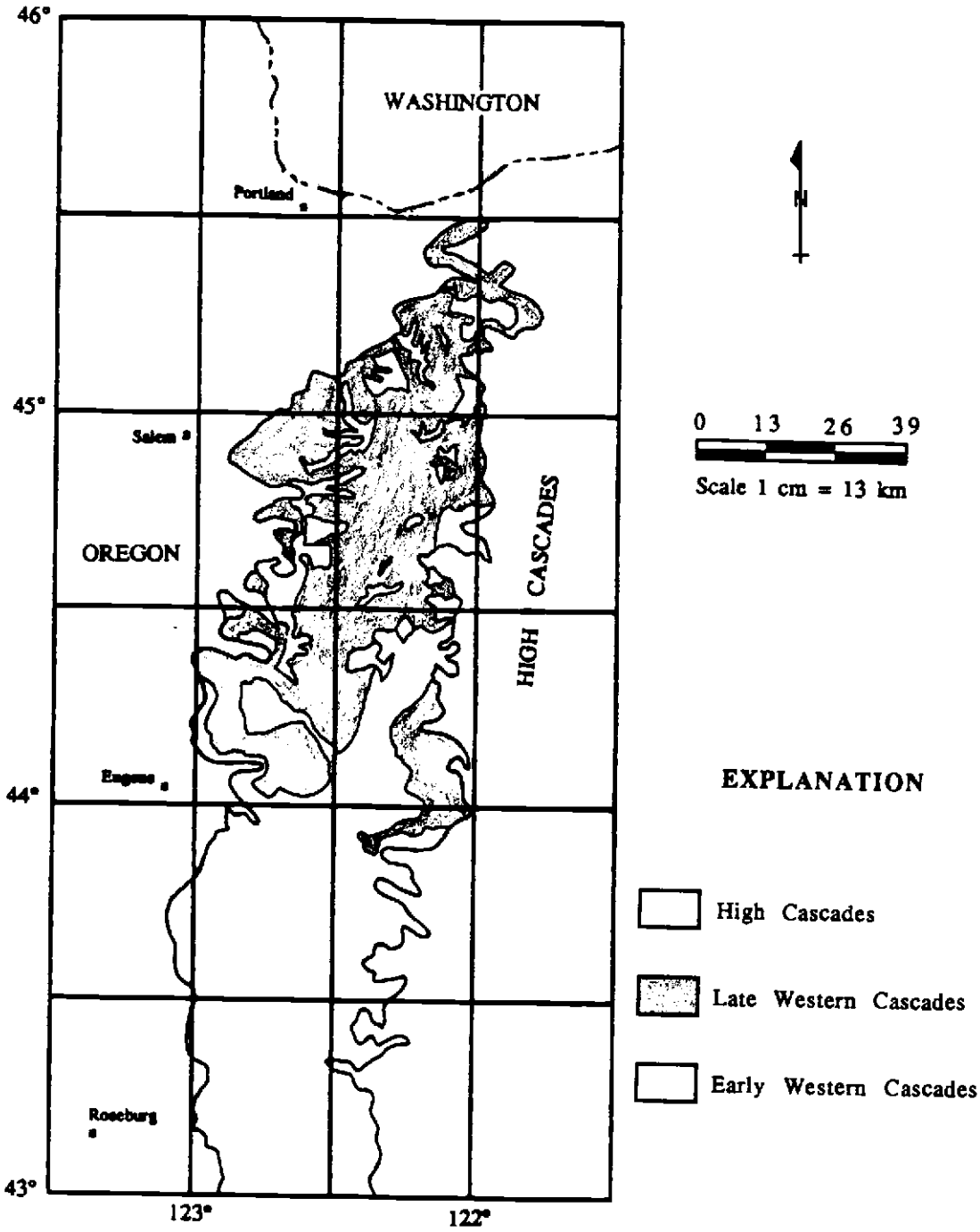

Figure 3- Generalized distribution of volcanic rocks within the Western Cascades. Modified from Peck et al. (1964) and Wells and Peck (1961).

Volcanic Series by Peck et al. (1964), who correlated them in part with the Little Butte Formation of Wells (1956) in the Medford Quadrangle. Stratigraphic names given to rocks of this sequence include the Breitenbush Formation (Hammond, 1979; White, 1980b), Scorpion Mountain Lavas (White, 1980a), and other units depicted in Figure 4. These rocks crop out over most of the Western Cascades south of the McKenzie River east of Eugene, along discontinuous portions of the western edge of the subprovince, and along the axes of the Breitenbush and Clackamas anticlines (Peck et al., 1964). Thicknesses of this sequence have been estimated at 1,500 to 5,000 meters, with the average thought to be about 1,500 to 2,500 meters (Priest et al., 1983). The maximum exposed thickness is present along the west side of the range and decreases towards the eastern margin of the province (Peck et al., 1964). Along the South Santiam River, south of the study area (Figure 1), rocks of early Western Cascade age have been reported to consist of a lower unit of fine-grained tuffs and an upper unit of olivine basalt and basaltic andesite flows and breccias (Peck et al., 1964). The distribution of known vents of Early Western Cascade rocks is shown in Figure 5.

The Late Western Cascade episode includes the Sardine Formation of Thayer (1936), named for the assemblage of volcanic rocks at Sardine Mountain in the North Santiam River area (Figure 1). The Sardine Formation covers most of the Western Cascades north of the North Santiam River, the axis of the Sardine syncline north of the McKenzie River, and discontinuous areas to the south near the western margin of the High Cascades (Peck et al., 1964). It is composed of flows of basaltic to rhyolitic composition which are interbedded with andesitic to dacitic

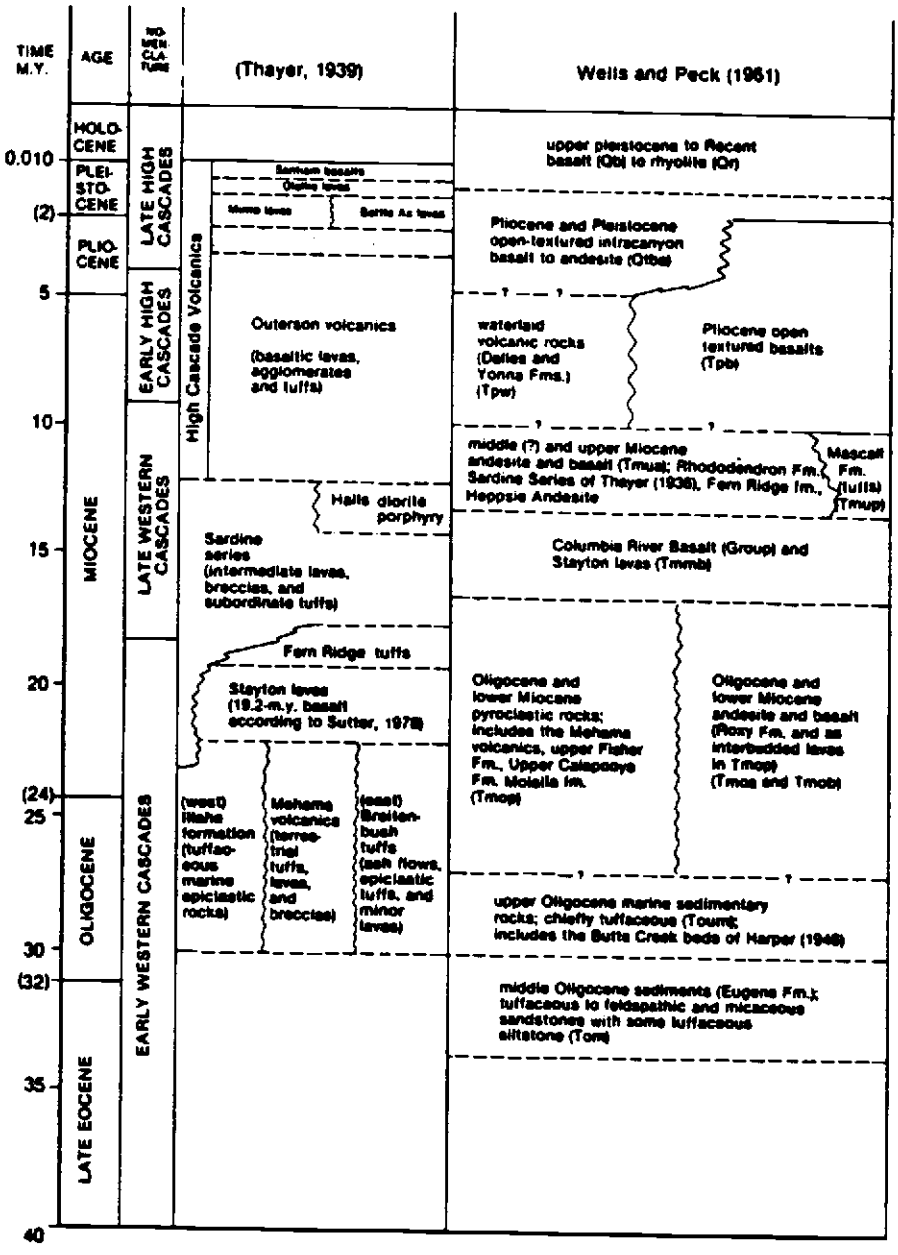

Figure 4- Regional stratigraphic units used by various geologists in the Western Cascades. (modified from Priest et al., 1983, with) geologic time boundaries of Armentrout, 1981).

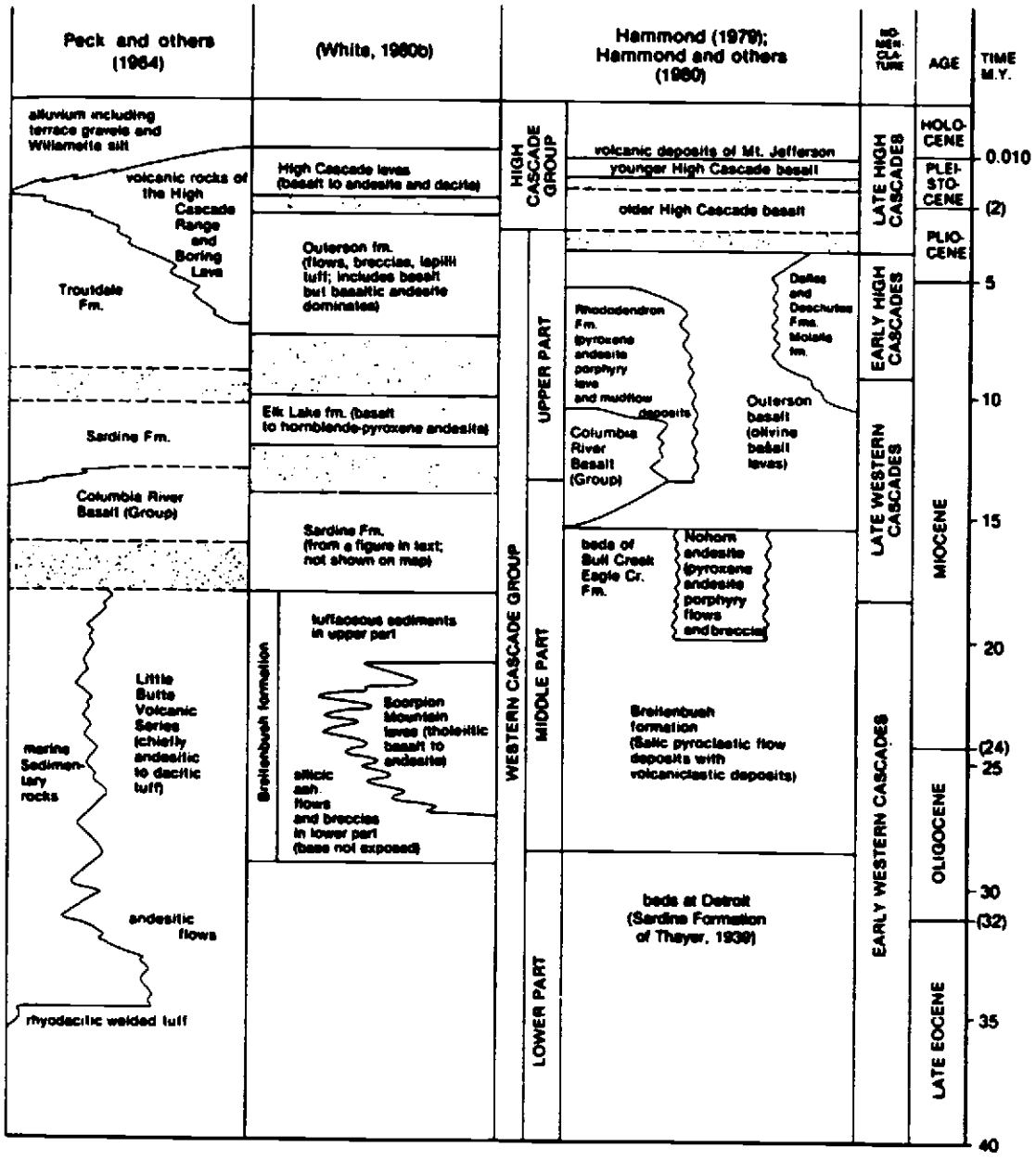

Figure 4- (continued)

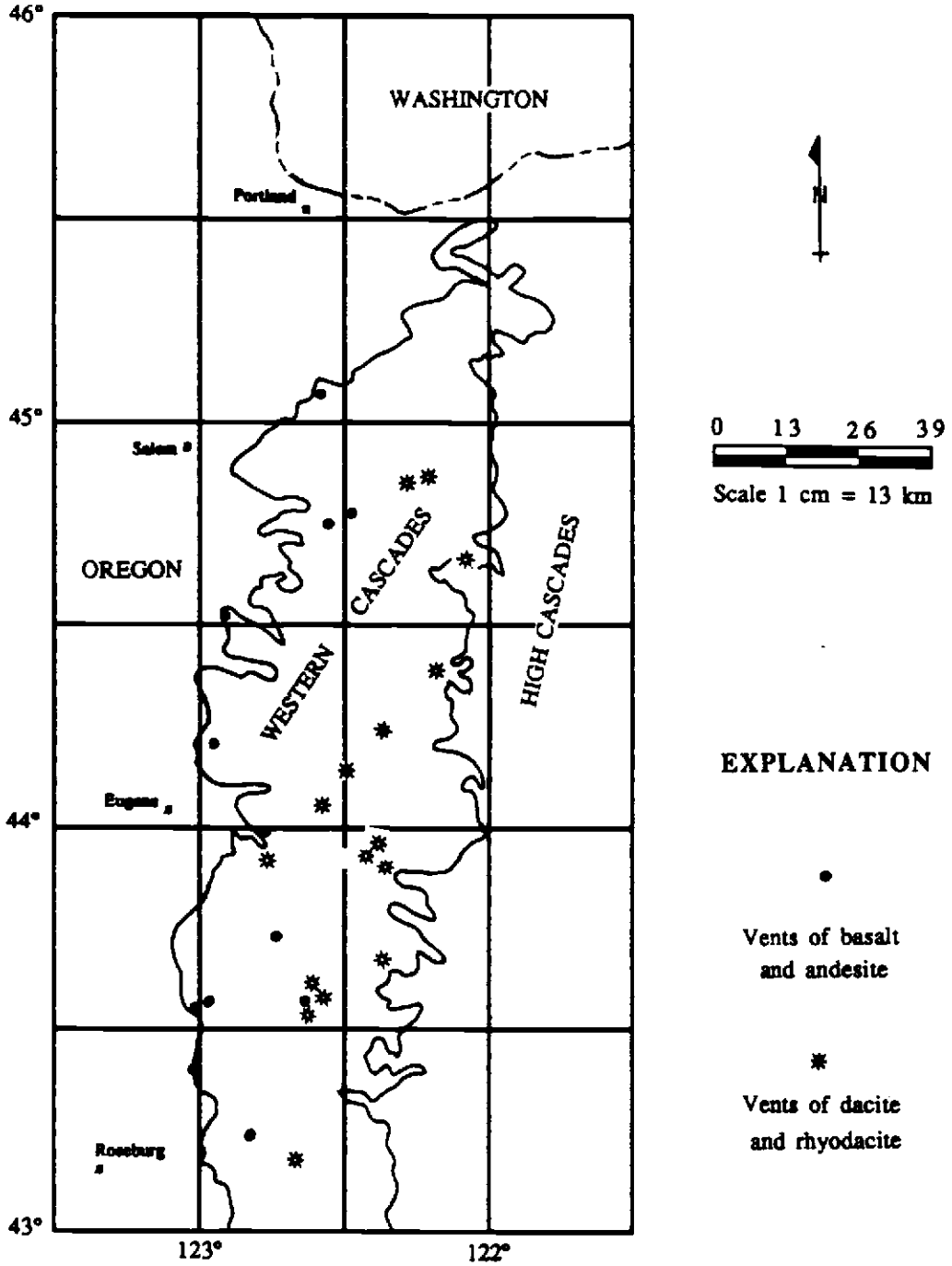

Figure 5- Vents of Early Western Cascade volcanic rocks (modified from Peck et al., 1964).

tuffs and extensive lahars. The dominant rock type is hypersthene andesite (Peck et al., 1964). Thicknesses of the formation average about 1,000 meters, but increase to a maximum of 3,500 meters near Detroit, presumably because of a concentration of vents in this area coupled with rapid subsidence of a basin along the eastern limb of the Sardine syncline (Peck et al., 1964). Vents have been identified in at least a dozen localities, including the Quartzville District, as depicted in Figure 6.

The axis of volcanism shifted to the east at about 9 Ma, corresponding to a change in the plate-tectonic regime, and produced the High Cascades (Priest, 1983). This subprovince is composed chiefly of voluminous eruptions of mafic, slightly alkaline, and iron-rich magmas from shield volcanoes which coalesced to form a broad platform during the Pliocene (E.M. Taylor, 1968; Priest et al., 1983). These lavas were highly fluid, apparently the result of rapid passage through the crust along normal faults (E.M. Taylor, 1980), which may have formed in response to an increased extensional tectonic stress across the Cascades that was the result of a major plate reorganization about 10-8 Ma (Priest et al., 1983).

Volcanic rocks of the Early High Cascade episode include olivine tholeiitic basalt flows that have a distinctive diktytaxitic texture, and minor andesites, dacites, and tuffs. Basalt and andesite flows of this age extended from vents located along the western margin of the High Cascades into the Western Cascades subprovince, where they are now found along the tops of high ridges, as shown on Figure 3 (Peck et al., 1964; Wells and Peck, 1961).

Volcanic rocks of the Late High Cascade episode are compositionally similar to those of Early High Cascade affinity (Priest et al, 1983). Rocks

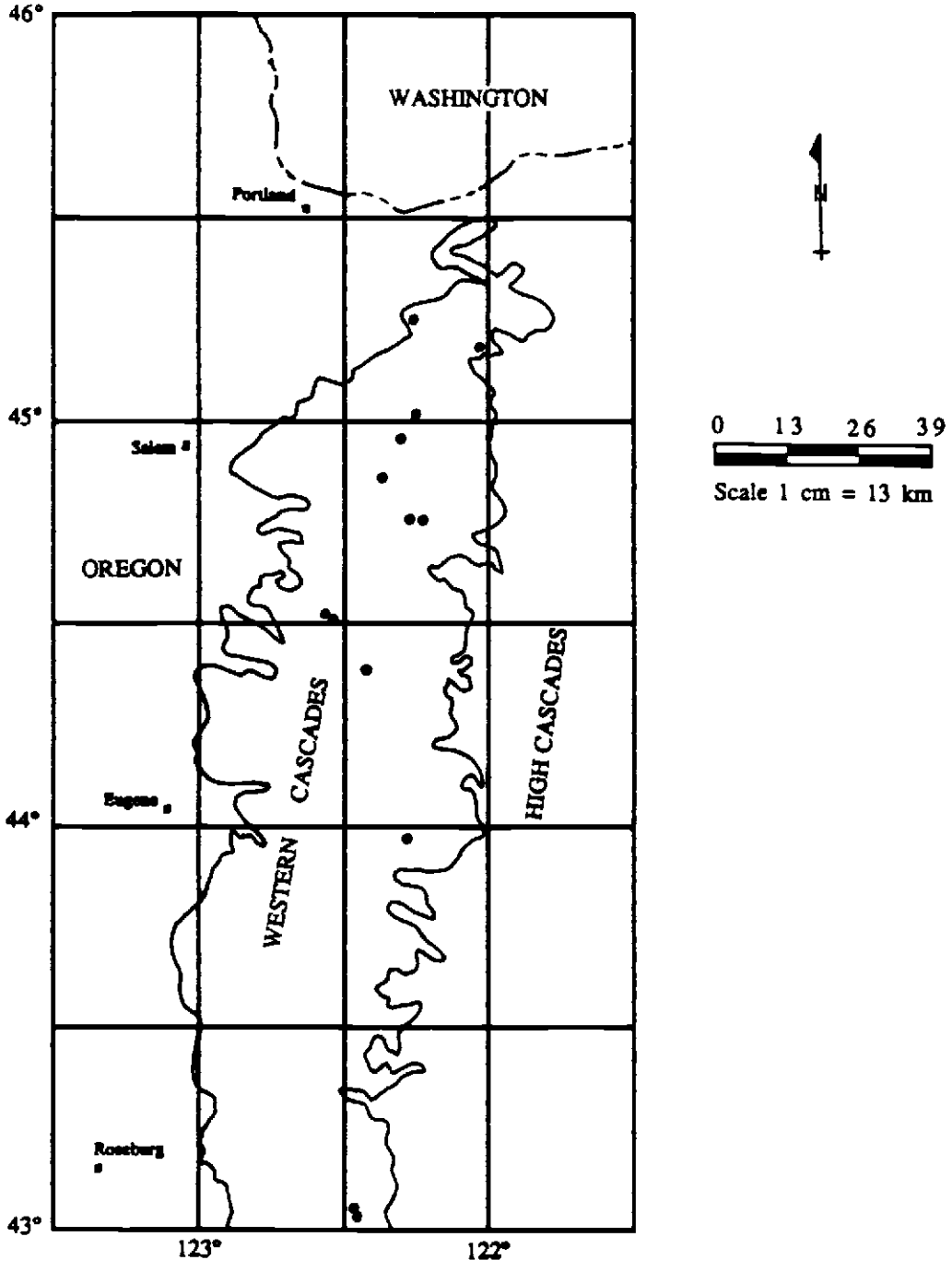

Figure 6- Vents of Sardine Formation volcanic rocks (modified from Peck et al., 1964).

of this age are present as intracanyon flows in a few localities within the Western Cascades, and are accompanied by a few small cinder cones that represent the last volcanic events in the subprovince. The distribution of the Late High Cascade volcanic rocks within the Western Cascades is dependent on contemporary drainage patterns, in sharp contrast with that of the Early High Cascade units (E.M. Taylor, 1980). Stratovolcanoes of intermediate to silicic composition were built on the mafic platform during the Quaternary period and created the majestic snow-capped peaks of the contemporary High Cascades. Volcanic activity has continued into the Holocene with the eruption of basaltic lavas from vents along the crest of the High Cascades (Priest et al., 1983).

Intrusive rocks in the Western Cascades include plutons of intermediate composition with ages ranging from 9 m.y. to 22 m.y. (Sutter, 1978; Power et al., 1981), and a compositionally diverse system of dikes and plugs. These intrusions range in size from small dikes less than one meter wide to stocks several kilometers in diameter. They are present along a linear belt that extends roughly north-south through the various historic mining districts (Callaghan and Buddington, 1938), as shown in Figure 7. Compositions of the intrusive rocks span the entire range from gabbro to granite, although intermediate varieties are the most abundant (Buddington and Callaghan, 1936). Common rock types include quartz diorite, granodiorite, diorite, tonalite, and quartz monzonite (Power, 1984). Granites have been reported from the Nimrod Stock (Buddington and Callaghan, 1936), and along the Middle Santiam River (Munts, 1978). Granitic rocks are also present in some of the mining districts (Power, 1984), including the Quartzville district (Munts, 1978) and the area of

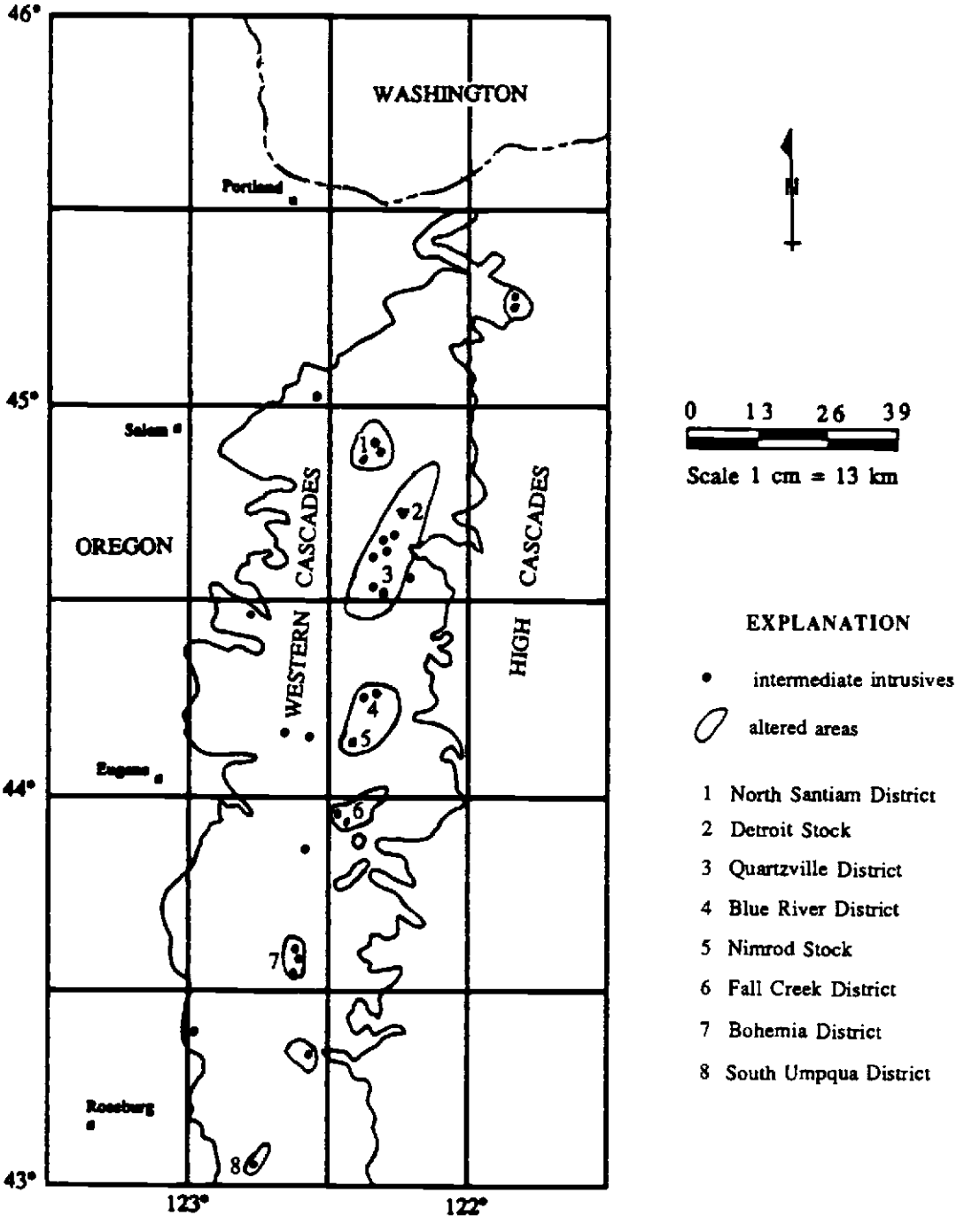

Figure 7- Distribution of stocks of intermediate composition, areas of alteration, and location of mining districts, in the Western Cascades. Modified from Peck et al. (1964) and Power (1984).

this study. Plugs and dikes of basaltic composition are present in the study area, and have been reported from the Quartzville district (Berg, 1961; Munts, 1978). Porphyritic textures are common to nearly all intrusive rocks found in the Western Cascades (Buddington and Callaghan, 1936; Power, 1984).

Hydrothermal alteration and mineralization accompanied the emplacement of these intrusions in all of the mining districts (Callaghan and Buddington, 1938), and led to the formation of precious and base-metal deposits which are thought to represent the "tops" of porphyry-copper deposits (Power, 1984). Indeed, a small porphyry-style copper deposit has been recently identified in the North Santiam district (Field et al., 1987).

Erosion of this volcanic-plutonic arc within the Western Cascades by glaciers and streams during the Quaternary has removed the parent volcanoes and resulted in a moderately to deeply dissected topography.

VOLCANIC ROCKS

Volcanic rocks of the Quartzville area consist of a series of basaltic to rhyodacitic flows and pyroclastic deposits of Late Oligocene to mid-Miocene age that are overlain in some locations by Pliocene and Quaternary basalt flows, presumably of High Cascade origin. A generalized volcanic stratigraphic column of the study area is presented in Figure 8.

Rocks of the Yellowbottom-Boulder Creek area are divided into units on the basis of similar lithologies, following the terminology used by Berg (1961) and later slightly modified by Munts (1978). The Miocene units, in order of decreasing age, are the lower andesite, lower pyroclastic, intermediate andesite, intermediate basalt, upper pyroclastic tuff, upper pyroclastic, and rhyodacite units. Extensive field descriptions of these units are provided by Munts (1978), and the reader is referred to his thesis for a more detailed and complete discussion.

Berg (1961) and Munts (1978) have suggested that the oldest two units mentioned above are correlative with the Little Butte Volcanic Series of Oligocene age. However, a published description of the Little Butte Volcanic Series (Peck et al., 1964, p. 13-14) states that the top of this unit is composed of several thousand meters of andesitic to dacitic pyroclastic rocks, and that the base of the Sardine Formation is marked by thick flows of hypersthene andesite. Thus, rocks exposed along Green Peter Reservoir (Figure 1) have the characteristics of the Little Butte Volcanic Series, whereas those of the lower andesite unit are similar to the Sardine Formation. In addition, rocks of the reservoir area display alteration

GENERALIZED VOLCANIC STRATIGRAPHIC COLUMN

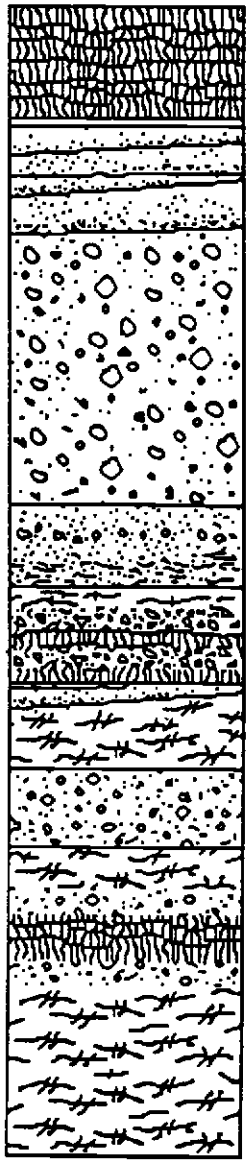

0 100

Vertical scale:
1 cm = 100 m

Pliocene Flows (Tb) - Diktytaxitic, open-textured olivine basalt of High Cascade affinity

Rhyodacite Unit (Tr)- rhyodacite flows and tuffs

Upper Pyroclastic Unit (Tup)- lacustrine tuff (top) and laharic breccias

Upper Pyroclastic Tuff Unit (Tupt)- tuff-breccia, ash-flow tuff, and welded tuff

Intermediate Basalt Unit (Tib)- dacite flows (top), and basalt flows interbedded with volcanic breccias

Intermediate Andesite Unit (Tia)- lacustrine tuff (top), and andesite flows

Lower Pyroclastic Unit (Tlp)- lapilli tuff, tuff-breccia, and ash-flow tuff

Lower Andesite Unit (Tla)- andesite and basalt flows. autoclastic breccia, and occasional laharic breccias

EXPLANATION

basalt

dacite

lacustrine tuff

andesite

laharic breccia

lapilli tuff

ash-flow tuff

Figure 8- Generalized volcanic stratigraphy of the Quartzville area (after Berg, 1961 and Munts, 1978).

restricted to the growth of zeolites and quartz in small vugs, and exhibit a subdued outcrop style. In contrast, rocks of the lower andesite unit are propylitically altered and form massive, blocky outcrops that are similar to other rock units thought to be of Miocene age in the district.

Comparison of the chemical composition of lower andesite unit rocks to that published for rocks of the Little Butte Volcanic Series and Sardine Formation (Power, 1984; Peck et al., 1964) reveals a resemblance between the Sardine Formation and the lower andesite unit (see Tables 2 and 3). Specifically, basaltic andesites of both the Sardine Formation and the lower andesite unit contain lower concentrations of TiO_2, MgO, and K_2O, and higher Na_2O, than those of the Little Butte Volcanic Series. Therefore, the close lithic and chemical similarity between the lower andesite unit and published descriptions of the Sardine Formation, coupled with the contrast in alteration and outcrop style from those exposed along the reservoir, suggest that the entire sequence within the study area belongs to the Sardine Formation and thus is of Miocene age. Furthermore, the volcanic rocks along the reservoir may be Oligocene, in which case the lower andesite unit represents the base of the Sardine Formation in the Yellowbottom-Boulder Creek area.

Pliocene basalt flows cap Galena Ridge along the southern border of the study area and are the chief constituent of glacial till in the Boulder Creek drainage. These basalts display diktytaxitic textures and columnar jointing, and they are thought to be the basal flows of the Early High Cascade episode (Priest et al., 1983; Munts, 1978). A sequence of relatively unaltered andesite flows in the Packers Divide area along the northern border of the map area is possibly correlative with those of

Galena Ridge. These flows have been thought to be Pliocene by some investigators (Priest et al., 1983), although others (Berg, 1961; Peck et al., 1964; Munts, 1978) have previously assigned them to the Quaternary. This controversy has been resolved by a K-Ar age determination of the basalt on Galena Ridge of 6.3 m.y. (Verplanck, 1985).

An intracanyon basalt flow that partially fills the valley of Canal Creek and parts of Dry Gulch, along the eastern edge of the map, and two cinder cones near this flow, represent the last pulse of volcanic activity in the District. The latter features are thought to be young, perhaps 10,000 years B. P. or less. Evidence for this young age was provided by Munts (1978), who observed that one of the cinder cones overlies glacial debris.

Volcanic rocks of the Yellowbottom-Boulder Creek area are classified according to the scheme of Le Maitre (1984). This method uses subdivisions based on total alkalis versus silica, as shown in Figure 9, and is consistent with megascopic field names given to these rocks. Attempts to use the mineralogical classification proposed by Streckeisen (1979), which defines rock types on the basis of the proportions of quartz, plagioclase, and alkali feldspar, are unsatisfactory because of the difficulty in obtaining modal data for finely crystalline volcanic rocks and the problem of distributing normative albite between plagioclase and alkali feldspar. Although modal analyses determined for these volcanic rocks are practically devoid of alkali feldspar and quartz, the CIPW normative data (Appendix A) indicate that these minerals should be present. Factors which may bear on this problem include incorporation of quartz and alkali feldspar into residual fluids, which subsequently crystallized as glass or very fine-grained matrix, and difficulties in trying

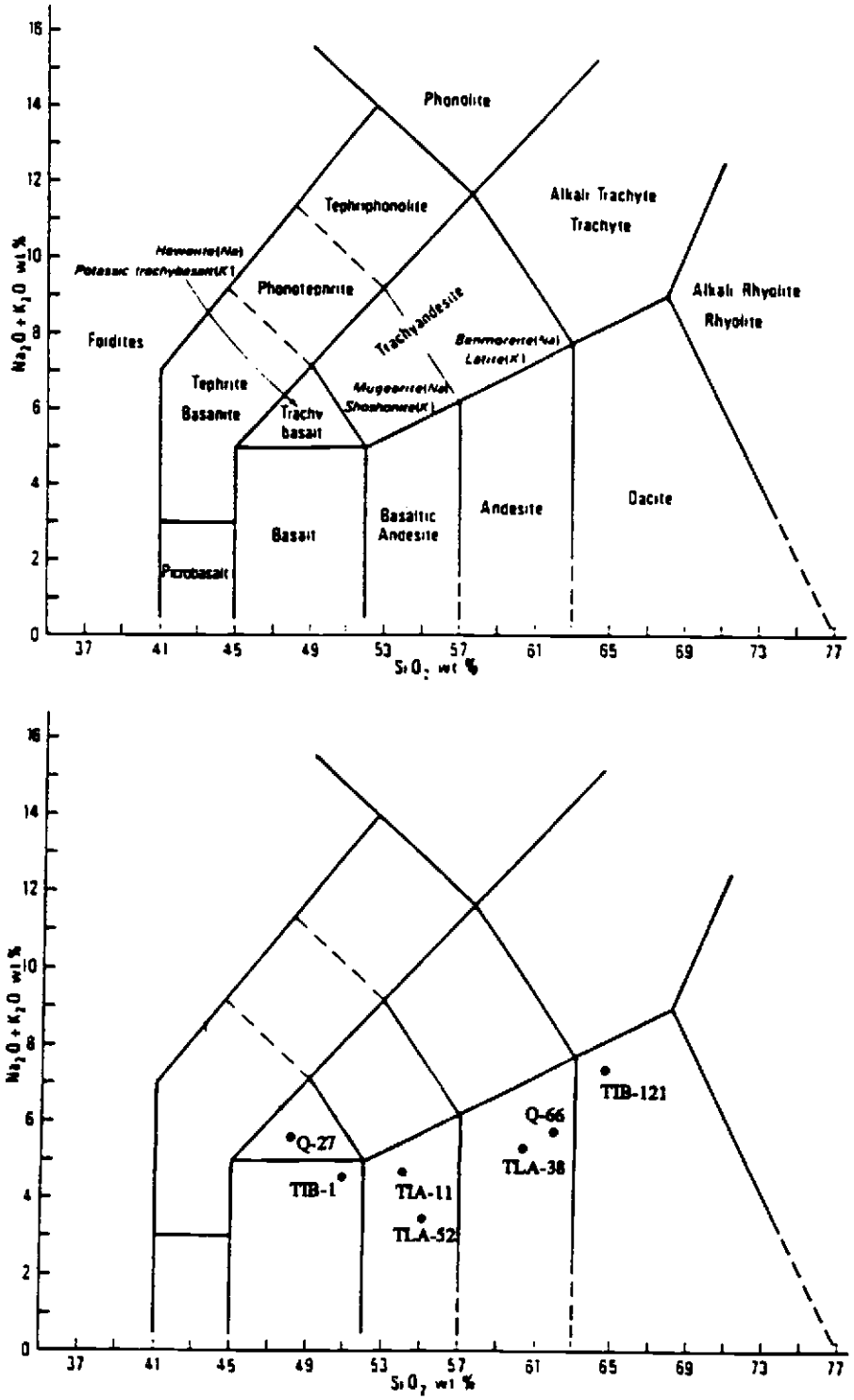

Figure 9- Classification of volcanic rocks from the Yellowbottom-Boulder Creek area using the TAS (total alkalis vs. silica) diagram of Le Maitre (1984).

to identify finely crystalline phases. The problem of the distribution of albite was recognized by Le Maitre (1976a), who gave a general formula for correcting the data. However, attempts to use this method in the present study resulted in the shifting of all data points toward the alkali feldspar apex and into fields of classification that are not consistent with megascopic field names given to the rocks.

Lower Andesite Unit (Tla)

The lower andesite unit is composed of flows of dense pyroxene andesite, nearly aphyric basaltic andesite, interflow layers of autoclastic breccia, and minor thin laharic breccias. These rocks crop out in the western half of the Yellowbottom-Boulder Creek area and have an average dip of approximately 10° SE. Rocks of this sequence are also present along the eastern edge of the Quartzville district, as mapped by Munts (1978). Berg (1961) stated that the unit is at least 360 meters thick. It forms massive, smooth outcrops along Quartzville Creek, Packers Gulch, and the lower part of Boulder Creek.

Pyroxene andesites of this sequence are medium bluish-gray color (5 B 5/1), and are nearly aphyric to porphyritic in texture. Porphyritic phases locally contain large phenocrysts of plagioclase up to 1.2 centimeters across. Basaltic andesites are very dense, medium dark gray (N 4) in color, and aphyric to porphyritic in texture.

Thick, dense flows of basaltic andesite, separated by autoclastic breccias and occasional mudflows, crop out in the Packers Gulch drainage. Layers of autoclastic flow breccia are common along Quartzville Creek and

Packers Gulch. These rocks range from bluish-grey to purplish-red, which indicates that oxidizing conditions were prevalent during their development, and they contain angular to rounded clasts of andesite or basalt of varying sizes recemented by aphyric andesitic material. The origin of these flow breccias may be mechanical and the result of the movement of the flow itself, or they may have been caused by fragmentation which resulted from contact with water-saturated ground causing phreatic explosive brecciation (Fisher and Schmincke, 1984).

A few thin mudflows are also present in this unit, mostly in the Packers Gulch area. They are typically about 4 meters thick and consist of clasts of andesite, basalt, dacite, and rhyodacite of various sizes in a fine-grained matrix.

Petrography and Petrochemistry

Modal mineralogical analyses for an andesite and a basaltic andesite from this unit are given in Table 1. Andesites (sample TLA-38) exhibit a pilotaxitic texture in thin section. Phenocrysts of calcic andesine (An_{48}), clinopyroxene, and occasional orthopyroxene are set in a groundmass dominated by plagioclase feldspar microlites of intermediate andesine composition (An_{49}).

Phenocrysts of andesine are up to 1 mm in length, display compositional zoning, and have been corroded internally by alteration processes which have replaced portions of the phenocrysts with calcite. Microphenocrysts of the pyroxenes have been completely altered to an assemblage of calcite, chlorite, and montmorillonite.

TABLE 1 - Modal mineralogical analyses (in percent) for samples of basaltic andesite (TLA-52) and andesite (TLA-38) from the lower andesite unit

Sample #	TLA-52	TLA-38
phenocrysts		
plagioclase[1]	26.1%	14.3%
orthopyroxene[2]	7.8	0.4
clinopyroxene[2]	--	3.4
olivine[3]	1.0	--
Fe-Ti oxides	1.0	1.0
groundmass		
plagioclase microlites	37.0	67.5
orthopyroxene[2]	4.0	--
clinopyroxene	--	5.0
Fe-Ti oxides	2.0	5.0
glass	21.0	--
quartz	--	3.0
apatite	acc.[4]	acc.

[1]weakly altered to clays and calcite
[2]completely altered to chlorite, calcite, and clays
[3]partially altered to iddingsite along fractures
[4]accessory (very minor) quantity

The groundmass consists of randomly oriented microlites of andesine which average 0.1 mm in length, interstitial clinopyroxene, minor quartz and apatite, and abundant, small, and rounded blebs of Fe-Ti oxides. Groundmass clinopyroxenes have also been converted to calcite, chlorite, and clay minerals. Two size populations of Fe-Ti oxides are present. The larger are euhedral and appear to be phenocrystic in origin, whereas smaller crystals are more abundant, rounded, and interstitial to microlites of andesine.

Basaltic andesites from the Packers Gulch drainage (Table 1 - sample TLA-52) contain phenocrysts of zoned calcic andesine (An_{46}) and orthopyroxene set in a hyalopilitic groundmass consisting of sodic andesine (An_{36}) microlites, brown glass, Fe-Ti oxides, and orthopyroxene.

Phenocrysts of andesine are up to 2.5 mm in length, exhibit compositional zoning, and are partially corroded along the margins. These crystals have been partially altered to clay minerals. Phenocrysts of orthopyroxene are up to 1.8 mm across and have been completely replaced by chlorite and calcite. Both feldspar and pyroxene phenocrysts are clustered together and provide textural evidence that they were formed simultaneously. Additionally, a few ghosts of olivine phenocrysts that have been altered to iddingsite and quartz are sparingly evident. Also present are skeletal crystals of ilmenite euhedra that are thought to be associated with the breakdown of mafic minerals, as they usually are at or near the former sites of pyroxenes.

Microlites of andesine in the groundmass average 0.1 mm in length and are randomly arranged in a matrix of brown glass. As was noted for

the sample of andesite described previously. Fe-Ti oxides are in two size ranges indicating formation as both phenocryst and groundmass constituents.

Chemical analyses of lower andesite unit rocks are presented in Table 2. Names originally assigned to these rocks in the field are consistent with those subsequently determined on the basis of chemical classification as previously shown in Figure 9. Comparisons of these rock compositions to the average analyses of basaltic andesites and andesites from the Little Butte Volcanic Series and andesites from the Sardine Formation, as summarized by Power (1984) and Peck et al. (1964) and tabulated in Table 3, show that samples of the lower andesite unit are grossly similar to those of the Sardine Formation. Volcanic rocks from the Little Butte Volcanic Series consistently contain higher FeO_T, MgO, and TiO_2 than those of the Sardine Formation, with the exception of the basaltic andesites of Peck et al. (1964). However, because these analyses were performed as early as the 1930's, the data may not be entirely reliable.

The samples of basaltic andesite and andesite from the Yellowbottom-Boulder Creek area (Table 2) are variably depleted in alumina as compared to the various averages listed in Tables 3 and 4. This apparent deficiency may relate to the abundance of plagioclase phenocrysts, as Ewart (1976) has demonstrated a strong positive correlation between the content of Al_2O_3 and modal phenocrystic plagioclase feldspar. Both samples were collected from the upper part of the lower andesite unit, which as previously mentioned contains fewer and smaller phenocrysts of plagioclase feldspar than similar rock types from lower horizons in this unit. Accordingly, it is suggested that the rocks from the upper part of

TABLE 2- Major oxide (in percent) and metal (in ppm) analyses for samples of basaltic andesite (TLA-52) and andesite (TLA-38) from the lower andesite unit

Elemental oxide	TLA-52	TLA-38
SiO_2	55.03%	59.40%
TiO_2	1.00	1.12
Al_2O_3	16.74	15.58
Fe_2O_3	3.00	2.09
FeO	3.43	4.12
MnO	0.11	0.12
MgO	3.22	2.13
CaO	6.91	5.12
BaO	0.03	0.06
Na_2O	3.33	3.64
K_2O	0.15	1.75
P_2O_5	0.35	0.39
LOI	4.40	2.64
TOTAL	97.70	98.16
Metals		
Cu	7 ppm	25 ppm
Mo	1	1
Pb	7	8
Zn	35	50
Ag	0.4	< 0.3

TABLE 3- Average major element compositions of basaltic andesites and andesites from the Sardine Formation and Little Butte Volcanic Series

	Basaltic andesites				andesites	
	1	2	3	4	5	6
SiO_2	53.8%	53.6%	55.2%	54.2%	61.1%	58.8%
TiO_2	1.32	1.10	1.34	1.25	0.72	0.89
Al_2O_3	17.8	17.9	16.2	16.3	17.3	17.7
Fe_2O_3	--	--	--	3.1	--	--
FeO	9.3	7.7	9.3	6.1	5.5	7.0
MnO	0.16	--	--	0.15	0.09	--
MgO	3.7	5.3	5.4	4.7	3.1	3.4
CaO	8.3	8.5	8.2	8.6	5.3	6.6
Na_2O	3.5	3.5	3.1	2.7	4.0	3.6
K_2O	0.77	0.39	1.13	1.06	1.45	0.91
P_2O_5	0.19	--	--	0.17	0.13	--
ΣH_2O	1.65	--	--	--	--	--
TOTAL	101.0	99.6	99.9	98.3	98.7	98.9

1- average of 4 analyses from the Sardine Fm., from Peck et al. (1964)
2- average of 4 analyses from the Sardine Fm., from Power (1984)
3- average of 6 analyses from the Little Butte Volcanic Series, from Power (1984)
4- average of 2 analyses from the Little Butte Volcanic Series, from Peck et al. (1964)
5- average of 2 analyses from the Sardine Fm., from Peck et al. (1964)
6- average of 4 analyses from the Sardine Fm., from Power (1984)

TABLE 4- Average major element compositions of basaltic andesites and andesites

	1	2	3	4
SiO_2	53.41%	55.4%	59.20%	59.21%
TiO_2	0.79	0.81	0.76	0.78
Al_2O_3	17.75	17.6	16.82	17.32
Fe_2O_3	3.24	3.4	2.90	1.14
FeO	6.25	6.1	4.50	5.72
MnO	0.17	0.21	0.14	0.13
MgO	4.78	4.3	3.20	3.59
CaO	9.54	9.1	6.88	7.04
Na_2O	2.60	2.7	3.30	3.45
K_2O	0.68	0.43	1.29	1.42
P_2O_5	0.14	0.16	0.17	0.19
ΣH_2O	0.71	0.78	0.87	--
TOTAL	100.06	101.0	100.03	99.99

1- average island-arc basaltic andesite, from Ewart (1976)
2- average low-K orogenic basaltic andesite, from Gill (1981)
3- average island-arc pyroxene andesite, from Ewart (1976)
4- average calc-alkali andesite, from Ewart (1982)

the unit are depleted in alumina as the result of flotation of plagioclase phenocrysts from lower portions of the magma chamber. As a consequence of this mechanism, plagioclase crystals that collected at the top of the magma chamber were erupted in the lower flows of the sequence, whereas the depleted liquids in the lower portion of the chamber were subsequently erupted and deposited on top of these early flows. To test this hypothesis, densities of the magmas were calculated using the method of Bottinga and Weill (1970) assuming a temperature of 1150° C for both magmas. The magma densities calculated were 2.74 for the basaltic andesite and 2.63 for the andesite. Because the specific gravity of plagioclase (An_{45}) crystals is approximately 2.67 (Deer, Howie, and Zussman, 1966), the flotation of plagioclase feldspar crystals is a possible fractionation mechanism for the basaltic andesite, but not for the andesite.

Basaltic andesites from this unit are notably depleted in FeO_T, MgO, and CaO when compared to their average orogenic and island-arc counterparts (Table 4), but they contain somewhat higher concentrations of TiO_2 and Na_2O. These compositional differences may possibly be explained by fractionation of calcic plagioclase feldspar and pyroxenes. Andesites are comparable to the average analyses in FeO_T and Na_2O, but deficient in MgO and CaO and contain higher TiO_2.

Lower Pyroclastic Unit (Tlp)

The lower andesite unit is conformably overlain by a succession of pyroclastic rocks that includes lapilli ash-fall tuffs, tuff breccia, ash-flow

tuff, and welded tuff. This pyroclastic unit ranges from 0 to 100 meters in thickness. It is normally poorly exposed except in roadcuts and the channels of major streams. The erosional pattern of stream channels cut in the pyroclastic unit differs markedly from that in the underlying flow rocks; the former is linear and smooth whereas the latter is undulatory and irregular. Elsewhere, especially in the vicinity of the Yellowbottom Stock along Quartzville Creek (Plate 1), this unit consists of lapilli tuff that contains interbedded flows of andesite and basalt a meter or two in thickness. The lower pyroclastic unit at this location is interpreted to have been deposited by a series of pyroclastic flows that alternated with periods of lava extrusion, although deposition by lahars or hyperconcentrated streams is also a possibility.

Color of the lapilli tuffs is generally a greenish gray (5 G 6/1) as a result of chlorite and epidote replacement of the matrix. These tuffs consist of angular to rounded clasts of andesite, basalt, dacite, rhyodacite, and occasional pumice fragments in a fine-grained matrix of ash. Approximately 90 percent of the clasts are in the lapilli size range, with the remainder being cobble-sized. The clasts are non-vesicular to vesicular and generally matrix-supported. Bedding structures in this tuff are absent from outcrops and hand specimens.

The lower pyroclastic unit elsewhere in the Yellowbottom-Boulder Creek area consists of fine- to coarse-grained ash-flow tuffs which range in color from white to light olive gray (5 Y 6/1). A roadcut in the northeast quarter of Section 25 exposes a welded tuff. This tuff is a dusky yellow color (5 Y 6/4) and contains flattened lumps of pumice and broken crystals in a matrix of ash. The degree of welding is moderate.

Similar tuffs have been reported from other parts of the Quartzville District, including Red Heifer Pass (Munts, 1978).

Intermediate Andesite Unit (Tia)

The intermediate andesite unit consists of flows of andesite and basaltic andesite that are interbedded with volcanic breccias and lapilli tuffs, and andesitic lacustrine tuff. Thickness of the unit is estimated from outcrops to be 110 meters. Weathering characteristics are similar to those of the lower andesite unit, although the outcrops are generally not as massive.

The unit can be divided into two parts. The lower section consists of dense flows of aphyric to highly phyric pyroxene andesite and basaltic andesite. This lower section is well exposed along Quartzville Creek, near the center of the northern boundary of Section 29, as interbedded flows of pyroxene andesite and basaltic andesite, monolithic volcanic breccias, and lapilli tuffs. The tuffs consist of rounded fragments of various lithologies in a fine-grained ash matrix, and are greenish-gray (5 G 8/1) on both fresh and weathered surfaces. Approximately 90 percent of the clasts are in the lapilli size range, with a few fragments up to 10 centimeters in diameter. Occasional pumice fragments are also present and indicate that these rocks were deposited by the aerial accumulation of ash particles.

The upper part of the intermediate andesite unit consists of a series of light bluish gray (5 B 7/1), epiclastic, andesitic tuffs that apparently were deposited by the reworking of the underlying rocks by streams

during a hiatus in volcanic activity. These tuffs are overlain unconformably by basalts of the intermediate basalt unit, as depicted in Figure 10. Sedimentary structures that can be identified in hand specimen include graded bedding, low-angle cross-stratification, sediment slumping, and microfaulting of bedding. Some tuffs in the unit are well laminated. Rip-up clasts are present in one outcrop. One tuff bed that is exposed for about 6 meters along the bottom of Quartzville Creek near the confluence with Canal Creek, is vesiculated. Vesicles in this tuff are spherical to sub-spherical, up to 0.5 cm across, and coated with fine ash. The gas that formed these vesicles was probably steam, either derived from rain water that percolated through the still-hot ash or from water-saturated ground beneath the deposit (Fisher and Schmincke, 1984). This vesiculated tuff also contains calcite-filled cavities up to 5 centimeters in diameter.

Another variety of tuff, exposed in roadcuts in the southwest corner of Section 20, was apparently deposited by fallout of fine ash. This tuff is thinly laminated and about 1 meter thick. Accretionary lapilli up to 3 mm across are present in a fine-grained, very light gray-colored (N 8) matrix. Accretionary lapilli form when raindrops pass through eruption clouds and cause agglutination of fine ash particles to yield a spherical ball (Moore and Peck, 1962).

Petrography and Petrochemistry

Basaltic andesites from this unit display abundant phenocrysts of calcic labradorite (An_{64}), clinopyroxene, and orthopyroxene in a very fine-grained groundmass observed in thin section. Modal and chemical

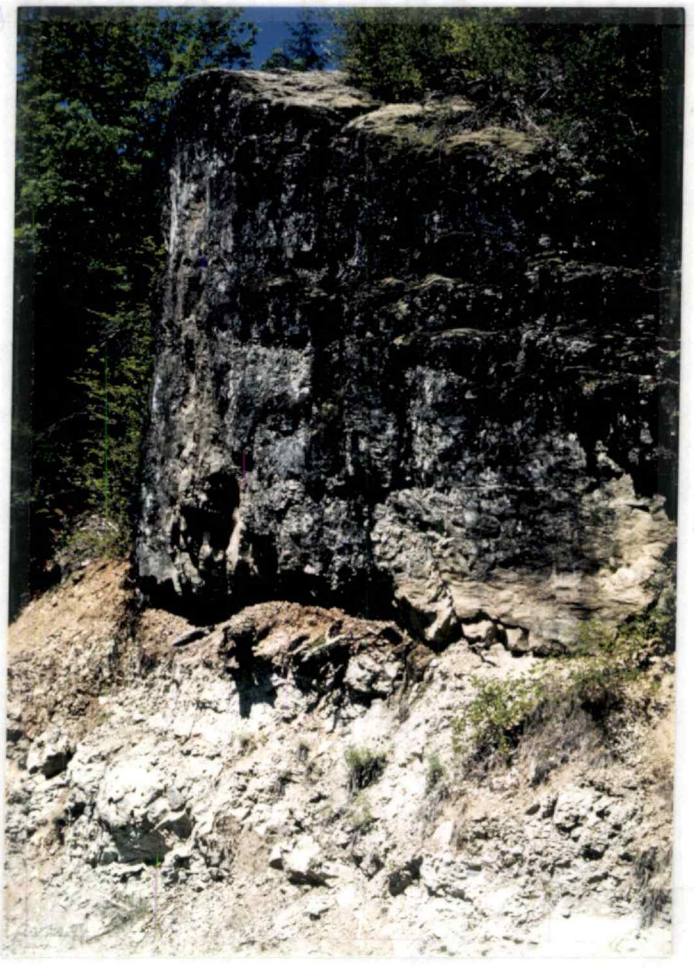

Figure 10- Contact between basalts of the intermediate basalt unit (above) and lacustrine tuffs of the intermediate andesite unit.

analyses for a single sample (TIA-11) of this rock are presented in Table 5. Phenocrysts of labradorite have been fractured and internally corroded, and are up to 2.5 mm in length. Euhedral phenocrysts of clinopyroxene are abundant and fresh in appearance. Most are about 0.3 mm in longest dimension, but a few are as large as 1 mm. Two generations of orthopyroxene phenocrysts are present. These consist of large, early orthopyroxene crystals that have been altered to an assemblage of chlorite, quartz, and epidote, and smaller (presumably later) phenocrysts that are relatively unaltered. The groundmass consists of nearly equal proportions of plagioclase feldspar microlites and brown glass, and lesser amounts of Fe-Ti oxides and accessory apatite. Alteration minerals present are chlorite, montmorillonite, epidote, quartz, and pyrite.

The chemistry of this rock (Table 5), with the exception of its higher alumina content, is remarkably similar to that of basaltic andesites of the lower andesite unit (Table 2), and other rocks of the Sardine Formation (Table 3). As was noted for rocks of the lower andesite unit, these andesites may also exhibit a strong correlation between phenocrystic plagioclase and alumina content. This sample (TIA-11) was taken from the lower part of the unit, which suggests that it was erupted from the top of the magma chamber. Accordingly, the large percentage of plagioclase phenocrysts and relatively high alumina content in this rock may be the result of accumulation of plagioclase crystals by flotation.

TABLE 5- Modal mineralogical and major oxide analyses (in percent), and metal analyses (in ppm) for a sample of basaltic andesite (TIA-11) from the intermediate andesite unit

Mineral		elemental oxide	
phenocrysts		SiO_2	54.04%
plagioclase[1]	45.3%	TiO_2	1.04
orthopyroxene[2]	4.6	Al_2O_3	18.09
clinopyroxene	6.3	Fe_2O_3	3.03
groundmass		FeO	3.96
plagioclase	19.0	MnO	0.13
glass[3]	20.0	MgO	3.40
Fe-Ti oxides	3.8	CaO	7.58
apatite	1.0	BaO	0.03
		Na_2O	3.98
		K_2O	0.75
		P_2O_5	0.39
		LOI	3.16
		TOTAL	99.58
		Metals	
		Cu	145 ppm
		Mo	<1
		Pb	18
		Zn	175
		Ag	0.5

[1]weakly altered to clay minerals
[2]moderately altered to chlorite, quartz, and epidote
[3]devitrified

Intermediate Basalt Unit (Tib)

Unconformably overlying lacustrine tuffs at the top of the intermediate andesite unit are interbedded basalt flows and volcanic breccias, and dacite flows, of the intermediate basalt unit (see Figure 10). These rocks are comparatively well-exposed, and form outcrops on steep slopes as well as in roadcuts and streams. Thicknesses average 125 meters, with a maximum of about 150 meters in the northern part of the Yellowbottom-Boulder Creek area. Float is better preserved than that from other rock units in the area, and is a useful aid in mapping. The intermediate basalt unit is also identified by a pervasive hackly fracturing, which is common to all lithologies. This fracturing tends to break the rocks into irregular-shaped fragments up to 10 cm across.

Basalts of the sequence are very dense, nearly aphyric, and medium dark bluish-gray in color (5 B 4/1). As was noted for the basaltic andesites of Packers Gulch, they contain stringers and veinlets of quartz despite a generally low intensity of alteration. The best exposures of these rocks are near the confluence of Quartzville and Canal Creeks and along the lower portion of Canal Creek. Basalt flows at the confluence area contain a prevalent joint set that strikes N 11° W and parallels the course of Canal Creek, which suggests that structure may play a role in the development of the drainage patterns of the area. This location is also one of the few areas in the Quartzville area where the attitude of rocks can be readily observed and measured. The top of a basalt flow exposed in the bed of Quartzville Creek strikes N 23° E and dips 18° SE.

Volcanic breccias are interbedded with the basalt flows in the lower three-quarters of the unit. These clast-supported breccias consist of angular fragments of basalt, dacite, andesite, and rhyodacite in a fine-grained matrix. These breccias average 5 meters in thickness and commonly appear reddish in color as a result of oxidation.

Basalt flows of this unit also form the "Temple", a beautiful swimming hole along Quartzville Creek bordered by towering outcrops of basalt, as shown in Figure 11. A large block of rock has been downdropped along a series of right-stepping faults at this location, presumably in association with the emplacement of the Yellowbottom Stock.

Dacite flows comprise the upper part of the unit, and are best exposed in the center of Section 20. These rocks are very fine-grained and exhibit flow-banding of alternating white and light bluish gray (5 B 7/1) material. A pervasive lamination gives these flows the appearance of tuffs in the field.

Petrography and Petrochemistry

Samples representing a basalt flow at the confluence of Canal Creek and Quartzville Creek and the dacite flow from Section 20 were examined in thin section. Modal mineralogical analyses of these rocks are given in Table 6.

Basalt sample TIB-1 consists of phenocrysts of calcic labradorite (An_{64}), and euhedral microphenocrysts of clinopyroxene, in a fine-grained, pilotaxitic groundmass dominated by calcic andesine (An_{45}) microlites and volcanic glass, as shown in Figure 12. Phenocrysts of plagioclase display corroded outlines indicating partial resorption, are

Figure 11- Wall of the "Temple", a towering outcrop of basalt along Quartzville Creek formed by faulting.

TABLE 6- Modal mineralogical analyses (in percent) for samples of basalt (TIB-1) and dacite (TIB-121) from the intermediate basalt unit

Sample #	TIB-1	TIB-121
phenocrysts		
plagioclase[1,2]	18.5%	14.4%
clinopyroxene[3]	0.7	--
Fe-Ti oxides	--	0.5
groundmass		
quartz	tr.	--
orthoclase	--	5.0
plagioclase[2]	65.0	10.0
clinopyroxene[3]	10.0	--
Fe-Ti oxides	3.0	1.0
glass	2.5	65.5
apatite	acc.	--
pyrite[4]	--	3.6

[1]weakly altered to clays (TIB-1)
[2]completely altered to sericite, quartz, and clays (TIB-121)
[3]weakly altered to chlorite and epidote
[4]hydrothermal origin

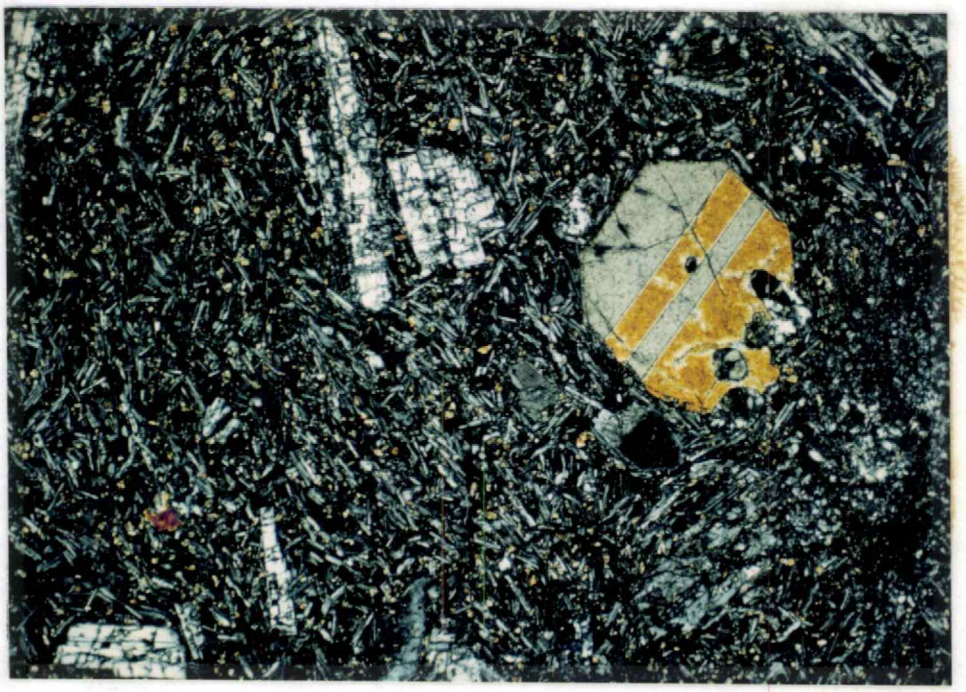

Figure 12- Photomicrograph of basalt sample TIB-1 (crossed polars). Width of field is 3.3 mm.

frequently broken, and are up to 1.5 mm in length. Phenocrysts of clinopyroxene are up to 0.8 mm across and have sharp outlines, which indicates that they apparently remained stable during the resorption event. Orthopyroxene phenocrysts formed twice during the crystallization history of this rock. The first phase produced large phenocrysts which were subsequently altered to chlorite, epidote, and quartz, whereas crystals of the later phase are smaller and nearly unaltered.

The groundmass consists of nearly equal proportions of glass and andesine microlites that average 0.1 mm in length. Interstitial to the microlites are equant crystals of clinopyroxene and rounded Fe-Ti oxides that average 0.05 mm in diameter. Other minerals present in trace amounts include quartz and apatite.

Alteration is of low intensity and consists mainly of the replacement of mafic phenocrysts by chlorite, epidote, and montmorillonite. Additionally, a few thin veinlets of quartz cut this specimen. Major oxide analyses of intermediate basalt unit rocks are presented in Table 7. As compared to an average of quartz normative basalts, sample TIB-1 is deficient in FeO_T, MgO, TiO_2, and K_2O, and contains excess Al_2O_3.

A second more-altered basalt sample (TIB-24) was also examined. This rock is finer grained, aphyric, exhibits a trachytic texture of plagioclase feldspar microlites in a glassy matrix, and also contains abundant, rounded Fe-Ti oxides in the groundmass. It exhibits a higher alteration intensity than other rocks of the confluence area, as several generations of veinlets cut the thin section. The quartz veinlets formed first and are associated with areas of quartz replacement of the

TABLE 7- Major oxide (in percent) and metal (in ppm) analyses for samples of basalt (TIB-1) and dacite (TIB-121) from the intermediate basalt unit

Elemental oxide	TIB-1	TIB-121	ave. basalt[1]	ave. dacite[2]
SiO2	50.96%	64.78%	51.6%	65.01%
TiO2	1.05	0.85	1.6	0.58
Al2O3	17.46	15.51	16.4	15.91
Fe2O3	2.77	2.36	3.2	2.43
FeO	4.67	1.90	7.4	2.30
MnO	0.13	0.16	0.17	0.09
MgO	4.72	1.40	5.6	1.78
CaO	9.59	1.58	9.8	4.32
BaO	0.06	0.09		
Na2O	2.99	4.06	2.5	3.79
K2O	1.48	3.32	0.8	2.17
P2O5	0.41	0.35	0.21	0.15
LOI	1.68	2.54		
Σ H2O + CO2			0.7	1.25
Metals				
Cu	40 ppm	12 ppm		
Mo	<1	6		
Pb	5	19		
Zn	20	50		
Ag	< 0.3	0.4		

[1]Average of 715 quartz normative basalts, from Manson (1967)
[2]Data from Le Maitre (1976b)

groundmass. These veinlets are cut by two generations of epidote veinlets, which are in turn cut by yet a later set containing calcite. These veinlets may have had different origins. For example, the quartz veinlets may have been formed by heated groundwaters that leached silica from volcanic glasses and redeposited it along fractures, whereas the later epidote and calcite veinlets may have formed during hydrothermal alteration processes associated with the emplacement of nearby intrusive rocks.

Dacite flows from the upper part of the sequence display a trachytic texture in thin section. Phenocrysts of plagioclase feldspar up to 2 mm in length and fewer phenocrysts of Fe-Ti oxides are contained in a matrix of devitrified glass, sparse plagioclase microlites, and Fe-Ti oxides. Phenocrysts of plagioclase feldspar are aligned along a preferred orientation that coincides with the color-banding observed in hand specimen, and are euhedral, unbroken, and display sharp outlines. Pyrite cubes are aligned along fractures that also parallel this preferred direction. The presence of foliation suggests that the dacite may possibly be pyroclastic in origin. However, the preferred interpretation of this foliation is that it represents a primary trachytic flow texture upon which subsequent hydrothermal fracturing and mineralization was superimposed.

The sample of dacite has been altered to a phyllic-argillic assemblage of sericite, kaolinite, quartz, chlorite, montmorillonite, and pyrite. Alteration makes determination of the plagioclase feldspar compositions impossible, although the high Na_2O content of the rock suggests that the mineral may be as sodic as oligoclase or albite.

Dacite sample TIB-121 contains abundances of the major oxides similar to those of the average dacite (Table 7). Notable exceptions are CaO, which is depleted, and K_2O, which is enriched. These changes may be the result of hydrothermal alteration of plagioclase. The formation of sericite requires the addition of potassium and the concomitant leaching of calcium from the plagioclase feldspar. Alternatively, this rock may represent a derivative of the basalts from lower in the unit. Fractional crystallization of calcic plagioclase feldspar is likely to enrich the remaining melt in Na_2O and K_2O and deplete it in CaO. Phenocrysts of plagioclase in the basaltic rocks are significantly more calcic than plagioclase feldspar microlites of the groundmass, and may indicate that the dacites were derived by fractional crystallization of the earlier basaltic magma.

Upper Pyroclastic Tuff Unit (Tupt)

This unit consists of a sequence of ash-flow tuffs, lapilli tuff, tuff-breccia, volcaniclastic breccia, and local interbedded basalt flows. Thicknesses are variable and are estimated to range from 90 to 150 meters. Exposures are poor and are confined mostly to roadcuts and streambeds. This unit displays the greatest variety of lithologies in the northeast corner of the Yellowbottom-Boulder Creek area. In Section 20, thin aphyric basalt flows are interbedded with a coarse-grained, greenish-gray colored (5 G 6/1) volcaniclastic breccia that has been called an agglomerate (Berg, 1961). This deposit contains rounded clasts of dacite, rhyodacite, andesite, and pumice in a matrix of fine- to coarse-

grained ash. The largest clasts are approximately 7 centimeters in diameter.

A laminated ash-fall tuff is exposed along the crest of the ridge in the center of Section 20. This tuff is very fine-grained, white on weathered surfaces, and very light gray (N 8) on fresh surfaces. The laminae, which average 5 centimeters in thickness, follow the undulations in the topography, which suggests that the deposit originated as a fall of pyroclastic material (Fisher and Schmincke, 1984).

Elsewhere in the Yellowbottom-Boulder Creek area, this unit consists of a moderately thick sequence of coarse-grained ash-fall and ash-flow tuffs. These tuffs are laminated, pale yellowish-brown (10 YR 6/2) in color, and display variable alteration. Epidote is the most common alteration product. The best exposure of these rocks is along the Boulder Creek access road in the center of Section 31. The tuffs at this locality break into slabs which range from 5 to 25 cm in thickness, and exhibit a wavy pattern of sideromelane glass shards that suggests a hydroclastic origin (Fisher and Schmincke, 1984). Color banding is evident on fresh surfaces and consists of laminae of light olive-gray (5 Y 5/2) (altered) and very light gray (N 8) (unaltered) tuffs.

Elsewhere in the study area, tuffs of the Tupt unit contain some broken crystals and pumice fragments up to 4 centimeters in diameter, especially near the top of the unit as exposed along the ridge near the north edge of Section 31. The rounded pumice indicates that these rocks were deposited by pyroclastic flows (Fisher and Schmincke, 1984). These deposits grade upward into lapilli tuffs, as exposed to the west of the

diorite outcrop in the southern part of Section 31 and along the eastern edge of Section 29.

Upper Pyroclastic Unit (Tup)

The upper pyroclastic unit is composed of extensive flows of laharic breccias that are overlain by epiclastic tuffs, and it exceeds 300 meters in thickness. The base of the unit is exposed along the ridge at the south edge of Section 30 and is placed at the first occurrence of laharic breccia above the Tupt tuffs. Laharic breccias of the Quartzville area consist of angular to rounded clasts of andesite, basalt, dacite, rhyodacite, and less commonly intrusive rocks, in a fine-grained matrix. Large blocks of autobrecciated andesite and volcanic breccias, and minor fragments of pumice, are also present. These lahars weather to flat, friable surfaces which parallel the topography. Carbonaceous material was not observed in these lahars.

Two units having different colors are present; one is greenish gray (5 G 6/1) and the other light brown (10 YR 6/4). Clasts range from a few millimeters to several meters in diameter, and some display features of weathering formed before incorporation into the lahar. Andesite clasts with well-developed weathering rinds up to 2.5 centimeters thick were observed along the road in the center of section 32.

These lahars are not confined to channels, but mantle steep slopes all over the Quartzville district. Most lahars of Pleistocene- Recent time are limited in extent and have been deposited in valleys or lowlands adjacent to volcanic centers. However, several examples are known of Tertiary

lahars which cover thousands of square kilometers, including some in the southern Cascade Range (Fisher and Schmincke, 1984). Collapse of crater walls and (or) failure of rain-soaked debris on steep volcanic slopes are the most likely causes of the lahars in the Quartzville area.

The upper part of the unit is composed of a sequence of epiclastic, andesitic tuffs that are best exposed in the headwall area of the easternmost cirque along Boulder Creek. These tuffs display poorly-defined normal graded bedding over a stratigraphic interval of about one meter. Most of the fragments are silt and sand-sized material, although some clasts are as large as 1.5 cm in diameter.

Reworking of the Tupt and lower Tup deposits by stream erosion and subsequent redeposition in local basins produced these water-laid tuffs, which are present throughout the Quartzville area. The widespread distribution and apparent lack of pyroclastic fragments within the tuffs suggest that a period of quiescence prevailed between the time of deposition of lahars of the Tup unit and the eruption of Pliocene basalt flows that cap Galena Ridge. These tuffs, as exposed in the Yellowbottom-Boulder Creek area, now dip to the southeast at about 20 degrees, presumably because of post-epiclastic sedimentation folding.

Rhyodacite Unit

A rhyodacite flow that is mantled by rhyodacitic ash-fall tuff is exposed over a small area along the north slope of Galena Ridge. The rhyodacite is yellowish-gray (5 Y 8/1) in color, highly fractured, and contains rounded phenocrysts of quartz. This rock also displays

Liesegang rings which are thought by some investigators to represent the fronts of advancing alteration solutions. The tuff is a pure white, aphyric, soft rock that has been strongly altered, mostly to clay minerals, and contains dissolution pits after former sulfides and (or) plagioclase.

These siliceous volcanics presumably are correlative with the rhyodacite unit exposed along ridge crests in the central portion of the Quartzville District as mapped by Munts (1978).

Petrography and Petrochemistry

Thin sections of the rhyodacite, as shown in Figure 13, display phenocrysts of calcic oligoclase (An_{28}), quartz, biotite, and orthoclase in a felsitic groundmass of plagioclase feldspar microlites, spherulites, clinopyroxene, quartz, orthoclase, and Fe-Ti oxides. The modal mineralogy of this sample (I-123) is given in Table 8.

Oligoclase phenocrysts are up to 3 mm in length and are rounded. Microphenocrysts of oligoclase, in contrast, have sharp outlines and are clustered together as glomerocrysts. Phenocrysts of quartz are up to 3 mm in diameter, have been rounded by resorption, are mantled by a reaction rim of orthoclase, and exhibit complex extinction patterns. A few orthoclase phenocrysts are present, as revealed by cobalt-nitrate staining of hand specimens. Phenocrysts of biotite measure up to 1 mm in the longest dimension. The presence of biotite in these rocks makes them unique to the Quartzville area. Argillic-phyllic alteration has affected most of the remaining primary constituents, and has led to the growth of clay minerals, sericite, and pyrite.

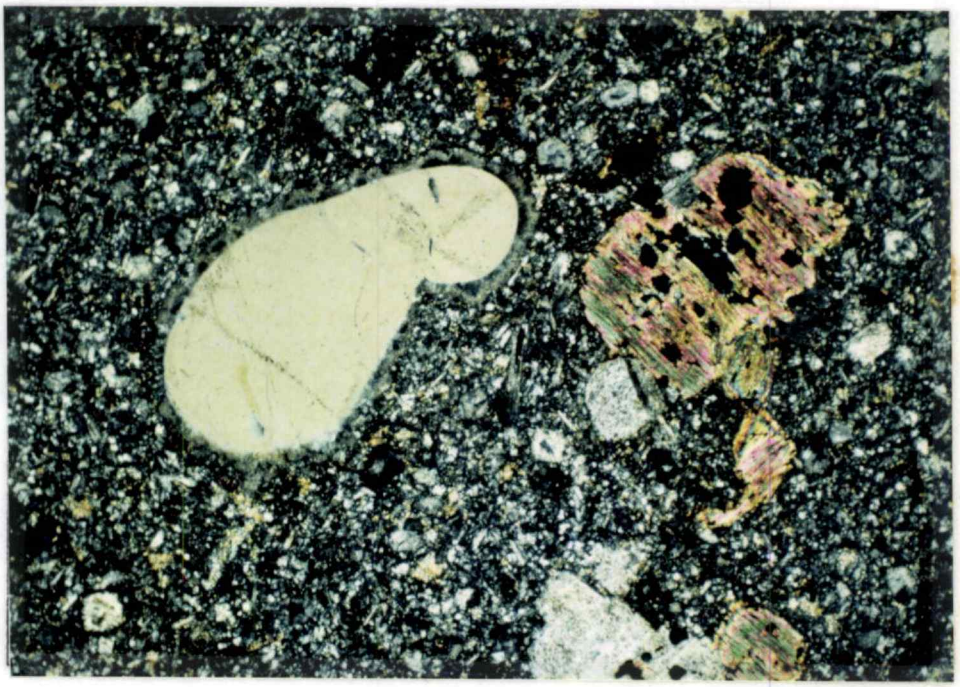

Figure 13- Photomicrograph of rhyodacite sample I-123 (crossed polars). Width of field is 3.3 mm.

TABLE 8- Modal mineralogical analyses (in percent) for a sample of the rhyodacitic dome (I-123)

phenocrysts	
quartz	4.0%
orthoclase	1.0
plagioclase[1]	11.7
biotite	1.3
groundmass	
quartz	1.0
orthoclase	10.0
plagioclase microlites[2]	49.0
clinopyroxene[3]	11.0
Fe-Ti oxides	1.0
glass	10.0

[1]moderately altered to sericite and clays
[2]weakly altered to sericite and clays
[3]moderately altered to chlorite

Petrographically, the tuff displays a clastic texture with grains of plagioclase feldspar, quartz, orthoclase, and Fe-Ti oxides. Some lighter-colored spots may represent ghosts of shattered plagioclase feldspar crystals, but this interpretation is uncertain because of the complete replacement of the primary minerals by clays, calcite, sericite, and epidote.

The rhyodacite was presumably emplaced as a dome and therefore sample I-123 is classified on the basis of modal mineralogy using the same diagram on which the intrusive rocks are defined (Figure 15). Although by this method the rock is classified as a quartz monzodiorite (andesite), it is likely that potassium feldspar and quartz are underestimated in the modal analysis. Staining of a slab of this sample with cobalt nitrate revealed significant quantities of potassium feldspar in the groundmass, as well as several phenocrysts of orthoclase.

Pliocene Volcanic Rocks

Flows of olivine basalt cap Galena Ridge, and clasts of this basalt are present in glacial till throughout the Boulder Creek drainage. These rocks are dark gray (N 3), vesicular, and diktytaxitic in texture. They are considered to be basal flows of the Early High Cascade episode (Priest et al., 1983; Munts, 1978; Berg, 1961). A sequence of andesite flows which cover a large area bordering the northwest corner of the Yellowbottom-Boulder Creek area are thought to be of the same age. Similar rocks also are present as two small plugs that intrude andesites of the lower andesite unit in the Packers Gulch area. Both the basalt and andesite

flows display columnar jointing, which has not been reported in compositionally similar units of the Sardine Formation, and are less altered than other rocks of the area.

These basalt and andesite flows overlie the Miocene section along an angular unconformity. In hand specimen, the andesite flows of the Packers Divide area display large phenocrysts of plagioclase feldspar set in a dense, dark gray (N 3), glassy groundmass.

Petrography and Petrochemistry

A thin section of andesite (sample Q-66) from Packers Divide was selected to represent the Pliocene volcanic rocks. Modal and chemical analyses of this rock are presented in Table 9. The andesite typically contains phenocrysts of calcic andesine (An_{44}), clinopyroxene, orthopyroxene, and Fe-Ti oxides are contained in a hyalopilitic groundmass of brown glass, calcic andesine (An_{45}) microlites and crystallites, and rounded crystals of Fe-Ti oxides. The phenocrysts of andesine are up to 5 mm in length, partially resorbed, and display well-developed compositional zoning. They are commonly clustered together with clinopyroxene forming glomerocrysts which range up to 8 mm across. Phenocrysts of clinopyroxene are euhedral and range up to 1.7 mm in diameter. One euhedral phenocryst of oxyhornblende was also observed, and is portrayed in Figure 14. The presence of oxyhornblende indicates that oxidizing conditions were prevalent at the time of crystallization (Nesse, 1986, p. 220); a not unexpected environment for lavas.

Microlites of andesine in the groundmass average 0.1 mm in length, and are randomly distributed in a matrix of brown glass. Other

TABLE 9- Modal mineralogical and major oxide analyses (in percent), and metal analyses (in ppm) for a sample of Pliocene andesite (Q-66)

Mineral		elemental oxide	
phenocrysts		SiO_2	61.59%
plagioclase	25.1%	TiO_2	0.73
orthopyroxene	4.9	Al_2O_3	15.77
clinopyroxene	5.6	Fe_2O_3	3.16
groundmass		FeO	2.03
plagioclase[1]	12.0	MnO	0.11
glass	48.3	MgO	2.55
Fe-Ti oxides	3.1	CaO	5.02
apatite	1.0	BaO	0.07
		Na_2O	3.76
		K_2O	2.13
		P_2O_5	0.29
		LOI	1.71
		TOTAL	98.92
		Metals	
		Cu	35 ppm
		Mo	<1
		Pb	8
		Zn	50
		Ag	< 0.3

[1] calcic cores selectively altered to chlorite and clay minerals

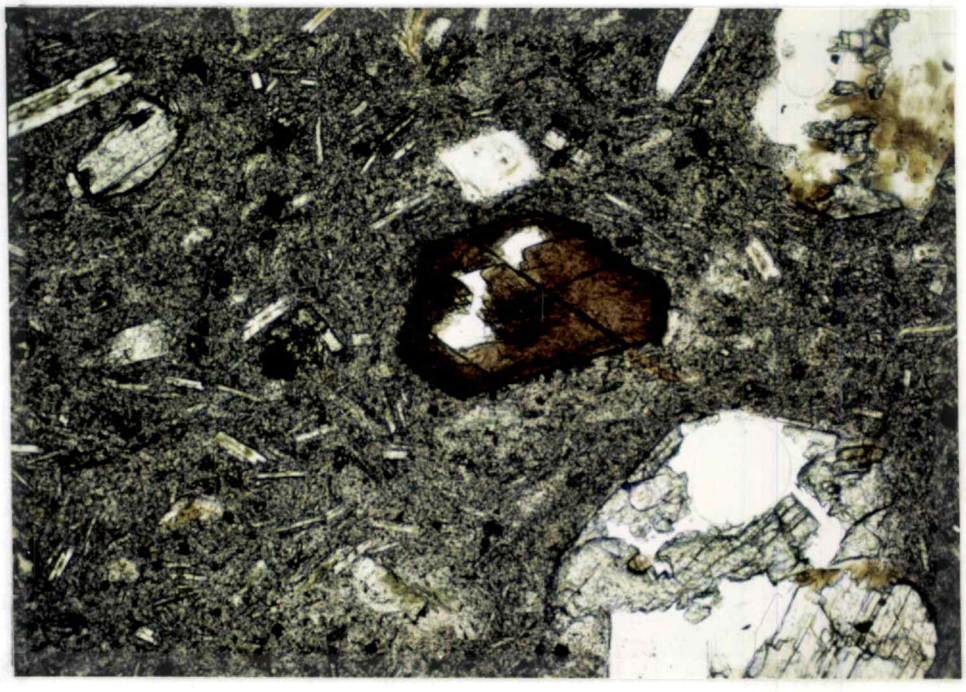

Figure 14- Photomicrograph of an oxyhornblende phenocryst in andesite sample Q-66 (plane light). Width of field is 1.3 mm.

groundmass constituents include plagioclase feldspar crystallites and rounded blebs of Fe-Ti oxides. Alteration intensity in this sample, and in related exposures of this rock type, is low, and consists mainly of the conversion of andesine to chlorite and epidote. This alteration has preferentially attacked the cores of smaller andesine phenocrysts that presumably were unstable because of their higher anorthite content.

The correlation of these flows is problematic. Chemically, sample Q-66 is nearly identical to andesites from the lower andesite unit (compare Table 9 to Table 2). Rocks from the early High Cascade episode, as defined by Priest et al. (1983), are dominantly basalt and basaltic andesite in composition and contain higher total-iron content than this sample shows. Additionally, rocks of High Cascade affinity may be expected to contain relatively high concentrations of P_2O_5, on the order of a full percent (Munts, 1978), and BaO (~0.35%), in contrast to the lower values (0.29% P_2O_5; 0.07% BaO) obtained for sample Q-66. However, these flows overlie the other volcanic units of the area along an angular unconformity, which clearly suggests that a considerable time interval elapsed between deposition of the Tup epiclastic tuffs and the rocks in question. The columnar jointing and unaltered nature of these flows is also dissimilar to units of the Sardine Formation as exposed elsewhere in the Quartzville district.

Quaternary Basalts

A single flow of olivine basalt partially fills the valley of Canal Creek along the eastern edge of the Yellowbottom-Boulder Creek area and

extends into Dry Gulch. The top of this flow forms a large topographically flat surface that is discernable on topographic maps. Because it fills a contemporary canyon, it is presumed to be Quaternary in age.

This basalt is medium light gray (N 6), contains small phenocrysts of olivine, and forms well-developed columns. The pattern of columnar jointing can be observed in a quarry along Canal Creek road, about one kilometer north of the Quartzville Access Road. Two cinder cones exposed in nearby roadcuts are possibly associated with this flow. These cinder cones are located in sections 21 and 22 of T 11 S, R 4 E, approximately 0.5 and 1 kilometer, respectively, from the eastern edge of the map area. They are the youngest volcanic features of the Quartzville District. Their age has been estimated as 10,000 years by Munts (1978), who stated that one of the cinder cones overlies glacial till thought to be between 10,000 and 12,000 years old (Williams, 1969).

Petrography and Petrochemistry

Petrographically, this basalt consists of euhedral phenocrysts of olivine in a groundmass of plagioclase feldspar microlites, clinopyroxene, Fe-Ti oxides, and minor apatite. Modal proportions of these phases and a chemical analysis are given in Table 10.

Two size populations of olivine and Fe-Ti oxides are present, which suggests that the magma resided in a shallow magma chamber for some time prior to eruption. The largest of the olivine crystals is 2.3 mm across. Vesicles are abundant and account for 14 percent of the rock volume. Minor alteration has affected this rock, the main products being

TABLE 10- Modal mineralogical and major oxide analyses (in percent), and metal analyses (in ppm) for a sample of Quaternary basalt (Q-27)

Mineral		elemental oxide	
phenocrysts		SiO_2	48.10%
olivine[1]	9.7%	TiO_2	1.47
Fe-Ti oxides	1.5	Al_2O_3	13.81
clinopyroxene	0.7	Fe_2O_3	5.35
groundmass		FeO	2.02
plagioclase	48.0	MnO	0.11
glass	0.6	MgO	9.40
Fe-Ti oxides	4.3	CaO	9.93
clinopyroxene	35.0	BaO	0.36
apatite	acc.	Na_2O	2.79
		K_2O	2.79
		P_2O_5	1.12
		LOI	0.93
		TOTAL	98.18
		Metals	
		Cu	20 ppm
		Mo	<1
		Pb	6
		Zn	30
		Ag	< 0.3

[1]weakly altered to iddingsite along fractures

chlorite and montmorillonite after plagioclase feldspar, and iddingsite along fractures in olivine phenocrysts.

This rock is classified as a trachybasalt on the total alkali-silica diagram (Figure 9). It is nepheline-normative (Appendix A) and thus slightly alkalic in nature. However, the composition of this basalt does not show great similarity to that of the average trachybasalt, as given in Table 11. Average trachybasalt analyses contain more FeO_T, Al_2O_3, and TiO_2, and much less MgO and CaO than the basalt from Canal Creek. When compared to the other averages presented in Table 11, the olivine basalt from Canal Creek is most closely similar to a low-Al transitional basalt, with the exception of deficiencies in TiO_2 and FeO_T.

A distinguishing chemical parameter of this and other rocks of Quaternary age in the area is the presence of high concentrations of P_2O_5 and BaO. Other trace metals, including Cr, Ni, and Co, are also anomalously enriched in these rocks, as revealed in an exploration soil-geochemistry survey performed by Orvana Resources Corporation (I. Thomson, Jan. 1988, personal communication).

TABLE 11- Average major element compositions of alkalic and transitional basaltic rocks

	1	2	3	4
SiO_2	48.6%	49.21%	46.51%	47.30%
TiO_2	1.7	2.40	2.63	2.41
Al_2O_3	15.5	16.63	13.32	13.85
Fe_2O_3	2.6	3.69	1.98	1.98
FeO	8.7	6.18	9.90	9.91
MnO	0.17	0.16	0.17	0.40
MgO	8.4	5.17	9.85	9.51
CaO	10.3	7.90	11.16	10.89
Na_2O	2.3	3.96	2.63	2.02
K_2O	0.6	2.55	0.80	1.31
P_2O_5	0.23	0.59	0.36	0.42
ΣH_2O	0.9	1.47	--	--
TOTAL	100.0	99.91	99.31	100.0

1 - average olivine tholeiite, from Manson (1967)

2- average trachybasalt, from Le Maitre (1976b)

3- average low-Al alkali basalt, from Wilkinson (1986)

4- average hypersthene-bearing, low-Al transitional basalt, from Wilkinson (1986)

INTRUSIVE ROCKS

Intrusive rocks of the Yellowbottom-Boulder Creek area are dikes, plugs, and small stocks of basaltic to granitic composition. Some of these bodies are probably hypabyssal equivalents of the volcanics. The largest intrusive body in the study area is a quartz monzodiorite stock that covers approximately 0.5 km^2 and for which the informal name Yellowbottom Stock is proposed. Outcrops of this stock are best exposed along Quartzville Creek immediately east of Yellowbottom Campground for a distance of several hundred meters. Several other dikes and small stocks of intermediate composition are present elsewhere in the study area. Compositions show these intrusions to include diorite, quartz monzodiorite, quartz monzonite, and tonalite, as portrayed in Figure 15. Other intrusions range in composition from basaltic (three mafic plugs near Yellowstone Creek), to rhyolitic. Small plugs and dikes of andesitic, basaltic, dacitic, rhyodacitic, and rhyolitic composition are also present within the area. A portion of Quartzville Creek, extending from the outcrop of the Yellowbottom Stock for a distance of 0.8 kilometer to the west, exposes a swarm of dikes thought to be associated with the emplacement of the stock. This swarm incorporates dikes of basaltic, andesitic, and dacitic compositions that are aligned N 20° W and dip northeast at 60-70 degrees. A pervasive joint set in the host andesite flows parallels these dikes, and narrow linear zones of argillic-phyllic alteration are present in the host between some of these dikes.

Most of the intrusions appear to be similar or slightly younger in age than the volcanic host rocks, but some, especially the mafic dikes, may

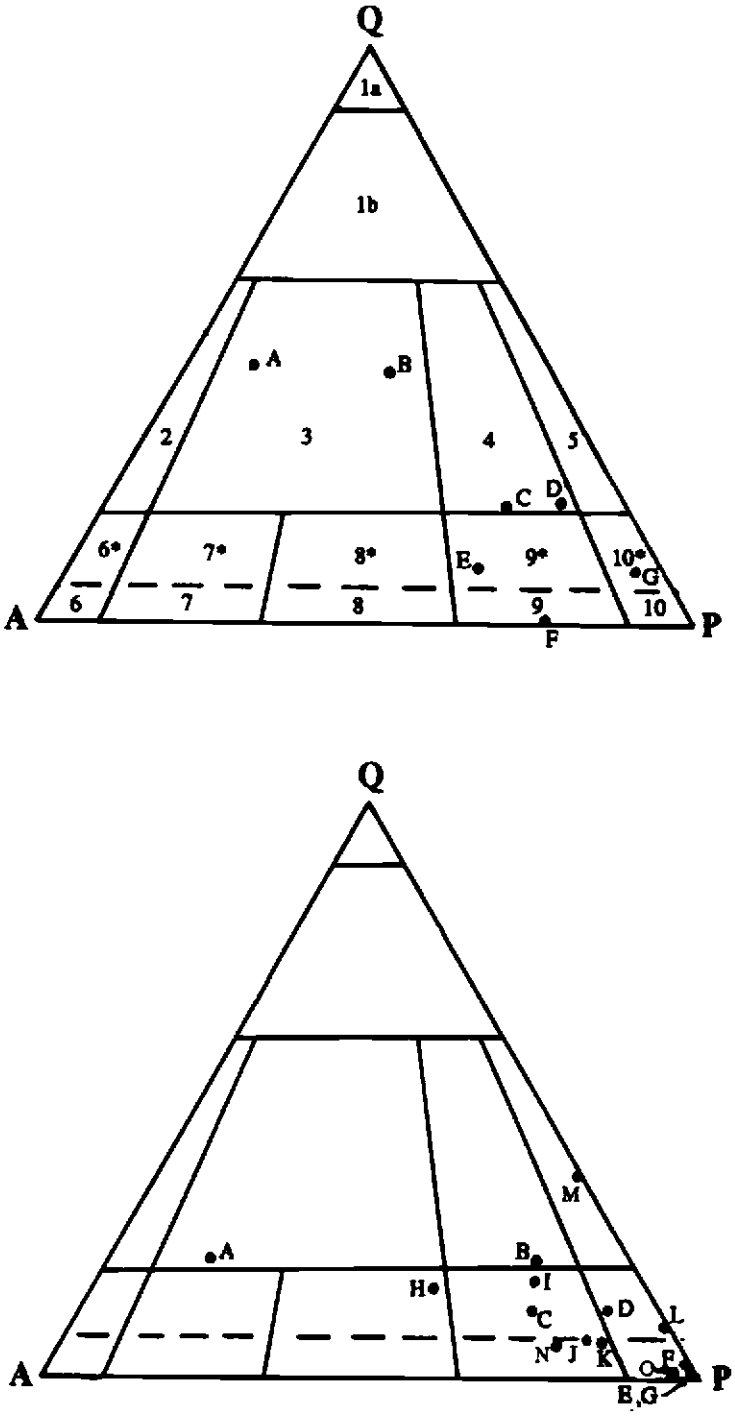

EXPLANATION

Apices:

Q- Quartz
A- Alkali-feldspar
P- Plagioclase

Nomenclature:

1a- Quartzolite
1b- Quartz-rich granitoids
2- Alkali-feldspar granite
3- Granite
4- Granodiorite
5- Tonalite
6*- Alkali-feldspar quartz syenite
7*- Quartz syenite
8*- Quartz monzonite
9*- Quartz monzodiorite/quartz gabbro
10*- Quartz diorite/quartz gabbro/ quartz anorthosite
6- Alkali-feldspar syenite
7- Syenite
8- Monzonite
9- Monzodiorite/monzogabbro
10- Diorite/gabbro/anorthosite

Rock samples:

A- I-18
B- I-111
C- I-14
D- I-33
E- I-42
F- I-29
G- I-59
H- I-101
I- I-21
J- I-123
K- I-142
L- I-92
M- I-151
N- I-17
O- I-147

Figure 15- IUGS classification of intrusive rocks from the study area, based on normative mineralogy (top), and modal mineralogy (bottom).

be Pliocene or Quaternary, as indicated by their lack of intense alteration and localization along fault zones.

Diorites and Related Rocks

The Yellowbottom Stock is a coarse-grained, porphyritic quartz monzodiorite that has a salt-and-pepper appearance in outcrop. It is the largest intrusive body in the Quartzville area. The best exposures of the stock are along Quartzville Creek, immediately east of Yellowbottom Campground, and along the road north of this area in the southwest corner of Section 20. Several other dioritic intrusives in the immediate vicinity, including the large body exposed in the center of Section 19, are compositionally similar, and may in fact be part of the same pluton and merge with it at depth.

Intruded into the quartz monzodiorite are aphyric dikes of a light bluish gray (5 B 7/1) dacite, which range from a few centimeters to 2 meters in width. The emplacement of these dikes was controlled by pre-existing fractures in the pluton. The dacitic magma forced its way along small fractures in the rock and the resultant dikes thus may diverge at right-angles along intersecting fractures. This behavior indicates that magma forming the dikes was extremely fluid when injected into the main phase of the stock. Contacts between the dacite and quartz monzodiorite are sharp, but in places exhibit cuspate borders. This feature suggests that the quartz monzodiorite was largely solidified, but hot, when the dacitic dikes were emplaced.

A single granophyric dike was also observed in this stock. It is exposed along the road above the stream exposures, but cannot be traced into the creek. This dike is described in the section of this chapter entitled "Granophyric Dikes".

Small plugs and dikes of intermediate composition are present elsewhere in the map area and are locally associated with argillic-phyllic alteration over a short distance. One plug, exposed in the SE1/4 Section 31 in the Boulder Creek drainage, appears to have been injected along a fault zone. It is cut by a vein that contains drusy quartz and abundant jarosite as coatings. This vein was assayed at 580 ppb gold, 5.5 ppm silver and 50 ppm molybdenum.

A tonalite dike is exposed along the Boulder Creek road near the boundary between R. 3 E. and R. 4 E. This dike is 75 meters wide and badly weathered, as a consequence of intense argillic-phyllic alteration caused by hydrothermal activity that perhaps was related to the emplacement of this or other dikes in the area.

Petrography and Petrochemistry

The Yellowbottom quartz monzodiorite stock consists of phenocrysts of plagioclase feldspar and hornblende set in a seriate-textured matrix of plagioclase feldspar, quartz, orthoclase, Fe-Ti oxides, and minor accessory apatite. Modal mineralogy and chemical analysis of this rock are presented in Table 12.

Phenocrysts of plagioclase feldspar are euhedral and up to 7 mm in length. Many have been altered to an assemblage of sericite, kaolinite,

TABLE 12- Modal mineralogical and major oxide analyses (in percent), and metal analyses (in ppm) for a sample of quartz monzodiorite from the Yellowbottom Stock (I-14)

Mineral		oxide	I-14	ave. monzonite[1]
phenocrysts		SiO_2	61.45%	62.60%
plagioclase[2]	32.3%	TiO_2	0.80	0.78
hornblende[3]	10.6	Al_2O_3	15.11	15.65
		Fe_2O_3	2.48	1.92
groundmass		FeO	2.45	3.08
quartz	10.0	MnO	0.08	0.10
orthoclase	16.0	MgO	2.65	2.02
plagioclase	30.0	CaO	4.46	4.17
Fe-Ti oxides	1.0	BaO	0.08	--
apatite	acc.	Na_2O	3.88	3.73
		K_2O	2.46	4.06
		P_2O_5	0.29	0.25
		LOI	1.57	1.17
		TOTAL	97.76	99.53
		Metals		
		Cu	12 ppm	
		Mo	1	
		Pb	4	
		Zn	30	
		Ag	< 0.3	

[1]average monzonite from Le Maitre (1976b)

[2]moderately altered to sericite, clays, and epidote

[3]completely altered to chlorite, calcite, epidote, and pyrite

epidote, and pyrite. This alteration has made the optical determination of plagioclase feldspar compositions largely impossible.

Hornblende (?) phenocrysts are up to 3 mm long. Hydrothermal alteration has replaced all of the hornblende (?) with aggregates of chlorite, calcite, epidote, and pyrite, which has imparted a greenish cast to the rock. This alteration has rendered the sample unsuitable for K/Ar dating, which had been one of the original objectives of the thesis.

The groundmass consists of anhedral crystals of quartz, alkali and plagioclase feldspars, apatite and Fe-Ti oxides. Much of the groundmass has a seriate texture, whereas other portions are very fine-grained and consist of a cotectic mixture of quartz and alkali feldspar.

As compared to the average monzonite of Le Maitre (1976b), the rocks from the Yellowbottom Stock are deficient in K_2O and contain more Fe_2O_3, but similar FeO_T (Table 12). The apparent deficiency in K_2O may be the result of using a monzonite for the comparison instead of a quartz monzodiorite (monzonites plot closer to the alkali-feldspar apex of the IUGS classification diagram).

Several other intermediate intrusives were examined in thin section, and their modal analyses are given in Table 13. All have phenocrysts of plagioclase feldspar in varying proportions. Textures range from seriate to porphyritic. All have been strongly altered, with the exception of one diorite dike exposed along Canal Creek at the east margin of the study area.

The tonalite is unusual in that it contains blebs of pyrite within phenocrysts of quartz. This pyrite has the appearance of droplets within the quartz, although less commonly elsewhere the sulfides may be

Table 13- Modal mineralogical analyses of intermediate intrusive rocks

sample #	I-17[1]	I-147[2]	I-151[3]
phenocrysts			
quartz	1.8%	--	35.1%
plagioclase	31.9	31.1%	60.4
clinopyroxene	5.9	4.0	0.9
orthopyroxene	--	5.7	--
Fe-Ti oxides	0.7	--	--
pyrite	--	--	3.7
groundmass			
quartz	2.0	1.0	--
orthoclase	15.0	2.0	--
plagioclase	36.5	36.7	--
clinopyroxene	5.0	15.0	--
Fe-Ti oxides	1.0	4.0	--
apatite	acc.	0.5	acc.
zircon	--	--	0.6

[1]Monzodiorite dike from Quartzville Creek
[2]Diorite dike from Canal Creek
[3]Tonalite plug from Boulder Creek

localized along fractures. The appearance of this pyrite surrounded by unfractured quartz, coupled with the drop-like morphology of the pyrite crystals, suggests an magmatic origin for this pyrite. Separation of an immiscible sulfide melt from the silicate melt and entrapment of this sulfide liquid within crystallizing phenocrysts of quartz provides one possible explanation for this unusual occurrence of pyrite.

Basaltic Dikes

Dikes of basaltic composition are abundant in the Yellowbottom-Boulder Creek area, but many cannot be recognized except where they are exposed in streambeds. Some dikes are propylitically altered and are interpreted to be hypabyssal equivalents of basalt flows of the lower andesite and intermediate basalt units. In contrast, others are fresh, intrude fault zones, and are interpreted to be younger and of Pliocene or Quaternary age.

The older dikes, represented by sample I-29, are dense, aphyric to porphyritic, and range from light to dark bluish gray in color (5 B 3/1 to 5 B 6/1) on both fresh and weathered surfaces. Dikes of altered porphyritic basalt are numerous in the area.

A porphyritic dike of basaltic composition, 6 meters in width, is exposed in Quartzville Creek 0.5 kilometer west of the Yellowbottom Recreation Site. This sample (I-42) is representative of the set of younger dikes. This rock is relatively unaltered, with only minor chlorite replacement of some mafic phenocrysts, and is dark gray (N 3).

Petrography and Petrochemistry

Thin sections of basaltic dikes representing each of the two age groups have been examined. The older fine-grained basalts contain sparse phenocrysts of plagioclase feldspar, orthopyroxene, and clinopyroxene in a pilotaxitic to sub-trachytic groundmass of plagioclase feldspar microlites, glass, quartz, orthopyroxene, and Fe-Ti oxides. The phenocrysts have usually been altered to chlorite, calcite, and quartz, and mafic components of the groundmass have been converted to chlorite and montmorillonite.

Sample I-29 is porphyritic in texture, and contains oligoclase (An_{23}) and clinopyroxene phenocrysts in a hyalopilitic groundmass dominated by glass and oligoclase (An_{24}) microlites. Modal mineralogical and chemical analyses of this rock are presented in Table 14. Phenocrysts of oligoclase are up to 4 mm in length, euhedral, and have been slightly resorbed. Those of clinopyroxene are up to 2 mm across, commonly twinned, and have been replaced by clay minerals along fractures. The groundmass consists of relatively large microlites of plagioclase feldspar, averaging 0.3 mm in length and set in a matrix of glass. Other groundmass components include rounded Fe-Ti oxides, quartz, clinopyroxene, and apatite. Much of the mafic component of the groundmass has been replaced by chlorite and clays.

This rock contains less CaO and more Na_2O and K_2O than basalts from the intermediate basalt and lower andesite units, whereas it is, with the exception of silica content, most similar to the Pliocene andesites. This suggests that these dikes may be substantially younger than the rocks

TABLE 14- Modal mineralogical and major oxide analyses (in percent), and metal analyses (in ppm) for a sample of a basaltic dike (I-29)

Mineral		elemental oxide	
phenocrysts		SiO_2	51.37%
plagioclase[1]	29.3%	TiO_2	0.86
clinopyroxene[2]	4.5	Al_2O_3	15.68
		Fe_2O_3	2.82
groundmass		FeO	3.47
quartz	tr.	MnO	0.13
plagioclase[1]	20.0	MgO	4.07
clinopyroxene[2]	8.0	CaO	4.93
Fe-Ti oxides	5.0	BaO	0.09
glass	33.0	Na_2O	4.62
		K_2O	2.63
		P_2O_5	0.30
		LOI	4.89
		TOTAL	95.86
		Metals	
		Cu	30 ppm
		Mo	<1
		Pb	13
		Zn	35
		Ag	< 0.3

[1]moderately altered to clays, calcite, epidote, and sericite
[2]weakly altered to chlorite and clays

they intrude. The large LOI may be partially explained by the presence of considerable calcite replacing phenocrysts of plagioclase.

The younger porphyritic dikes display abundant phenocrysts and microphenocrysts of labradorite (An_{57}), clinopyroxene, and less commonly orthopyroxene phenocrysts, in a glassy groundmass. Chemical and mineralogical analyses of sample I-42 are provided in Table 15. Labradorite phenocrysts are up to 4 mm in length and commonly exhibit compositional zoning patterns. These crystals are unaltered, although some resorption has occurred, whereas microphenocrysts of labradorite have been partially altered to chlorite. This alteration has selectively attacked the centers of crystals, presumably because of the higher anorthite content. Clinopyroxene is present as two generations of phenocrysts. The larger crystals are up to 1.5 mm across and are presumably older as they have been altered to chlorite and calcite. In contrast, the smaller clinopyroxene phenocrysts are unaltered. A few phenocrysts of orthopyroxene are large (up to 3 mm), and they have been slightly resorbed, but are unaltered. The groundmass consists of microlites of plagioclase feldspar, Fe-Ti oxides, and small quantities of clinopyroxene in a matrix of black glass.

Chemical analysis of this sample (Table 15) reveals a general compositional resemblance to basalts of the intermediate basalt unit with respect to most oxides, but having higher K_2O and lower CaO. Nonetheless, the almost complete lack of alteration suggests that this dike is much younger than the rocks which it intrudes.

TABLE 15- Modal mineralogical and major oxide analyses (in percent), and metal analyses (in ppm) for a sample of a porphyritic basaltic dike (I-42)

Mineral		elemental oxide	
phenocrysts		SiO_2	55.98%
plagioclase	33.3%	TiO_2	0.91
clinopyroxene[1]	13.1	Al_2O_3	15.59
orthopyroxene	0.6	Fe_2O_3	2.47
groundmass		FeO	4.03
plagioclase	14.0	MnO	0.12
Fe-Ti oxides	8.0	MgO	3.92
clinopyroxene	2.0	CaO	7.56
glass	29.0	BaO	0.05
		Na_2O	2.88
		K_2O	3.30
		P_2O_5	0.40
		LOI	1.93
		TOTAL	99.14
		Metals	
		Cu	35 ppm
		Mo	<1
		Pb	7
		Zn	25
		Ag	0.3

[1]older phase cpx completely altered to chlorite and calcite

Andesitic Dikes and Plugs

Dikes and small plugs of andesitic composition are present throughout the Yellowbottom-Boulder Creek area and many of these may have been feeders for the flows of andesite. The dike rocks are dark greenish gray (5 G 4/1) to medium bluish gray (5 B 5/1) on fresh surfaces, but are usually weathered to shades of tan. These dikes may be the hypabyssal equivalents of volcanic rocks belonging to the lower and intermediate andesite units. Textures of these intrusions range from aphanitic to strongly porphyritic, the latter in small plugs scattered throughout the study area.

Petrography and Petrochemistry

Major-oxide chemistry and modal mineralogy of an andesitic dike (sample I-33) is presented in Table 16. This rock displays a sub-trachytic texture of oligoclase (An_{21}) microlites, which average 0.1 mm in length, and interstitial quartz, clinopyroxene (?), orthoclase, and rounded Fe-Ti oxides. Mafic minerals have been completely altered to chlorite, preventing their identification by optical methods. A few phenocrysts of plagioclase feldspar are present but these have been largely altered to an assemblage of epidote and chlorite. Voids similar in shape to phenocrysts of plagioclase feldspar occupy about three percent of the rock by volume, and suggest the removal of these crystals by weathering, hydrothermal alteration, and (or) plucking during preparation of the thin section.

TABLE 16- Modal mineralogical and major oxide analyses (in percent), and metal analyses (in ppm) for a sample of an andesitic dike (I-33)

Mineral		elemental oxide	
phenocrysts		SiO_2	59.56%
plagioclase[1]	0.3%	TiO_2	1.40
		Al_2O_3	15.42
		Fe_2O_3	2.88
groundmass		FeO	4.38
quartz	8.6	MnO	0.13
orthoclase	5.0	MgO	1.99
plagioclase	58.0	CaO	2.63
Fe-Ti oxides	3.1	BaO	0.08
clinopyroxene[2]	25.0	Na_2O	5.11
		K_2O	1.21
		P_2O_5	0.50
		LOI	2.63
		TOTAL	97.92
		Metals	
		Cu	20 ppm
		Mo	<1
		Pb	8
		Zn	110
		Ag	0.3

[1]moderately altered to epidote and chlorite
[2]completely altered to chlorite

The sub-trachytic texture and relative scarcity of phenocrysts in this dike indicate that the magma was injected in a very fluid state, perhaps along a fault zone associated with the emplacement of the Yellowbottom Stock.

This rock chemically resembles andesites from the lower andesite unit but with slightly higher FeO_T and Na_2O, and lower K_2O and CaO. These changes may have resulted from hydrothermal alteration. Rectangular voids in the rock suggest the removal of phenocrysts of plagioclase feldspar either by supergene weathering or hypogene hydrothermal leaching, which may have contributed to the loss of CaO.

Dacitic and Rhyodacitic Dikes and Plugs

Dikes and plugs of dacitic to rhyodacitic composition are the most numerous intrusive rock type in the area. Four subsets of dacite intrusions are recognized.

Most common are aphyric-textured dikes with a light bluish-gray (5 B 7/1) color, represented by sample I-142. These intrusions are prevalent in the dike swarm along Quartzville Creek that has invaded the Yellowbottom Stock, as depicted in Figure 16, as well as in many other parts of the study area. Those observed range from a few centimeters to 2 meters in width.

A second type of dacitic dike, represented by sample I-101, ranges from pale pink (5 RP 8/2) to very light gray (N 8) on fresh surfaces, and tends to weather to a moderate yellowish-brown (10 YR 5/4). This type of dike is shown in Figure 17 intruding pyroclastic rocks of the upper

Figure 16- Dacitic dike intruding quartz monzodiorite of the Yellowbottom stock. Note the multiple intrusions of dacite.

Figure 17- Dacitic dike intruding laharic breccia of the upper pyroclastic unit.

pyroclastic unit. These dikes may actually be rhyolitic in composition, but chemical analyses were not performed because of extensive alteration. However, the classification of these rocks based on modal mineralogy is quartz monzonite (Figure 15).

A third type of dacitic dike, exemplified by sample I-21, has a similar modal composition to the second type but exhibits a trachytic texture. Colors are light olive-gray (5 Y 6/1) where unaltered, and dark yellowish-brown (10 YR 4/2) where weathered. These dike rocks have more quartz and less orthoclase than the previous group, and plot in the quartz monzodiorite field (Figure 15).

The fourth subdivision of dacitic intrusives is porphyritic in texture. These intrusions, some of which contain rounded quartz phenocrysts, are generally larger than the other types of dacitic intrusions and are both dikes and small plugs. These features have been described before (Peck et al., 1964; Munts, 1978) under the misnomer dacite porphyry. That term should be restricted to rocks that contain at least 50 percent phenocrysts by volume. The color of these rocks ranges from very light bluish-gray (5 B 8/1) to yellowish-gray (5 Y 8/1) on fresh surfaces, and they generally weather to a grayish-brown (5 YR 3/2).

Two types of porphyritic dacite intrusives are recognized: with quartz phenocrysts and without them. Both types have similar modal proportions of quartz, as those without phenocrysts contain more silica in the groundmass. Although samples of these rocks plot in the quartz diorite field on the QAP diagram (Figure 15), the glassy groundmass precludes an accurate assessment of the modal percentage of quartz.

Cobalt-nitrate staining of the rock indicates that alkali feldspar is not present in appreciable quantities.

Petrography and Petrochemistry

Aphyric dacitic dikes exhibit a sub-trachytic texture of plagioclase feldspar microlites, which average 0.25 mm in length, and varying amounts of quartz, pyroxenes, Fe-Ti oxides, and orthoclase (Table 17, sample I-142). Phenocrysts of plagioclase feldspar up to 2 mm in length were formerly present, but have been altered to epidote and chlorite, rendering determination of plagioclase feldspar compositions by optical methods impossible. A few rounded phenocrysts of Fe-Ti oxides are also present. Hydrothermal fluids have reacted with this rock and replaced much of the primary mineralogy with a propylitic assemblage of minerals.

The second type of dacitic intrusion (Table 17, sample I-101) reveals a felsitic texture of oligoclase (An_{21}) microlites which average 0.1 mm in length. Interstitial to these microlites are anhedral crystals of quartz, orthoclase, Fe-Ti oxides, and accessory rutile. This sample also contains disseminated pyrite cubes up to 0.5 mm in diameter.

The third type of dacitic dike (Table 17, sample I-21) displays a trachytic texture of oligoclase (?) microlites, interstitial and equant-shaped crystals of quartz and orthoclase, and an unidentified mafic mineral (pyrite ?) that has been completely replaced by jarosite. Phenocrysts of plagioclase feldspar up to 1 mm in length compose less than one percent of the sample.

The fourth type is represented by two varieties: those with quartz phenocrysts and those without. Sample I-92 (Table 17), represents a

TABLE 17- Modal mineralogical analyses (in percent) for four types of dacitic dikes

Sample #	type 1[1] I-142	type 2[1] I-101	type 3[1] I-21	type 4[1] I-92
phenocrysts				
quartz	--	--	--	2.3%
plagioclase	5.0%	--	1.0%	16.7
clinopyroxene	--	--	--	3.6
Fe-Ti oxides	2.0	--	--	--
pyrite	--	3.0%	--	--
groundmass				
quartz	5.0	15.0	15.0	1.0
orthoclase	10.0	31.0	15.0	--
plagioclase	69.0	60.0	60.0	6.0
clinopyroxene	7.0	--	8.0	1.0
Fe-Ti oxides	2.0	1.0	1.0	1.0
glass	--	--	--	67.8
apatite	--	--	--	acc.

[1]type 1 - aphyric and light blue in color
type 2 - aphyric and pale pink in color
type 3 - medium-grained and trachytic in texture
type 4 - porphyritic

quartz phenocryst dike from an outcrop along the Boulder Creek road near the western edge of Section 31. This rock contains phenocrysts of quartz, plagioclase feldspar, and minor clinopyroxene set in a felsitic groundmass consisting mostly of devitrified glass. The phenocrysts of quartz are up to 3 mm in diameter and have been rounded and embayed. Those of plagioclase feldspar are up to 4 mm in length and have been altered to an assemblage of sericite, quartz, and clay minerals. In contrast, phenocrysts of clinopyroxene have been replaced by clays and Fe-Ti oxides. The groundmass of this rock consists of spherulites of devitrified glass, plagioclase feldspar microlites, clinopyroxene, Fe-Ti oxides, and apatite. Argillic-phyllic alteration has affected the groundmass minerals to a large extent, and for this reason major-element analysis of this rock was not obtained.

Sample I-111, which lacks quartz phenocrysts and was collected from an outcrop in a roadcut along the ridgecrest near the southern border of Section 30, is believed to be compositionally representative of the porphyritic dacite dikes. Modal mineralogical and major oxide analyses of this rock are presented in Table 18. In thin section, these porphyritic dacites display phenocrysts of oligoclase (An_{23}) in a fine-grained, felsitic groundmass of plagioclase-feldspar microlites, quartz, orthoclase, hornblende (?), and Fe-Ti oxides. The phenocrysts of oligoclase are unresorbed and up to 2 mm in length. They are usually clustered and may be associated with anhedral masses of pyrite. The groundmass has been flooded with jarosite that has replaced the mafic mineral phases and pyrite cubes.

TABLE 18- Modal mineralogical and major oxide analyses (in percent), and metal analyses (in ppm) for a sample of a porphyritic rhyodacite dike (I-111)

Mineral		oxide	I-111	ave. rhyolite[1]
phenocrysts		SiO_2	73.45%	72.82%
plagioclase[2]	13.9%	TiO_2	0.23	0.28
		Al_2O_3	12.89	13.27
groundmass		Fe_2O_3	2.51	1.48
quartz	15.0	FeO	0.19	1.11
orthoclase	10.0	MnO	0.01	0.06
plagioclase[2]	34.0	MgO	0.16	0.39
hornblende[3]	25.0	CaO	0.40	1.14
Fe-Ti oxides	0.5	BaO	0.12	--
pyrite[4]	1.5	Na_2O	3.25	3.55
		K_2O	3.74	4.30
		P_2O_5	0.16	0.07
		LOI	2.32	1.49
		TOTAL	99.43	99.96
		Metals		
		Cu	50 ppm	
		Mo	1	
		Pb	15	
		Zn	75	
		Ag	< 0.3	

[1] average rhyolite of Le Maitre (1976b)
[2] weakly altered to clays
[3] completely altered to chlorite and epidote
[4] completely altered to jarosite and hematite

In terms of major oxide components, this rock is compositionally similar to the average rhyolite of Le Maitre (1976b).

Granophyric Dikes

A fine-grained dike of granitic composition intrudes the Yellowbottom Stock and is exposed along the Quartzville access road 0.25 km east of Yellowbottom Campground. This dike is 3 meters wide, pinkish-gray (5 YR 8/1) in color on both fresh and weathered surfaces, and contains cubes of pyrite. Intrusions of this composition have been previously reported in the Western Cascades (Peck et al., 1964; Munts, 1978), and have been referred to as aplites. These dikes are invariably enclosed by dioritic stocks.

Petrography and Petrochemistry

The granophyric dike consists of peculiar square-shaped phenocrysts of quartz set in a groundmass of anhedral plagioclase feldspar, spherulitic orthoclase, quartz, and apatite, as shown in Figure 18. Modal mineralogical and major oxide analyses of this rock are provided in Table 19. The quartz is present both as euhedral phenocrysts and as a major constituent of the groundmass. Phenocrysts of quartz are up to 1.5 mm in diameter and of an unusual cubic morphology. This square form suggests that the mineral originally crystallized as ß-quartz, and subsequent quenching of the magma preserved the crystal shape associated with that quartz phase. These phenocrysts are mantled by spherulitic orthoclase. Phenocrysts of plagioclase feldspar are up to 2.5

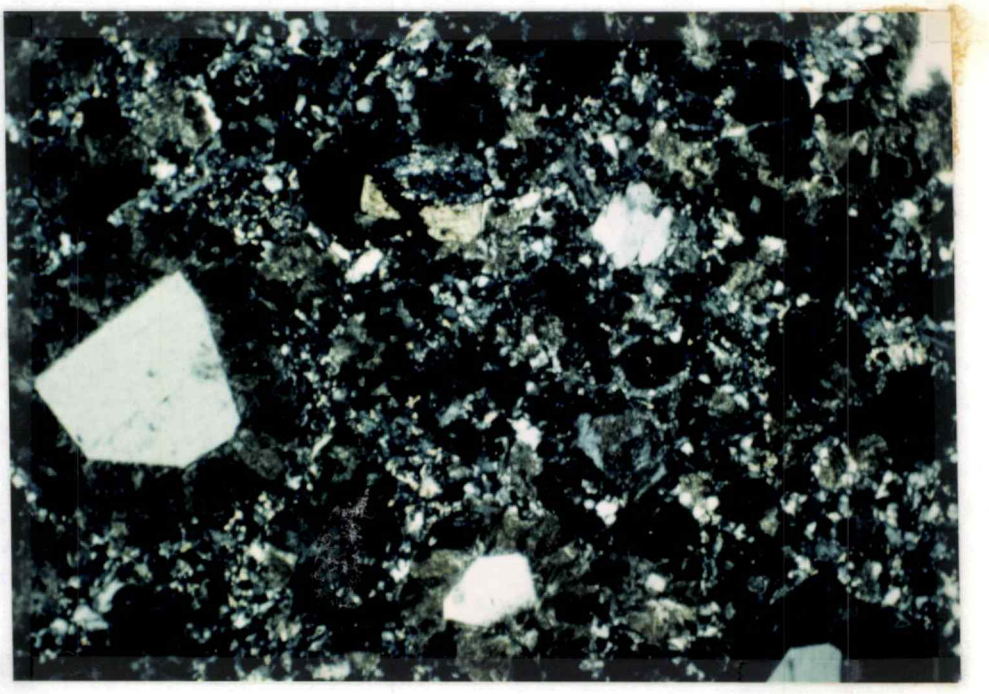

Figure 18- Photomicrograph of a granophyric dike (crossed polars). Note the unusual habit of quartz and spherulitic orthoclase. Length of field is 10 mm.

TABLE 19- Modal mineralogical and major oxide analyses (in percent), and metal analyses (in ppm) for a sample of granophyric dike (I-18)

Mineral		oxide	I-18	ave. granite[1]
phenocrysts		SiO_2	74.68%	71.08%
quartz	4.4%	TiO_2	0.11	0.40
hornblende[2]	0.4	Al_2O_3	11.57	11.26
		Fe_2O_3	1.22	4.28
groundmass		FeO	0.22	2.19
quartz	16.5	MnO	0.03	0.11
orthoclase[3]	27.0	MgO	0.14	0.25
spherulitic		CaO	1.32	0.84
orthoclase[3]	35.5	BaO	0.10	--
plagioclase[3]	15.0	Na_2O	0.40	4.92
pyrite	1.2	K_2O	7.13	4.21
apatite	acc.	P_2O_5	0.13	0.07
		LOI	1.21	0.39
		TOTAL	98.26	100.00
		Metals		
		Cu	9 ppm	
		Mo	<1	
		Pb	5	
		Zn	9	
		Ag	< 0.3	

[1]average peralkaline granite of Nockolds (1954)
[2]completely altered to sericite and calcite
[3]strongly altered to sericite and clays

mm in length and have been partially altered to sericite and clay minerals. A few ghosts of hornblende (?) are also present, but are now completely replaced by sericite and calcite, and they represent the primary mafic phase of this host.

This granophyric dike is compositionally unique, as it is chemically unlike any of the averages for silicic igneous rocks that have been published by Le Maitre (1976b) or Nockolds (1954). It is similar in alumina content, total alkalis, MgO, and CaO to the average peralkaline granite of Nockolds (1954), but is depleted in FeO_T. In addition, the K_2O content is very high. Presumably, the original composition of this rock has been modified by hydrothermal alteration that may have included the addition of quartz and potassium feldspar.

Mafic Plugs

Three mafic plugs are present in the Yellowbottom-Boulder Creek area, all located within Section 35 near the western boundary of the map. Two are exposed along the Quartzville access road within 0.4 kilometers of each other, with the third near the center of the western edge of Section 35. These plugs share several features in common, being domal in shape, weakly altered, high in iron content, and dark gray (N 3) on fresh and weathered surfaces. Two of the three plugs also exhibit a radial-and-concentric pattern of jointing.

These intrusions have been previously described as Quaternary in age, associated with the last pulse of volcanic activity in the region (Berg, 1961; Munts, 1978). However, they lack the distinctive chemical

signature of other rocks in the area known to be of that age (i.e., high P_2O_5 and BaO; nepheline-normative) and have been propylitically altered, which suggests that they are similar in age to the volcanic rocks they intrude.

Petrography and Petrochemistry

A sample of mafic plug (I-59) was examined in thin section and analyzed for major oxides and metals. The results of these determinations are presented in Table 20. Petrographic analysis reveals phenocrysts of calcic labradorite (An_{65}), clinopyroxene, and orthopyroxene set in a seriate groundmass of plagioclase-feldspar microlites, pigeonite, Fe-Ti oxides, and apatite. Ghosts of former olivine (?) phenocrysts are also present. Phenocrysts of labradorite are up to 3 mm in length and fractured, but relatively unaltered. This fracturing of plagioclase feldspar may have been artificially induced, as the sample was taken from a quarry. Euhedral phenocrysts of clinopyroxene up to 1 mm in length are present in small amounts. Orthopyroxene phenocrysts have been replaced by chlorite and are mantled by clinopyroxene. Olivine (?) is present as ghosts of euhedral crystals which display hexagonal outlines and fractures filled with iddingsite, as shown in Figure 19. These crystals are up to 8 mm in longest dimension, and have been completely replaced by an assemblage of quartz, clay minerals, and chlorite. The groundmass of this rock is composed of a seriate fabric of plagioclase- feldspar microlites of undetermined composition, abundant rounded crystals of Fe-Ti oxides, interstitial pigeonite, and accessory apatite.

TABLE 20- Modal mineralogical and major oxide analyses (in percent), and metal analyses (in ppm) for a sample of a mafic plug (I-59)

Mineral		oxide	I-59	ave. gabbro[1]
phenocrysts		SiO_2	50.24%	50.14%
plagioclase[2]	28.6%	TiO_2	1.18	1.12
clinopyroxene	0.8	Al_2O_3	19.20	15.48
orthopyroxene[3]	3.8	Fe_2O_3	4.23	3.01
olivine[4]	5.5	FeO	5.54	7.62
groundmass		MnO	0.20	0.12
plagioclase[2]	38.0	MgO	3.42	7.59
Fe-Ti oxides	10.0	CaO	10.10	9.58
pigeonite	13.0	BaO	0.02	--
apatite	acc.	Na_2O	2.68	2.39
		K_2O	0.44	0.93
		P_2O_5	0.31	0.24
		LOI	1.21	0.93
		TOTAL	98.77	99.15
		Metals		
		Cu	80 ppm	
		Mo	<1	
		Pb	16	
		Zn	55	
		Ag	< 0.3	

[1]average gabbro of Le Maitre (1976b)
[2]weakly altered to clays
[3]completely altered to chlorite and epidote
[4]completely altered to chlorite, epidote, clays, quartz, and iddingsite

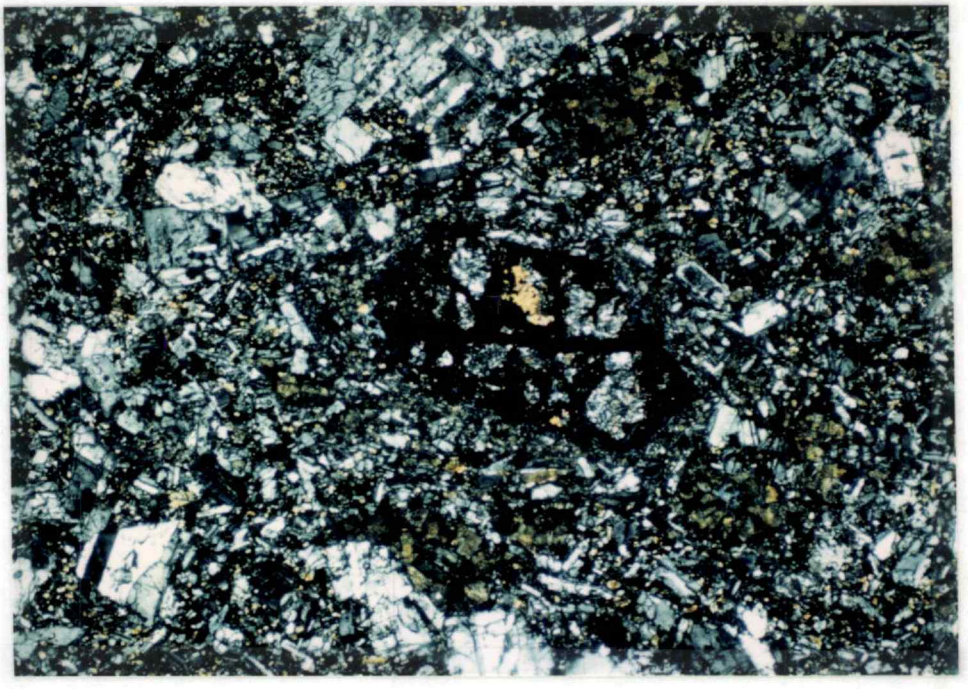

Figure 19- Ghost of an olivine (?) phenocryst in mafic plug sample I-59. Length of photomicrograph is 10 mm.

As compared to the average gabbro, this rock is deficient in MgO and contains excess Al_2O_3. These differences may in part be attributable to relatively large amounts of calcic plagioclase feldspar and, to a lesser extent, the possible presence of clinopyroxene.

UNCONSOLIDATED DEPOSITS

Unconsolidated deposits of Quaternary age in the Yellowbottom-Boulder Creek area include glacial drift, talus, terrace gravels along Quartzville Creek, and landslides and debris flows on steep slopes.

Glacial Deposits

Glacial drift is present in valleys of the Boulder Creek area, originating from three cirques cut into the north face of Galena Ridge. These deposits are composed of boulders of various sizes, nearly all of which are diktytaxitic basalt eroded from Galena Ridge, in an unsorted matrix of clay, silt, sand, and pebbles. The drift, where observed in roadcuts, ranges up to 8 meters in thickness.

The glaciers that left these deposits may have advanced and retreated more than once. Evidence for multiple glacial events is present at one outcrop along Boulder Creek road, where two stacked deposits of till can be distinguished.

The easternmost cirque is the largest glacial feature in the Yellowbottom-Boulder Creek area. An impressive headwall 200 meters high has been carved into the columnar jointed basalts of Galena Ridge, and the most extensive deposits of drift originated from this cirque. Drift extends to the main valley floor of Boulder Creek, from this and the other two cirques immediately west along Galena Ridge.

Evidence suggests that the glaciers extended down nearly to Quartzville Creek. A sudden steepening in the gradient of Boulder Creek

is present where a bridge crosses the creek in the northwest corner of Section 36. This inflection, at an altitude of 1400 ft (425 m), possibly represents the lower limit of the glacial advance. A remnant of drift is exposed along the access road above a breccia zone approximately 1/2 kilometer upstream from this bridge.

The elevation of these deposits is much too low for them to have been caused by the youngest episode of glaciation in the Cascades, which occurred 2,500 years ago but affected areas only between 7,000 (2,100 m) and 9,000 (2,750 m) feet in elevation (E.M. Taylor, 1968). Thus, it is likely that this glaciation event occurred during the Wisconsin Glacial Period, perhaps 10,000-12,000 years B.P.

River Terraces

River terraces consisting of rounded stream gravels and sand are common along Quartzville Creek at heights above the present river level of up to more than 20 meters. These deposits range from less than one to approximately 5 meters in thickness. In addition, several large terraces are present in the Yellowbottom area. Some are covered with old-growth trees approximately 200 years old, which suggests that they may contain deposits of unworked placer gold.

Landslides

Landslide scarps and debris are present at several localities, most notably two large slides in the lower part of Boulder Creek. One of these

slides remains intermittently active, and often covers the access road with debris. These deposits contain large blocks of rock mixed with unsorted material. Accordingly, they have a chaotic appearance. A large block of basalt from Galena Ridge has slid down the hill near the exposure of rhyodacite in Section 6. The presence of inclined bedding (flow banding) suggests that the block was rotated backwards during the mass-wasting event.

The steep terrain and wet climate of the area suggest that many more landslide features may be present. Because it is likely that much of the surface of this area has moved at one time or another, caution should be exercised in the interpretation of geochemical data such as that derived from soil surveys.

Talus

Small deposits of talus are present along Galena Ridge, and are composed of angular fragments of diktytaxitic basalt, whose columnar jointing facilitates in the formation of slide rock. These deposits overlie glacial drift in the same area, indicating a younger age and perhaps indirect association, as most of these deposits are found along the headwalls of the cirques excised into the ridge. Their development was probably accelerated by glacial erosion, which undermined Galena Ridge and led to slope instability.

STRUCTURE

The structural relationships of the Western Cascades are poorly understood. Analysis of aerial photographs of that subprovince reveals the presence of numerous lineaments (Priest et al., 1983), which can be roughly resolved into three sets oriented N 60° to N 20° W, N-S, and N 15-30° E. Although many of these features detected on the photos may be faults, their precise recognition on the ground is difficult to demonstrate because of insufficient mapping and poor exposures. Known faults of N-S orientation are concentrated along the eastern boundary of the Western Cascades. These structures bound blocks of High Cascade volcanic rocks that have been downdropped relative to adjacent areas to both the east and the west, beginning in early Pliocene time (E.M. Taylor, 1981; Priest et al., 1983).

North-trending faults are older than the others, with documented movements as early as 16 Ma (Beeson and Moran, 1979), and with recurrent activity extending into late Pliocene time (Peck et al., 1964). These faults may be related to lateral movement along a series of N 60° W lineaments which cross the Cascade Range and represent the western edge of Basin-and-Range style deformation (Lawrence, 1976). Many mineralized veins, breccia pipes, and intrusions in the mining districts of the Western Cascades are localized along these northwest-trending structures (Callaghan and Buddington, 1938; Power, 1984).

Although aerial-photograph lineaments of northeast-trending orientation are also numerous, only a few have been documented as faults (Priest et al., 1983). Several northeast-trending faults that show

both lateral and normal displacements have been recognized in the Breitenbush Hot Springs area (Hammond et al., 1982; White, 1980a,c). These faults cut the 11.8-9.8 m.y. Elk Lake Formation and are associated with a fold of middle Miocene age (White, 1980a).

A series of northeast-trending anticlines and synclines in the northern half of the Western Cascades were first described and named by Thayer (1936). These structures are depicted as continuous features on the map of the Cascades compiled by Wells and Peck (1961). However, Hammond et al. (1980, 1982) suggested that the gentle dips that characterize these folds may be related to interactions between fault blocks, or may possibly represent primary depositional dips. Some of these folds, including the Sardine Syncline which passes just east of the study area through the Quartzville District, expose rocks of the Sardine Formation in their hinge zones. The age of folding is poorly documented but has been suggested to be middle Miocene (White, 1980a,c).

The compressional style of deformation responsible for the folds and uplift-related normal faults during the Miocene changed to an extensional style during the early Pliocene. Evidence for this change in stress orientation is provided by voluminous eruptions of diktytaxitic basaltic lavas along the boundary between the Western Cascades and the High Cascades, and the formation of a graben-like feature bounded by normal faults which parallels the axis of the High Cascades (E.M. Taylor, 1981).

Widespread uplift of the central Western Cascades relative to the High Cascades during the last few million years has resulted in rapid downcutting of rivers and has produced the dissected topography of the present Western Cascades Range.

The structure of the Yellowbottom-Boulder Creek area is generally simple. Volcanic rocks dip between 10 and 20 degrees to the southeast, presumably into the hinge zone of the Sardine Syncline. Locally, some rocks depart from this orientation, probably owing to varying primary dips of the volcanic stratigraphy or tilting of blocks between faults. Several shear zones, which consist of parallel sheeted fractures of the volcanic host rocks, are commonly associated with mineralization (see Plates 1 and 2). One such feature intersects a cluster of shatter zones in the Boulder Creek drainage basin, which suggests that the shearing may have created a zone of weakness along which volatiles, either heated meteoric waters or fluids exsolved from a cooling pluton, were channeled to the surface.

Faults and Fractures

Numerous lineaments can be identified on aerial photographs of the Yellowbottom-Boulder Creek area (Plate 2), but only a few can be correlated with field evidence of faulting. Some of these lineaments correspond to sites of dike intrusion, which suggests that they may indeed be faults that provided access for the magma.

Normal faults can be documented in a few locations, most notably at the "Temple" (see Figure 11), where a right-stepping *en echelon* series of fractures is exposed. The traces of these faults can be readily observed on the aerial photos, and offsets can be demonstrated where they intersect Quartzville Creek at the "Temple". One strand of the fault at this location is defined as a gap 2 meters wide in the basaltic rocks that is

filled with fault gouge. This fault can be traced across the Champion B road immediately south of Quartzville Creek, where basalt flows of the intermediate basalt unit are in contact with tuffs of the lower pyroclastic unit. A lineament 0.3 km east of this location, which parallels the "Temple" fault zone, is postulated as a fault that bounds the eastern side of a graben-like structure. This fault system may possibly be associated with the emplacement of the Yellowbottom Stock.

Other lineaments in the vicinity of the stock may also be faults. Cross-section A-A' (Plate 1) reveals an apparent offset of the volcanic stratigraphy across the stock. This offset may have been accomplished by normal faulting along Yellowbottom Creek. Although field evidence for this fault is lacking, a lineament along the creek (see Plate 2), and the abrupt contact of the Yellowbottom Stock with rocks of the lower andesite unit at this location, suggest that such a structure may be present. An alternative explanation for this offset is the doming of the volcanic rocks as the result of intrusion of magma from below.

Prominent joint sets are present in many of the volcanic rock units in the area. Parallel sets of joints are associated with a swarm of dikes in the western half of Section 30 along Quartzville Creek, and may have played a role in the localization of these intrusions and associated hydrothermal alteration. Some joints may have controlled the location of stream channels, as shown in the confluence area of Quartzville and Canal Creeks, where Canal Creek has eroded a channel 25 feet deep through bedrock at the confluence.

Folds

Folding caused by regional compression has affected the Yellowbottom-Boulder Creek area. The Sardine Syncline trends northeasterly and passes through the center of the Quartzville District, immediately east of the study area. Volcanic rocks both to the east and west of the fold axis dip northwest and southeast, respectively (Munts, 1978). Volcanic rock units of the Yellowbottom-Boulder Creek area increase in southeast dip to as much as approximately 25 degrees towards this feature.

Other small folds are present elsewhere in the study area. Tuffs of the Tupt unit have apparently been drag-folded into the inferred fault in the center of Section 31. The dip of these tuffs changes from approximately 35 degrees adjacent to the fault, to less than 10 degrees 100 meters to the west. Drape folding is present in the laminated ash-flow tuffs exposed along the ridge top in central part of Section 20, and is interpreted to represent primary depositional dips of the tuffs on a topographically irregular surface.

Breccia Pipes and Breccia Zones

Several zones of brecciated rock are present in the Yellowbottom-Boulder Creek area. These breccias range in shape from linear to cylindrical, and presumably owe their origin to the emplacement of intrusions. Similar features are associated with mineralization in many porphyry-copper environments (Perry, 1961; Lowell and Guilbert, 1970;

Sillitoe and Sawkins, 1971; Field et al., 1974; Gustafson, 1978; Titley, 1981), and are commonly the hosts for ore. The occurrence of mineralized intrusive breccias, especially as swarms of simple pipes, has been correlated with the presence of concealed porphyry copper deposits at depth (Gilmour, 1977).

The origin of breccia pipes has been extensively debated by geologists. Mechanisms proposed include fluidization, solution-stoping, magma pulsations, phreatomagmatic explosions, and collapse into a vapor-bubble void.

Fluidization, as defined by Reynolds (1954), involves the release of a fluid phase from magma and the vertical transport of this fluid and particulate matter upward along fracture systems as a result of a high pressure gradient. This pressure differential is presumably caused by venting at the surface. Clasts are transported in suspension by the fluid and are deposited when channels become blocked or the pressure gradient decreases. This mechanism was proposed to account for the formation of breccias at the Warren Mining District in Arizona (Bryant, 1968), and at many localities elsewhere. However, more recent studies (Wolfe, 1980) have suggested that fluidization may not be a likely mechanism for the formation of all breccia pipes.

The hypothesis of solution-stoping, by Sillitoe and Sawkins (1971), proposes that breccias result from the collapse of wall rocks into a void created by corrosive hydrothermal fluids that evolved from a solidifying magma. These authors envisioned a gradual yet continuous outward and upward advance of alteration and fragmentation from a central area until equilibrium is established between the wall rocks and fluids.

Perry (1961) suggested that pulsations of magma were responsible for the formation of breccia pipes in the Cananea District, Mexico. The pulsations are driven by fluctuations in magma pressure and create a void into which rock may collapse to form the breccia.

Another hypothesis recently proposed by Wolfe (1980) attributes the formation of breccias to the interaction of magma with groundwater. The resulting phreatomagmatic explosions would create rounded to subrounded fragments ranging from several meters across to microns in size.

Norton and Cathles (1973) have developed a model for the formation of breccias in which a void space is created by the trapping of vapors beneath the chilled outer and upper rind of a pluton. Increasing vapor pressure during continued crystallization of the magma results in explosive piercement of the rind and fracturing of rocks above the pluton (Burnham, 1979). Collapse of rocks into the void space creates the breccia, which is subsequently altered by groundwaters which invade the system.

Currently, the most favored hypothesis is that of Norton and Cathles (1973) as subsequently modified by Burnham (1979).

All breccia zones in the study area have been mineralized to some extent, as indicated by abundant gossans and disseminated pyrite. Additionally, galena and sphalerite are present at one location. Several of the more important breccias in the study area are described below.

A quarry near the confluence of Quartzville Creek and Yellowstone Creek exposes a breccia zone that contains numerous sunbursts of tourmaline and cubes of pyrite in a matrix-supported, argillically-altered

breccia. Tourmaline is localized along fractures in the surrounding rocks for a distance of approximately 100 meters from the breccia, as is pyrite or its oxidized product, limonite. Iron staining is abundant. Chalcopyrite has been reported from this quarry by Munts (1978) and Gray (1977), but was not observed by myself. Five rock samples from this quarry were analyzed for trace metal content (samples T-53, A-54, TLA-55, T-56, and I-57), but failed to yield significant copper, with the largest value being only 18 ppm. This low value suggests that the zone has been leached, perhaps removing copper sulfides formerly present. Several small silicic dikes are also present in this quarry, and horizontal domal and vertical radial joints cut the rocks. The presence of silicic dikes and the high-temperature mineral tourmaline, together with the unusual joint patterns, suggest that the cupola of a stock may underlie this quarry at shallow depth.

Roadcuts in the extreme southeastern corner of Section 36 in the Boulder Creek drainage area expose a cluster of breccia "pipes". Because of steep slopes, the aerial distribution of these features cannot be determined. As exposed in the roadcuts, their contacts with the surrounding country rocks are diffuse. Gilmour (1977) and Sillitoe and Sawkins (1971) have stated that most breccia pipes are bounded by sharp contacts, commonly with concentric fractures extending into the wall rocks for a meter or so. The lack of sharp contacts indicates that these features may be more correctly referred to as "fracture" or "shatter" zones.

In outcrop, these clast-supported breccias contain angular clasts of andesite and dacite, which range up to 1 meter across, in a rock-flour

matrix that has been partially altered to sericite and clay minerals. The hydrothermal origin of the brecciation is evidenced by the elongate slabs of rock which have been wedged apart by the matrix , as shown in Figure 20. This matrix consists of abraded particles up to 0.5 cm in diameter which are supported by rock flour derived from the physical abrasion of rock fragments. Both the matrix and rock fragments contain disseminated pyrite, but other sulfides, if originally present, have been largely removed by weathering processes. Veins and irregular blebs of calcite are also common.

Sphalerite and galena are present in veinlets with calcite and quartz at the north end of the sequence of shatter zones. These veinlets are localized in a greenish-colored, tuffaceous host rock along the margin of the northernmost shatter zone, close to several outcrops of dioritic intrusions. The sphalerite is low in iron content and honey-colored. Disseminated pyrite is present in the wall rocks adjacent to the veinlets, but chalcopyrite was neither observed nor suggested from chemical analysis of the host rocks.

A breccia pipe is exposed near the boundary between Sections 36 and 31 in a roadcut of the Boulder Creek road. This pipe is approximately 25 meters across, and is bounded on both sides by sharp contacts with unbrecciated rocks of the lower andesite unit. The contact on the west side displays sheeted fractures which extend into the wall rocks for a distance of 0.5 meters. Clasts incorporated in this breccia are of varying sizes and up to 3 meters in diameter. These fragments are rounded, in contrast to the angular clasts of the shatter zones, which suggests that substantial transport may have occurred within this pipe. This breccia

Figure 20- Hydrothermal breccia texture in a shatter zone in Section 36.

displays strong argillic alteration, with nearly complete replacement of clasts and matrix by clay minerals. Pyrite is present as abundant, well-formed pyritohedrons up to 0.5 cm across. Patches of green clay (malachite and crysocolla ?) are moderately abundant and may suggest the former presence of copper sulfides. The rounded clasts, sheeted contacts, and strong argillic alteration, perhaps accomplished by groundwaters, suggest that this pipe vented at the surface.

Samples were not collected from this zone for geochemical analysis. However, it has been assayed in the past and found not to contain anomalous concentrations of gold (Jay Grant, U.S. Forest Service, July,1987, personal communication).

A linear zone of brecciated rocks is present in the northeast corner of Section 36. This zone changes markedly in character over a vertical distance of 500 feet. The lower part of the zone is approximately 5 meters in diameter, and is contained in the center of a dioritic plug. It consists of a hydrothermal breccia cemented by goethite, jarosite, quartz, and red hematite. Fractures are encrusted with hematite and goethite up to one centimeter thick, which suggests that a large volume of fluid was channeled along this zone. These brecciated rocks contain anomalous concentrations of gold (250 ppb), silver (5 ppm), copper (495 ppm), molybdenum (15 ppm), zinc (520 ppm), arsenic (976 ppm), antimony (56 ppm), and bismuth (53 ppm), as represented by samples B-86 and B-144 (Appendix B). At the top of the zone, massive silicification, exposed on a logging platform, has replaced the host rock with quartz. The zone widens to approximately 40 meters in this area, but cannot be traced in any direction beyond this point. Brecciated textures are

preserved in this rock, and several generations of quartz deposition can be distinguished. Finely disseminated pyrite is present at the highest topographic location, but metal values are depleted from background levels (samples B-112 and B-112a, Appendix B). The changes in mineralogy and alteration suggest that this breccia zone may have been a feeder conduit for a hot spring.

Field observations suggest that several mechanisms may have been responsible for the formation of breccia pipes and related features in the Yellowbottom-Boulder Creek area. The shatter zones in Section 36 are composed of angular fragments that have not been transported or abraded, which suggests that hydrofracturing of the rocks above the cupola of a magma chamber, as envisioned by Norton and Cathles (1973) and Burnham (1979), formed these breccias. Sphalerite and galena were deposited by fluids which invaded these fractures after brecciation. In contrast, the breccia pipe along the Boulder Creek road shows substantial abrasion and transport of clasts, and thus may have vented at the surface. These characteristics are similar to those of breccia pipes described from Chile by Sillitoe and Sawkins (1971). Accordingly, I postulate that this pipe may have been formed by the solution-stoping process proposed for the Chilean pipes.

MAJOR-OXIDE CHEMISTRY OF VOLCANIC AND PLUTONIC ROCKS

Volcanic and plutonic rocks of the study area display systematic variations of major-element oxides when plotted against silica on Harker diagrams (Harker, 1909), as depicted in Figure 21. Trends lines for the variation diagrams were constructed by simple linear regression of the data points utilizing the Statview program for the MacIntosh. These regression lines exclude samples Q-27 and I-59, which are clearly divergent from the main trends and, therefore, may not be cogenetic with the other rocks. For comparison, however, these samples are included on the diagrams. The trend lines for the volcanic and intrusive suites have different slopes for many of the elemental oxides; notably TiO_2, CaO, MnO, Na_2O, and P_2O_5. This variance in slope may be the result of a wider range of silica values for the intrusive rocks, differences in the intensity of hydrothermal alteration between the volcanic and intrusive rocks, or it may be an artifact of the small size of both data sets.

Data for the volcanic rocks display significantly less scatter than those for the plutonic rocks. This increased dispersal of the major-oxide data for the intrusive sequence may be the result of alteration processes. The plutonic rocks are generally more altered than their volcanic country rocks, perhaps because the hydrothermal fluids represent either meteoric waters that were heated by the plutons (see H.P. Taylor, 1971) or a primary magmatic component exsolved from plutonic magmas during cooling and crystallization (see Burnham, 1967 and 1979). Accordingly, nearly all intrusive rocks have been altered to some extent, and changes

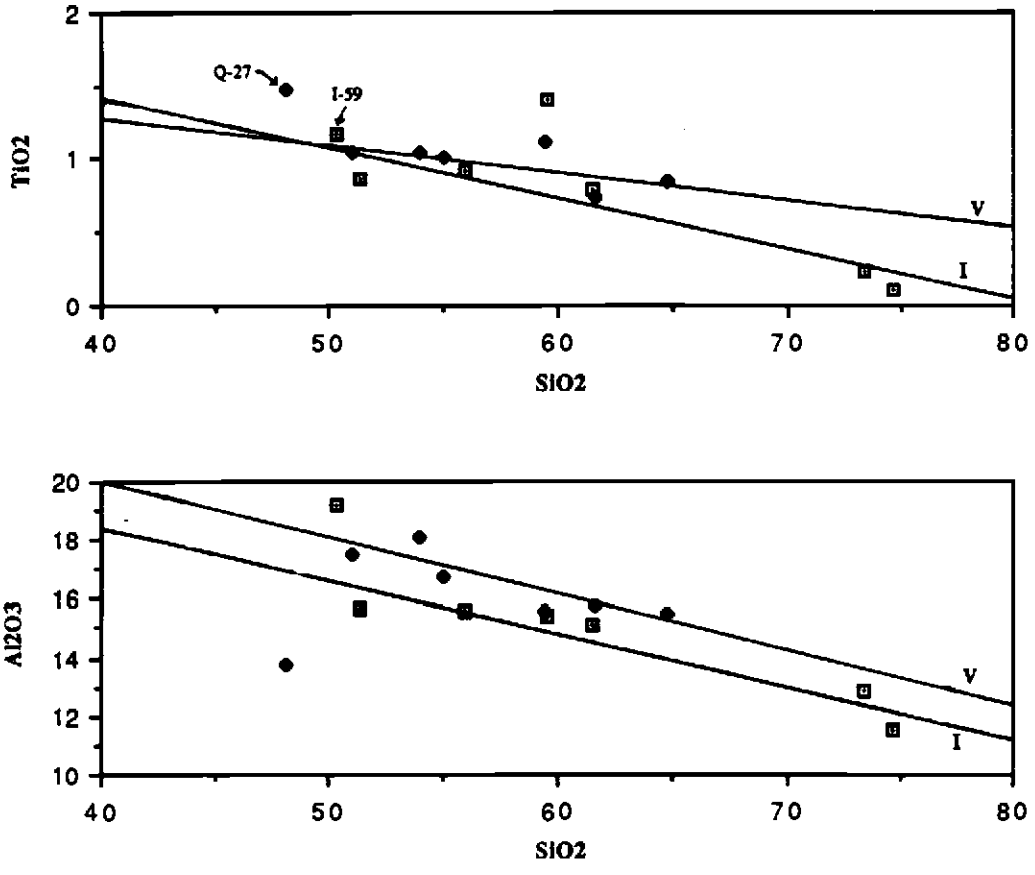

Figure 21- Harker variation diagrams of major oxide components in volcanic (closed diamonds) and intrusive (open squares) rocks of the study area (continued on the following two pages). Trend lines derived from simple regression of the data points, but exclusive of samples Q-27 (volcanic) and I-59 (intrusive).

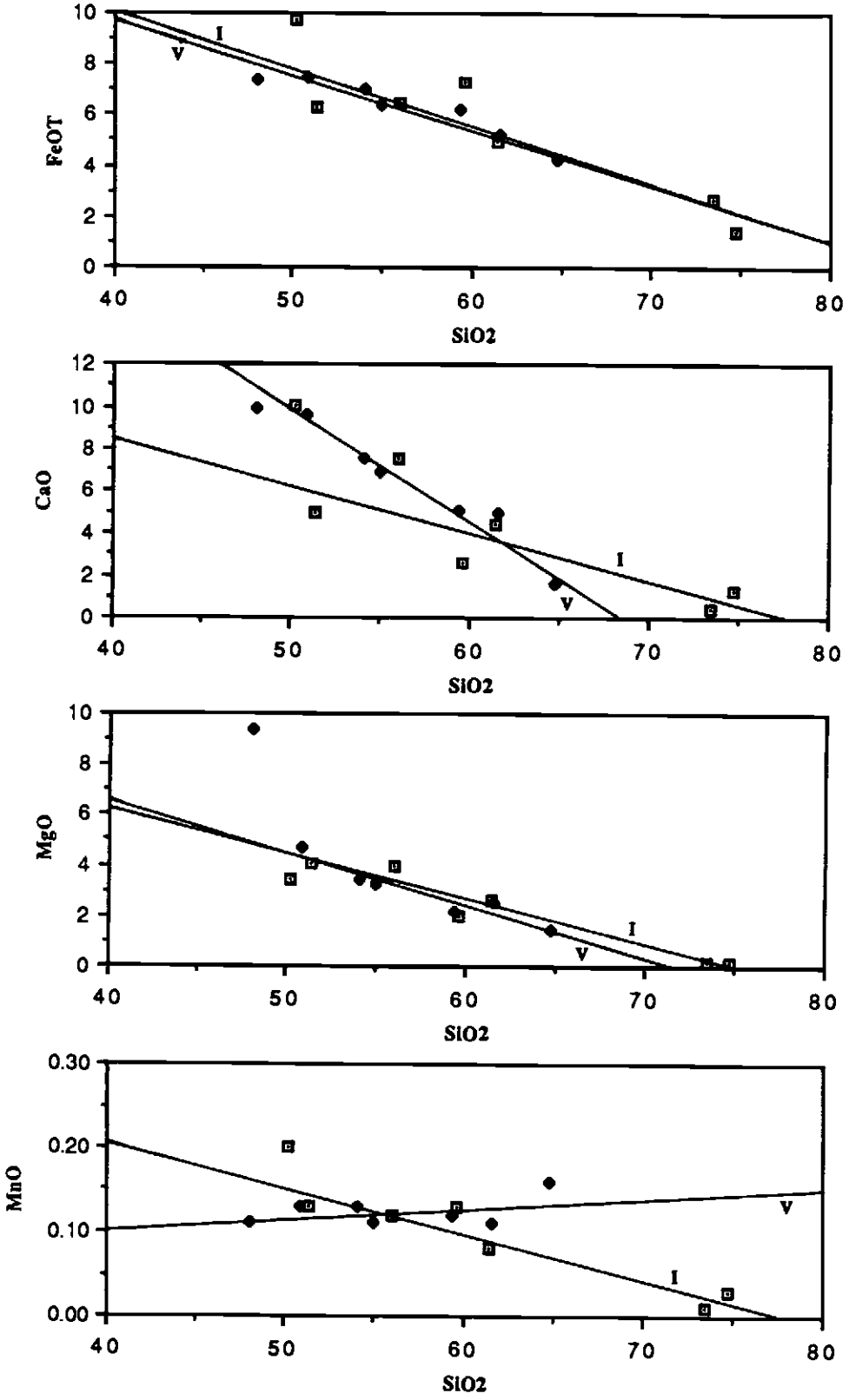

Figure 21 - continued

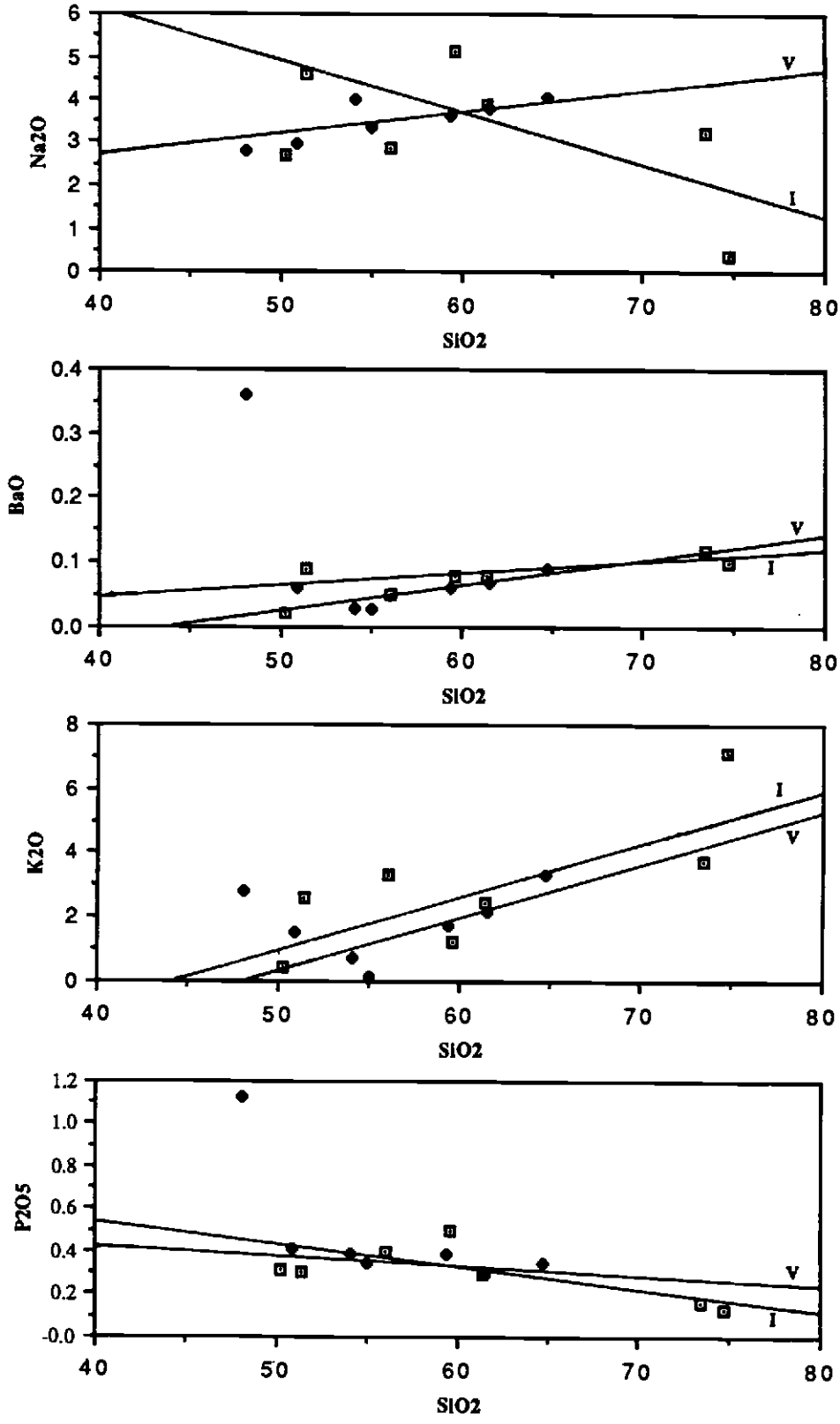

Figure 21 - continued

in the concentrations of some major oxides, notably K_2O, CaO, and Na_2O, may have occurred.

Harker diagrams show that with increasing silica content there is a regular decrease in the concentrations of Al_2O_3, TiO_2, FeO_T, MgO, CaO, and P_2O_5, whereas those of BaO and K_2O increase. These trends are typical of rock suites which have been differentiated from a single batch of magma (Cox, Bell, and Pankhurst, 1979). Volcanic and plutonic rocks of the Yellowbottom-Boulder Creek area may possibly have been derived from a common magma source; however, geologic evidence to support this idea is lacking. Additionally, dikes and plugs are present within all volcanic rock units in the area, with the exception of the Quaternary flows. This distribution suggests that the plutonic suite was emplaced during a relatively short time interval subsequent to deposition of the volcanic rocks, and therefore they may not be cogenetic. Petrologic modeling of the major oxide data was not attempted because of the probability that certain oxides, including Na_2O, K_2O, CaO, FeO, and Fe_2O_3, have had their concentrations changed by hydrothermal alteration.

MnO and Na_2O show divergent behavior, as both oxides decrease in the intrusive rocks but increase slightly in the volcanic suite. The dual behavior of Na_2O is most likely related to alteration. The intrusive trend line for Na_2O is strongly controlled by a granophyric dike (silica = 74.7%), which contains over 7 percent K_2O. Petrographic examination of this rock indicates that sericite replaces plagioclase feldspar, therefore, Na_2O may have been leached from this rock during sericitization. A possible reaction involving these mineral species is presented in the subsequent chapter on hydrothermal mineralization. Alternatively, the divergent

trend shown by Na_2O, and especially MnO, may be an artifact of the small size of the data set analyzed.

Two rock samples (I-59 and Q-27) consistently plot off trend, as previously mentioned. This divergence from the trend lines defined by other samples may suggest that those rocks were derived from a different magma source than the main sequence.

The first sample is the trachybasalt from Canal Creek (Q-27; silica - 48.1%), which is considered to be Quaternary in age from its distribution. Rocks of Quaternary age in the Western Cascades can be recognized chemically by a high concentration of BaO and P_2O_5 in contrast to older rocks of the region (Munts, 1978). Additionally, Quaternary rocks also contain high values of certain metals, notably Cr, Co, and Ni (Ian Thomson, Orvana Resources Corp., Jan., 1988, personal communication).

The other anomalous sample on the variation diagrams is represented by the major oxide data for a mafic plug (I-59; silica - 50.2%). This sample is enriched in CaO, MnO, and Al_2O_3 and depleted in total alkalis with respect to the main sequence of intrusive rocks. These differences are also suggestive of a Quaternary age for this intrusion. However, as will be discussed subsequently, there are other possible causes for the chemically anomalous behavior of this sample.

The effects of alteration on the chemistry of intrusive rocks from the Yellowbottom-Boulder Creek area are also evident from the plots of the alkali-lime (Peacock) index, as shown in Figure 22. This index, which is given by the value of SiO_2 at the cross-over point at which the percentage of CaO is equal to that of $Na_2O + K_2O$, is widely used to determine the magmatic affinity of rock suites. Values of the alkali-lime index between

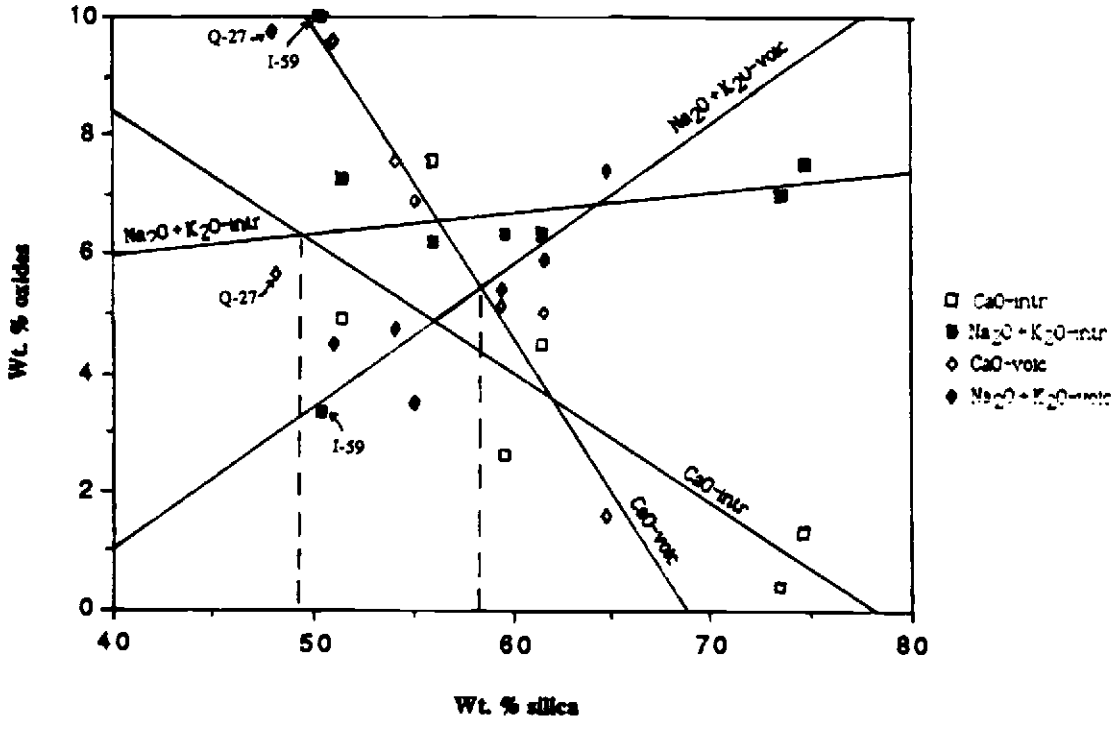

Figure 22- Peacock diagram for volcanic and intrusive rocks of the study area. Trend lines derived from simple regressions of the data points, exclusive of samples Q-27 (volcanic) and I-59 (intrusive).

55 and 61 percent are representative of the calc-alkaline igneous suite. The data from volcanic rocks yield a value of 58.5 percent silica for this index. Therefore, volcanic rocks from the Yellowbottom-Boulder Creek area are representative of a calc-alkalic sequence of magmatism. Data for the intrusive rocks (excluding sample I-59) give an index value of 49 percent silica, which is markedly different from that of the volcanic rocks. However, were sample I-59 to be included in the data set, the alkali-lime index would be raised to 56.5 percent, in closer agreement with that of the volcanic rocks.

Two interpretations of the data from the Peacock diagram for the intrusive rocks are possible. First, as suggested by Berg (1961), sample I-59 may be of a different and younger age than the main progression of intrusions. Provided this is the case, the main sequence of intrusive rocks are either alkalic in character, or have had their chemical composition modified by subsequent widespread hydrothermal alteration, a chemical change leading to a loss of CaO as a consequence of the conversion of plagioclase feldspar to sericite and clay minerals, which do not contain calcium. This type of alteration is observed in thin sections of most of the intrusive rocks from the area.

The second possibility is that sample I-59 is cogenetic with the other rocks, but that the variation diagrams contain insufficient data to define a linear trend. If it is assumed that the volcanic and intrusive rocks are cogenetic, and should therefore have a similar magmatic affinity, then the second explanation is more plausible. Furthermore, hydrothermal alteration in the Yellowbottom-Boulder Creek area is most likely the same age (Miocene), or slightly younger, than the dioritic plutonic rocks.

Accordingly, I consider sample I-59 and the other mafic plugs present in the area to be of Miocene age.

Major oxide data are plotted on AFM and NKC ternary variation diagrams in Figures 23 and 24. These diagrams plot the proportions of $Na_2O + K_2O$, $FeO + Fe_2O_3$, and MgO (AFM), and Na_2O, K_2O, and CaO (NKC), respectively. The approximate trends revealed by these diagrams for the volcanic and intrusive rocks are consistent with those of the calc-alkaline rocks as defined by Nockolds and Allen (1953).

Data for the intrusive rock samples display considerable scatter on the ternary variation diagrams, as was previously noted for the Harker diagrams. This variability is attributed to alteration of the intrusive rocks by hydrothermal fluids, as supported by dispersal of these data on the NKC diagram. The three oxides used to construct this diagram are, to a large extent, involved in fluid-rock reactions, and their concentrations are likely to have been changed during hydrothermal alteration.

Major-oxide compositions of samples of both volcanic and intrusive rocks, as plotted on the AFM diagrams, reveal a trend towards alkali enrichment relative to the oxides of iron and magnesium. Major-oxide compositions of the volcanic samples also follow the calc-alkaline trend of Nockolds and Allen (1953), when plotted on the NKC diagram, whereas those of the intrusive rocks display more variability. This study shows that some intrusive rocks from the Quartzville District are anomalously enriched in K_2O with respect to other intrusive rocks from the Western Cascades mining districts, a trend that was also revealed by Power (1984). The cause of this enrichment of K_2O is unknown. The composition of the mafic plug (I-59) falls within the tholeiitic field of

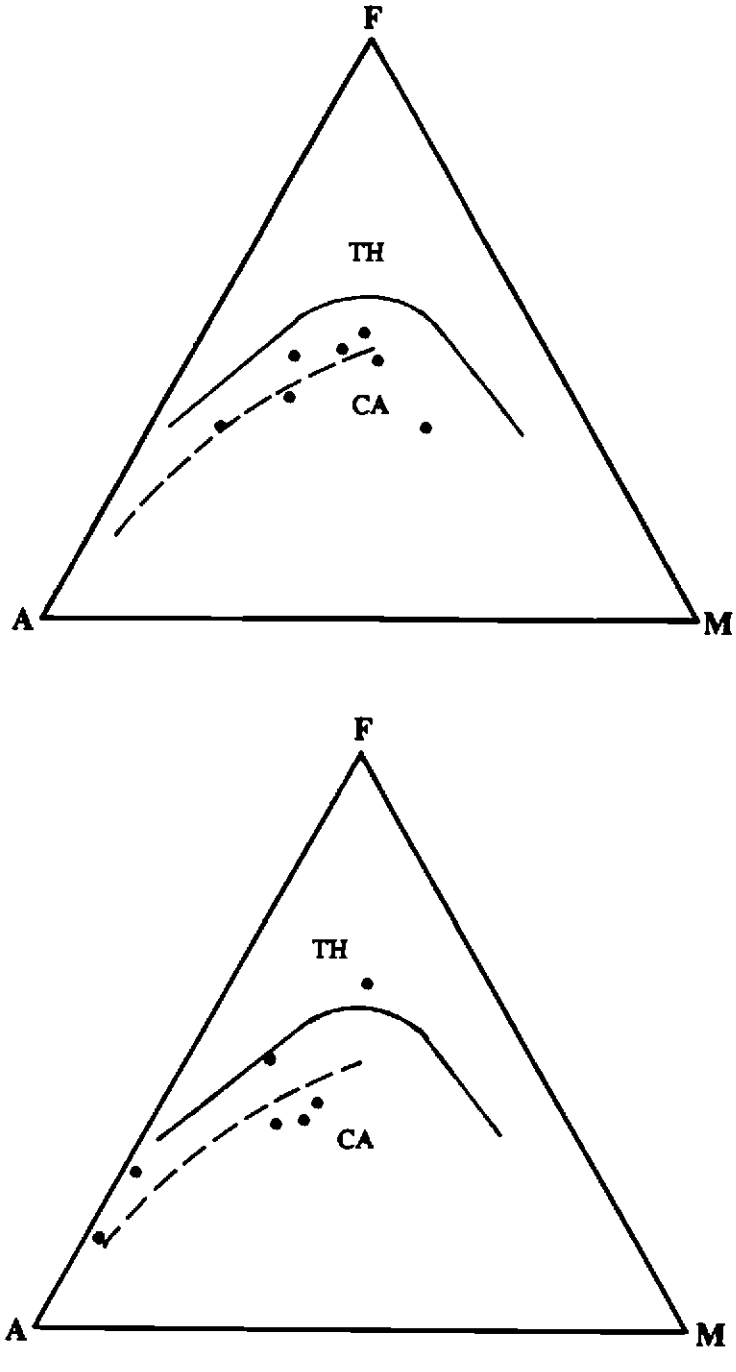

Figure 23- AFM ternary diagrams for volcanic (top) and plutonic (bottom) rocks of the study area (A = $Na_2O + K_2O$, F = $FeO + Fe_2O_3$, M = MgO). Solid line separates the tholeiitic and calc-alkaline fields of Irvine and Baragar (1971); dashed line is the calc-alkaline trend of Nockolds and Allen (1953).

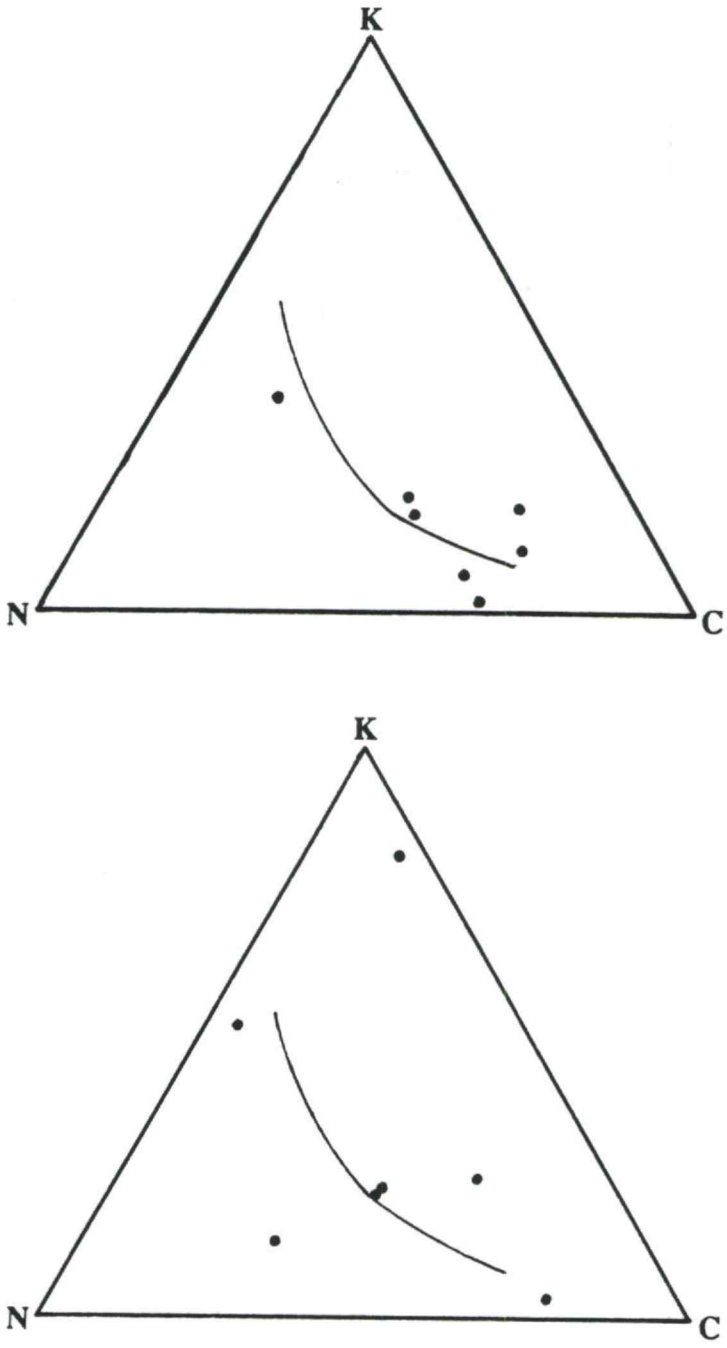

Figure 24- NKC ternary diagrams for volcanic (top) and intrusive (bottom) rocks of the study area (N - Na_2O, K - K_2O, C - CaO). Solid line is the calc-alkaline trend of Nockolds and Allen (1953).

Irvine and Baragar (1971), as plotted on the AFM diagram, as a consequence of the high iron content of this rock. All other samples plot within the calc-alkaline field.

The major-oxide chemistry of plutonic rocks from the study area and from the Western Cascades in general is similar to that of island-arc terranes, including the Southern California batholith (Nockolds and Allen, 1953), the Caribbean and southwestern Pacific (Kesler et al., 1975; Titley and Beane, 1981), and Pacific Northwest (Field et al., 1975) areas. The main difference in major-element chemistry between plutonic rocks associated with porphyry-type mineralization in island-arc regions and those of cratonic environments is the relative paucity of potassium in the former (Kesler et al., 1975). Most rocks from the Quartzville area also contain very little potassium feldspar, and it nearly always occurs as a late-stage mineral in the groundmass. The island-arc character of intrusive rocks from the study area is illustrated in Figure 25, which distinguishes rocks of cratonic and island-arc affinities based on distributions of SiO_2 versus $Na_2O + K_2O$ (Titley and Beane, 1981). Although there is some overlap of the two rock suites as plotted on this diagram, most samples of cratonic character will plot above the diagonal line, whereas most of those from island arc terranes will plot below it.

Depletion of K_2O in the plutons of island-arc terranes is considered to be representative of the more primitive nature of the magmas which formed these plutons as compared to those of cratonic regions (Kesler et al., 1975). Accordingly, island-arc magmas are derived from the mantle with little or no contamination from crustal material. Rocks of the Western Cascade mining districts contain K_2O concentrations intermediate

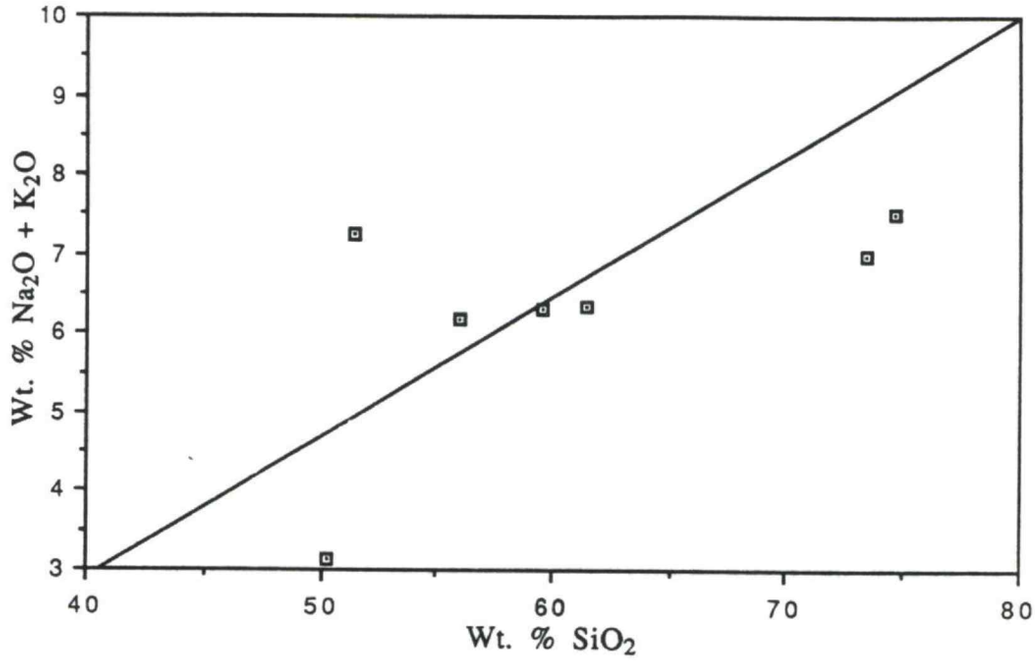

Figure 25- Alkali-silica diagram of intrusive rocks from the Yellowbottom-Boulder Creek area. Most samples from cratonic suites plot above the diagonal line whereas most of those from island arc terranes plot below it (Titley and Beane, 1981).

between those of the Caribbean and those of the southwestern U. S. (Power, 1984), and suggest that some crustal contamination or assimilation of subducted sediments into the magmas may have occurred in the Western Cascades (Power, 1984). This interpretation is substantiated by the presence of normative corundum in several of the samples (numbers TIB-121, I-18, I-33, I-111, A-35, TLA-39, and T-53) from the study area (Appendix A), and in other mining districts of the Western Cascades (Power, 1984). The presence of corundum in the normative analyses indicates an oversaturation of alumina, and is suggestive of the assimilation of crustal materials rich in aluminum. An alternative explanation is the hydrothermal formation of clay minerals that contain a higher percentage of alumina than the host minerals (dominantly plagioclase feldspars).

HYDROTHERMAL MINERALIZATION

Although the Yellowbottom-Boulder Creek area lacks any historical record of mineral production, the presence of several geologic and geochemical features found during this investigation are suggestive of economic mineralization. Prospects in the area are limited to a few small test pits excavated into veins in the vicinity of the confluence of Yellowstone Creek and Quartzville Creek. Features which warrant additional examination include large areas of pervasive propylitic alteration, zones of argillic-phyllic alteration, quartz-bearing porphyritic intrusions, breccia pipes, linear zones of intense silica replacement, and geochemically anomalous concentrations of base and precious metals. Alteration is often accompanied by disseminated pyrite, and less commonly by traces of galena and sphalerite. Quartz-carbonate-sulfide veins are present in a least one location. Argillic-phyllic alteration is localized along shear zones, faults, and lineaments, and in areas of brecciated rocks. These breccias are of several types, as has been discussed in a previous chapter. Anomalous metal concentrations are commonly, but not always, associated with these breccias. Silver is as high as 5.5 ppm in one breccia, which also contains 580 ppb gold. A single sample from a shatter zone in the Boulder Creek area apparently contains 11,420 ppb gold and 21 ppm silver. Several dikes and small plugs of dacitic composition contain quartz phenocrysts, are mineralized, and are associated with areas of argillic-phyllic alteration.

ALTERATION

All rocks of the Yellowbottom-Boulder Creek area, with the exception of those of Quaternary age, have been hydrothermally altered to some extent, presumably in association with the emplacement of the intrusive units. This alteration was accomplished by heated fluids which reacted with and replaced the primary minerals of the host rocks with several common assemblages of hydrothermal minerals. The assemblage produced is determined by several factors that include the primary mineralogy and chemistry of the host rocks, composition of the fluids, and temperature, pressure, and redox conditions of the system. These alteration assemblages normally display lateral and vertical zonations as a result of chemical and thermal gradients in the hydrothermal system.

Alteration intensity of rocks in the study area ranges from minor, selective clay and chlorite replacement of groundmass mafic minerals, to complete and pervasive replacement of all phases by quartz. Four different types of alteration are recognized: propylitic, argillic-phyllic, silica, and tourmaline-quartz. The alteration types in this study are largely, but not exclusively, those recognized in porphyry-copper districts and other mineralized areas by Burnham (1962), Creasy (1966), Meyer and Hemley (1967), Lowell and Guilbert (1970), Rose (1970), and Rose and Burt (1979).

Diagnostic alteration minerals are used to distinguish the various types. The propylitic alteration assemblage is characterized by calcite, epidote, albite, and chlorite; argillic by clay minerals of the kaolinite and montmorillonite groups; and phyllic by sericite. The argillic-phyllic

assemblage recognized in the study area combines minerals of both the argillic and phyllic assemblages from porphyry copper districts (Burnham, 1962; Lowell and Guilbert, 1970). However, it is designated the argillic-phyllic assemblage because the diagnostic mineral phases are usually fine-grained, intermixed, and physically similar in appearance, and thus are difficult to distinguish by optical examination. Potassic alteration, defined by secondary K-feldspar and (or) biotite, is not present in the Quartzville area, although it has been reported from other mining districts of the Western Cascades (Schriener, 1978; Schaubs, 1978; Olson, 1978). Silica is commonly a product of the various alteration reactions, with the result that quartz may be present in all of the alteration assemblages.

Alteration of the rocks of the Quartzville District, and other mining districts of the Western Cascades, is similar to that described for porphyry copper deposits at Bingham, Utah (Moore, 1978), El Salvador, Chile (Gustafson and Hunt, 1975), and San Manuel, Arizona (Lowell and Guilbert, 1970), and vein deposits at Butte, Montana (Meyer et al., 1968).

At San Manuel, the "typical" alteration zonation has been described by Lowell and Guilbert (1970), and serves as the model to which other porphyry copper districts are compared. This model consists of a central zone of potassic alteration, followed successively outward by concentric zones of phyllic and argillic alteration and a fringing zone of propylitic alteration that extends for considerable distance beyond. Changes in the sulfide mineralogy accompany the different alteration types, with centrally deposited bornite and chalcopyrite (and less commonly molybdenite and (or) chalcocite and covellite) giving way to pyrite at

peripheral locations. The most productive ore is found at the interface between the potassic and phyllic zones, and occurs as an ore "shell" containing 1-3 percent chalcopyrite. Lead, zinc, and silver mineralization is commonly present in veins at and beyond the peripheral zone of abundant pyrite.

Hydrothermal fluids responsible for alteration may be exsolved from cooling magmas undergoing solidification as a result of the concentration of water and incompatible elements during crystallization of anhydrous mineral phases (Burnham, 1967; 1979). Alternatively, groundwater in the vicinity of an intrusion may be heated and circulated through the rocks. Although the intrusion acts as a "heat engine" to drive the convection, it does not actually supply the water (see Meyer et al., 1968).

The primary reaction mechanisms for alteration of silicate minerals are hydrolysis, hydration, and base exchange (Hemley and Jones, 1964; Meyer and Hemley, 1967). Hydrolysis reactions consume H^+ ions and liberate an equivalent amount of cations to the fluid. This mechanism is characteristic of argillic and phyllic alteration and releases excess SiO_2 to solution, leading to supersaturation of silica in the hydrothermal fluids (Hemley and Jones, 1964). One result of these reactions is to replace feldspars with sericite and clay minerals while releasing K^+ ions to solution. Hydration reactions involve the combination of H_2O with other substances, as in the conversion of anhydrite to gypsum. Base-exchange reactions may lead to the formation of albite from calcic plagioclase by the replacement of calcium with sodium.

Major-oxide chemistry and mineralogical data for samples representing the various alteration assemblages discussed in this chapter

are presented in Table 21. A summary and comparison of these data to a sample which represents the unaltered equivalent of the altered rocks (TLA-38) is presented in Figure 26. Samples A-35, TLA-39, and T-53 are representative of the argillic-phyllic, propylitic, and tourmaline-quartz assemblages, respectively. Figure 26 was constructed from the major oxide data, and the specific gravity determined for each sample (Appendix A), to allow the concentrations of the various oxides to be reported in grams per cubic centimeter. This format provides for a better direct comparison of the gains and losses of major oxides in these samples. It should be noted that the geologic relationship of sample T-53 to the unaltered equivalent (TLA-38) has not been established, as is discussed more completely later, in the section on the tourmaline-quartz assemblage.

The pattern of argillic-phyllic alteration in the Yellowbottom-Boulder Creek area suggests a meteoric source for the hydrothermal fluids responsible. Some dikes in the area are surrounded by alteration envelopes ranging from several centimeters to several meters in width. These envelopes change from argillic-phyllic next to the dike to intense propylitic alteration with disseminated pyrite farther away. Additionally, the dikes are usually altered strongly to propylitic or argillic-phyllic assemblages. The correlation between argillic-phyllic alteration and structures such as faults and shear zones is also apparent on Plate 2, and suggests that meteoric waters invading these structures led to the development of this assemblage. In contrast, the large areal extent of propylitically altered rocks at Quartzville and elsewhere, and the higher intensity of propylitic alteration in intrusive rocks, may imply that

Table 21- Major oxide analyses (in percent), trace metal concentrations (in ppm), and specific gravity for samples representing altered rocks and their unaltered equivalent (TLA-38)

oxide	TLA-38	TLA-39	A-35	T-53
SiO_2	59.40%	56.64%	65.12%	48.06%
TiO_2	1.12	0.84	0.83	0.98
Al_2O_3	15.58	17.25	15.98	16.63
Fe_2O_3	2.09	3.72	3.81	11.12
FeO	4.12	2.30	0.59	1.47
MnO	0.12	0.10	0.04	0.02
MgO	2.13	3.46	2.26	2.19
CaO	5.12	6.52	0.23	3.02
BaO	0.06	0.03	0.15	0.01
Na_2O	3.64	3.22	0.27	4.39
K_2O	1.75	0.60	4.04	1.95
P_2O_5	0.39	0.33	0.21	0.34
LOI	2.64	2.90	4.90	8.81
TOTAL	98.16	97.91	98.43	98.99
Metals				
Cu	25 ppm	10 ppm	10 ppm	18 ppm
Mo	1	1	< 1	< 1
Pb	8	12	3	9
Zn	50	35	35	15
Ag	< 0.3	< 0.3	< 0.3	0.3
S. G.	2.59	2.69	2.42	2.68

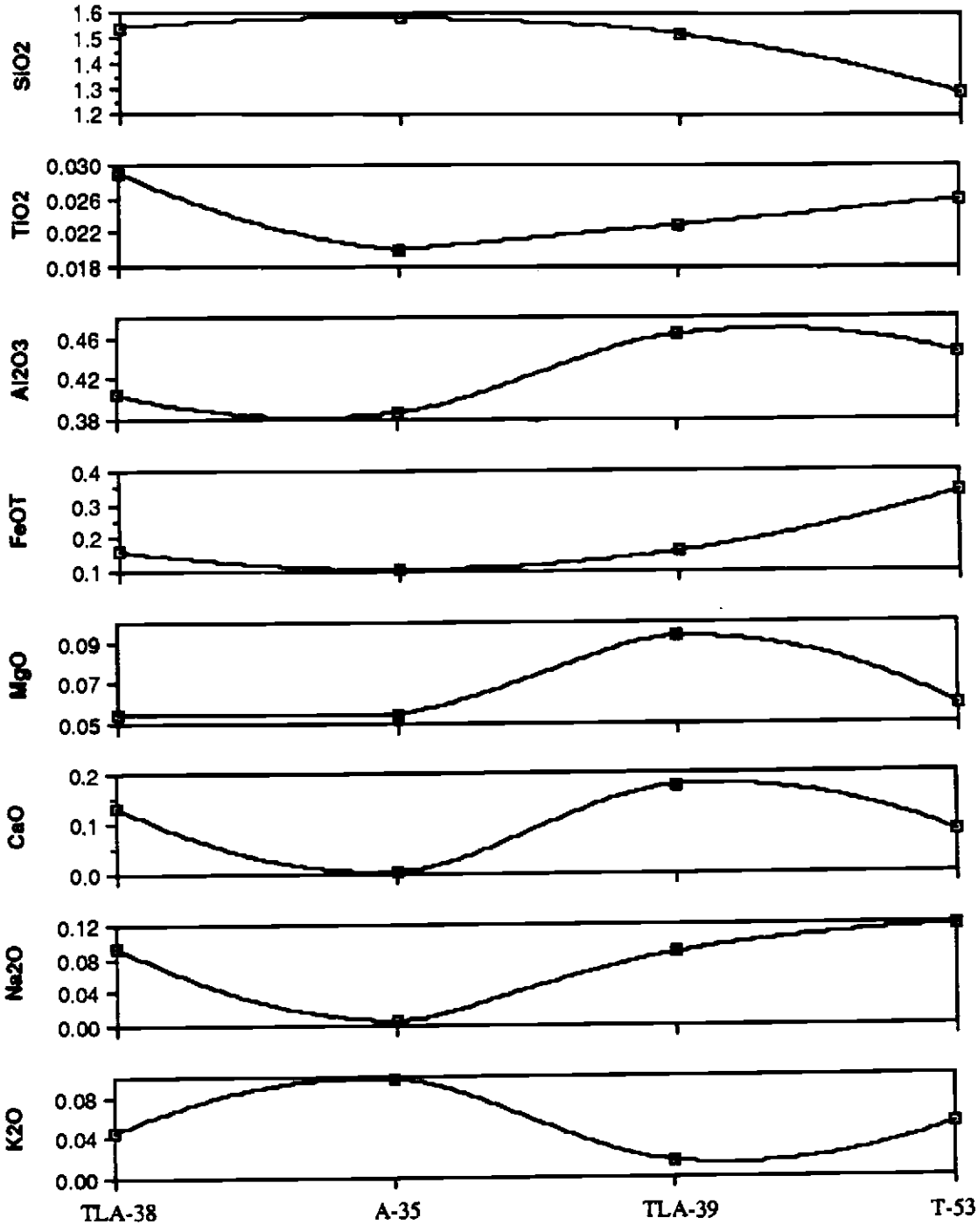

Figure 26- Chemical changes associated with argillic-phyllic (A-35), propylitic (TLA-39), and tourmaline-quartz (T-53) alteration, reported in grams per cubic centimeter. Sample TLA-38 represents the unaltered equivalent of the other samples.

magmatic waters were the fluids responsible for the formation of this assemblage. Sulfur-isotope data reported in this study and previously by Power (1984) suggest a magmatic source for the sulfur in sulfide minerals of the area. However, ^{18}O data for seven intrusive centers in the Western Cascades, according to H.P. Taylor (1971), indicate that rocks of the propylitic assemblage have been depleted in ^{18}O by an average 5 to 7 per mil. This major isotopic anomaly indicates a large-scale interaction of ^{18}O-depleted meteoric waters with the cooling plutons. This interaction is thought to have "overprinted" the earlier isotopic signature of magmatic fluids with that of meteoric waters.

Propylitic Assemblage

Propylitic alteration is widespread in the Yellowbottom-Boulder Creek area, the Quartzville area (Munts, 1978), and elsewhere in the Western Cascades (Buddington and Callaghan, 1936; Peck et al, 1964; Power, 1984; Field and Power, 1984; Field et al., 1987). It is present as alteration halos that surround the intermediate intrusions and all known occurrences of base and precious metal deposition in the Western Cascades. Alteration intensity of rocks in the Yellowbottom-Boulder Creek area ranges from a few percent of secondary chlorite selectively replacing groundmass minerals and mafic phenocrysts to a pervasive assemblage of chlorite, calcite, epidote, and pyrite replacing all phases of the host rock except quartz and apatite. Variable amounts of sericite, albite, quartz, magnetite, and clay minerals also are present in this assemblage. Because of difficulties in optical recognition, albite may be more common than reported, occurring as replacement rims around plagioclase

phenocrysts and microlites. The kinds and proportions of the individual alteration minerals are variable at different locations. Some rocks lack epidote or calcite, whereas others are cut by veins of one or both.

Sample TLA-39, an andesite from the lower andesite unit, is representative of typical propylitic alteration in the Yellowbottom-Boulder Creek area. Phenocrysts of plagioclase feldspar have been altered to an assemblage of epidote, quartz, and clay minerals. Clays (montmorillonite ?) occur as reaction rims around all plagioclase phenocrysts in the thin section. Mafic phenocrysts, presumably clinopyroxenes, have been replaced by aggregates of epidote, quartz, and calcite, with minor sericite and clay (montmorillonite ?). Groundmass mafic minerals have been altered to chlorite, clay (montmorillonite ?), and calcite, whereas the plagioclase microlites have been partially altered to clay minerals. Cubic pyrite and anhedral quartz are disseminated throughout the groundmass. Some pyrite has been altered to hematite, presumably as a result of weathering.

Sample TLA-39 has been depleted in the oxides of silicon, sodium, potassium, and titanium, as shown in Figure 26, when compared to a sample of less altered andesite (TLA-38) taken from an outcrop a few hundred feet away. Oxides of magnesium and calcium were apparently added during hydrothermal alteration. Oxides that display the greatest change are CaO, MgO, and K_2O, which suggests that calcium and magnesium metasomatism was a primary alteration mechanism. The predominance of chlorite in this assemblage also indicates that MgO was added to the host (Meyer and Hemley, 1967). The introduction of these oxides to the rock, presumably accompanied by CO_2, resulted in the

replacement of plagioclase feldspar by epidote and calcite, and the mafic minerals by chlorite and calcite. Analyses of the metal content of this sample indicate only background concentrations of Ag, Pb, Cu, Mo, and Zn.

Chemical equations can be written which model reactions that may take place during propylitic alteration, although each may be imprecise. For example, equation 1, which describes the conversion of andesine to clinozoisite and albite, may be as follows (Meyer and Hemley, 1967, p. 207):

$$2\ NaCaAl_3Si_5O_{16} + 2\ SiO_2 + Na^+ + H_2O \text{ ---> } Ca_2Al_3Si_3O_{12}(OH) + 3NaAlSi_3O_8 + H^+ \quad (1)$$

Note that this reaction liberates H^+ ions, which may then be available for subsequent hydrolysis reactions.

A sample of quartz monzodiorite from the Yellowbottom Stock (I-14) displays similar alteration to that in the andesite (TLA-39). Mafic minerals have been replaced by an assemblage of epidote, chlorite, and calcite, and phenocrysts of plagioclase feldspar were replaced by sericite and clay minerals (and possibly albite). The chlorite in this sample displays the anomalous "Berlin blue" interference color characteristic of pennine, which is the magnesium end-member of the chlorite series (Kerr, 1977), suggesting that magnesium metasomatism was a prevalent component of the alteration process. However, optical properties of chlorites are not always a reliable indicator of the composition or structure of these minerals (Nesse, 1986).

Some basaltic rocks of the lower andesite and intermediate basalt units contain irregularly-shaped veins and veinlets, stringers, and blebs of chalcedonic quartz that may range up to one-half meter in width. This quartz is typically white and blue chalcedony and dull to bright-red jasper. A sample of this jasper contains only background values of Au, Ag, Cu, Pb, Zn, and Mo, and thus has undergone very little metallization. The intensity of hydrothermal alteration of these basalts is comparatively weak, and consists mainly of minor quantities of chlorite and clay that replace the mafic groundmass minerals. These irregularly shaped veins and blebs in rocks of low alteration intensity, coupled with the low metal values, suggest that the quartz formed as the result of silica leached by heated groundwaters and subsequently redeposited in cooler environments. This style of alteration is observed only in flows from the lower andesite and intermediate basalt units, which collectively exhibit low intensities of alteration. Such occurrences of chalcedonic quartz and (or) quartz veins in basalt elsewhere are considered to be of similar origin (C. W. Field, September 1987, personal communication).

Argillic-Phyllic Assemblage

Argillic-phyllic alteration is present locally and is structurally-controlled in the Yellowbottom-Boulder Creek area, as shown on Plate 2. This alteration type is characterized by the replacement of plagioclase feldspar and mafic minerals by quartz, sericite, and clay minerals, and is normally accompanied by variable amounts of disseminated pyrite. Outcrops of argillic-phyllic alteration are markedly conspicuous, as the replacement of primary minerals by sericite and clays results in a

distinctly bleached appearance of the rock. Additionally, these outcrops are commonly iron-stained with limonite, that forms by the dissolution of pyrite in oxygenated groundwaters and subsequent deposition of jarosite, goethite, and hematite.

The most continuous areas of argillic-phyllic alteration are in and near several of the larger dioritic intrusions. Sample A-138 was collected from the dioritic rocks exposed in the center of Section 19 (Plate 1). Phenocrysts of plagioclase feldspar in the diorite have been altered to a fine-grained aggregate of sericite, clay minerals, and quartz. Groundmass minerals have been replaced by diffuse patches containing approximately 70 percent sericite and 30 percent clay (kaolinite ?). Phenocrysts of mafic minerals have been converted to epidote and pyrite. The original secondary pyrite content of this rock is estimated to have been about 10 percent by volume, but much of this pyrite was apparently removed by supergene leaching. Pyritohedron and cubic void spaces are present, usually in association with epidote, and are commonly infilled or lined with hematite and jarosite deposited as a result of the breakdown of pyrite. A few of these void spaces have a pyramidal shape, which suggests that chalcopyrite may have also been present. The reaction which describes the breakdown of pyrite under oxidizing conditions in the presence of water is as follows (Rose, 1970):

$$FeS_2 + 7/2O_2 + H_2O \longrightarrow H_2SO_4 + FeSO_4 \qquad (2)$$

Note that this reaction produces a strong acid. It is possible that much of the argillic-phyllic alteration has resulted from hydrogen-ion

metasomatism due to supergene leaching by this acid, and therefore these minerals may not be entirely hypogene (hydrothermal).

Some features observed in thin section also suggest that two episodes of alteration may have affected sample A-138. An early hydrothermal event resulted in the replacement of mafic phenocrysts by epidote and pyrite, with most of the pyrite being removed by leaching during a subsequent argillic-phyllic supergene event. Evidence to support this is the association of epidote, a propylitic mineral, with the void spaces formerly occupied by pyrite that may also have accompanied propylitic alteration.

Local zones of argillic-phyllic alteration are present along shear zones or fractured rocks in many parts of the Quartzville area. These zones are as much as 20 meters across, contain up to 10 percent disseminated pyrite, and have been pervasively silicified. Iron-oxide stains and void spaces are abundant, and indicate the former presence of sulfides that have been removed by supergene leaching.

Sample A-35 was collected from a local zone of argillic-phyllic alteration a short distance up Quartzville Creek from sample TLA-38. A thin section of this rock displays a fine-grained mixture of sericite and clays (kaolinite ?) replacing phenocrysts of plagioclase feldspar. The groundmass has been replaced by a mosaic of anhedral quartz, sericite, and clay minerals. Void spaces are mantled by hematite and jarosite, which also fill small fractures in the rock. Propylitic minerals are not present in this sample. Concentrations of the major oxides in sample A-35 are compared to those of the relatively unaltered andesite (TLA-38) in Figure 26. For this alteration assemblage, additions of SiO_2 and K_2O are

readily apparent, accompanied by large depletions in CaO and Na_2O and smaller decreases of FeO_T and TiO_2. These chemical changes are typical of hydrolysis reactions, which lead to the liberation of cations to the solution and the deposition of quartz as the result of a supersaturation of silica in H^+-rich hydrothermal solutions. Reactions which illustrate the conversion of plagioclase feldspar to sericite, clays, and quartz, are given in equations 3 and 4. Equation 3, modified from equations given by Rose and Burt (1979) and Creasy (1966) for the replacement of alkali feldspar by sericite and quartz, shows one possible reaction for the alteration of andesine to sericite and quartz:

$$NaCaAl_3Si_5O_{16} + 2H^+ + K^+ \longrightarrow KAl_3Si_3O_{10}(OH)_2 + 2SiO_2 + Na^+ + Ca^+ \quad (3)$$

Note that this equation satisfies the changes in chemistry observed for sample A-35, in that K_2O is added to the rock, whereas CaO and Na_2O are released to solution. The formation of kaolinite may occur as a secondary reaction involving the hydrolysis of previously-formed sericite (Rose and Burt, 1979; Creasy, 1966), as presented in equation 4:

$$KAl_3Si_3O_{10}(OH)_2 + H^+ + 3/2\ H_2O \longrightarrow 3/2\ Al_2Si_2O_5(OH)_4 + K^+ \quad (4)$$

Concentrations of the metallic elements are at only background levels in sample A-35.

Silica

Some rocks in the Yellowbottom-Boulder Creek area have been flooded with silica, usually without the formation of other alteration minerals. This type of alteration is usually present where host rocks have been brecciated, as shown in samples A-62, B-86, B-112, and B-112a. These rocks were brecciated and subsequently flooded by silica- supersaturated solutions that replaced the primary minerals with an interlocking mosaic of quartz. In some instances, fine-grained pyrite also was deposited with this quartz.

Silicification may take place either with the hydrothermal addition of silica to the host rock, or with selective base leaching that leaves quartz as a residual phase (Meyer and Hemley, 1967). Deposition of quartz is most readily accomplished by a decrease in temperature that accompanies the ascent of fluids from deeper depths in the conduit, or from the boiling of the ascending fluids (Rose and Burt, 1979). Silicification is commonly closely associated with the deposition of sulfide ores. In epithermal systems, silica is commonly a residual phase left by the leaching of bases by strong acids produced from the oxidation of H_2S (Rose and Burt, 1979).

Tourmaline-Quartz Assemblage

The fourth variety of alteration is present at the confluence of Quartzville and Yellowstone Creeks, associated with a breccia zone. This alteration assemblage includes tourmaline, pyrite, clay minerals, sericite, chlorite, quartz, and apatite. Tourmaline in the Western Cascades is

commonly associated with breccia pipes and copper mineralization (Power, 1984).

Tourmaline occurs as sunbursts of Fe-rich shorl, intergrown with cubes and irregular masses of pyrite. Mafic minerals have been replaced by clay minerals and minor quartz, whereas plagioclase feldspar has been replaced by coarse-grained sericite and clays. Some veinlets containing quartz, tourmaline, and pyrite have been observed in thin section (sample T-53). Voids of irregular shape are also present and suggest the removal of copper sulfides.

Major-oxide analysis of sample T-53, compared to a relatively unaltered andesite sample (TLA-38) in Figure 26, suggests depletion of SiO_2 and CaO, and addition of FeO_T, Al_2O_3, Na_2O, and K_2O. The concentration of iron has apparently more than doubled, corresponding to the deposition of large amounts of pyrite in the breccia zone. The apparent additions of Al_2O_3 and Na_2O may be indicative of the large amounts of clay minerals in the sample, whereas K_2O, presumably added by hydrothermal fluids, was fixed in sericite. However, the geologic relationship of this sample to that of the control sample (TLA-38) is not known, as mentioned on page 133. Both samples were collected from the same rock unit (lower andesite unit), but it cannot be determined whether the host rocks for the breccia zone were basaltic or andesitic. Volcanic rocks in the immediate vicinity of the breccia are similar in composition to that of sample TLA-38, but formation of this zone may have been accompanied by the translocation of wall rocks from depth, which may have possessed different major oxide chemistry than those at the present surface. Metallic element analyses of this sample indicate

that it is depleted in all metals relative to average background values from the area. This depletion may have resulted from the selective leaching of cations as a consequence of the hydrolytic reactions in the presence of acidic fluids that resulted in the replacement of plagioclase feldspar by sericite and clays.

Distribution of Trace Metals

Concentrations of silver, copper, lead, zinc, and molybdenum were determined for 45 samples by Chemical and Mineralogical Services of Salt Lake City, Utah. These analyses are representative of the spectrum of rock types, alteration, and mineralization present in the Yellowbottom-Boulder Creek area. Seven of these samples were also assayed for gold. An additional 23 analyses of altered rocks, vein material, and breccia zones from the study area were kindly provided by Orvana Resources Corporation. These analyses reported antimony, arsenic, nickel, bismuth, cobalt, barium, and potassium, in addition to the six metals previously named. Stream sediment was collected from each of the five major drainages in the area, and submitted for silver, copper, lead, zinc, and molybdenum analyses. Complete results of these determinations are listed in Appendix B, and sample locations are shown on Plate 3.

In order to maintain consistency of the data from the study area, only the results from Chemical and Mineralogical Services are used in the discussion of metal distribution. A large set of chemical analyses of volcanic and intrusive rocks from the Western Cascades exists, which were previously performed by this company.

Comparisons of the values obtained for Ag, Cu, Pb, Zn, and Mo to the average concentrations for granodiorite, for Caribbean intrusions associated with porphyry copper deposits, and for Western Cascade rocks are presented in Table 22. Rocks of the study area are depleted in Cu, Pb, and Zn compared to all the others listed. This depletion of base metals may be the result of the inclusion of oxidized samples in the data set, which may have been leached of these elements. Silver values for rocks of the study area and the Western Cascades in general are higher than the listed averages, perhaps as a result of ubiquitous propylitic alteration present in all mining districts of the subprovince.

Threshold values of the various metals for the rocks of the study area are presented in Table 23. These values were determined graphically from log-probability plots of metal concentrations versus cumulative frequency, as depicted in Figure 27. Plotted in this way, a linear distribution indicates a simple log-normal population of samples. Multi-modal populations are characterized by two or more line segments, and the inflections between these segments define the different sample populations (Lepeltier, 1969). Distributions of Cu, Pb, Zn, and Ag display well-defined inflections separating background values from mineralized values (Figure 27). Background is defined as the average (mean) of the normal range of concentrations in unmineralized rocks of an area (Levinson, 1974), and presumably represents the primary magmatic metal content. Mineralized samples reflect the hydrothermal addition of metals. Threshold values for the study area rocks are comparable to the averages for the Pacific Northwest, but lower for Cu, Pb, and Mo as compared to the average Western Cascade rocks (Table 23).

Table 22- Comparison of metallic element concentrations from the study area with published averages. Metal values in ppm (Au in ppb).

metal	Study area		Western Cascades[1]		Average granodiorite[2]	Caribbean intrusions[3]
	average[4]	range	average[4]	range	average	average
Ag	.28	.2-5.5	.4	< .2-151	.07	--
Cu	22	4-495	35	5-91,000	30	61
Pb	8.5	2-930	20	4-90,000	15	7.5
Zn	35	3-520	40	5-72,000	60	50
Mo	.64	< 1-50	2	< 1-455	1	--
Au	5.5	< 2-580	3	< 2-4,250	--	--

[1]Field et al., 1987
[2]Turekian and Wedepohl, 1961
[3]Kesler et al., 1975
[4]average background value, excluding mineralized samples

Table 23- Threshold values determined from cumulative frequency diagrams.

metal	study area	Western Cascades[1]	Pacific Northwest[2]
Ag	.6 ppm	.6 ppm	1 ppm
Cu	60	80	50
Pb	20	50	30
Zn	90	70	100
Mo	< 1	4	1
Au	8 ppb	6 ppb	--

[1]Field et al., 1987
[2]Field et al., 1974

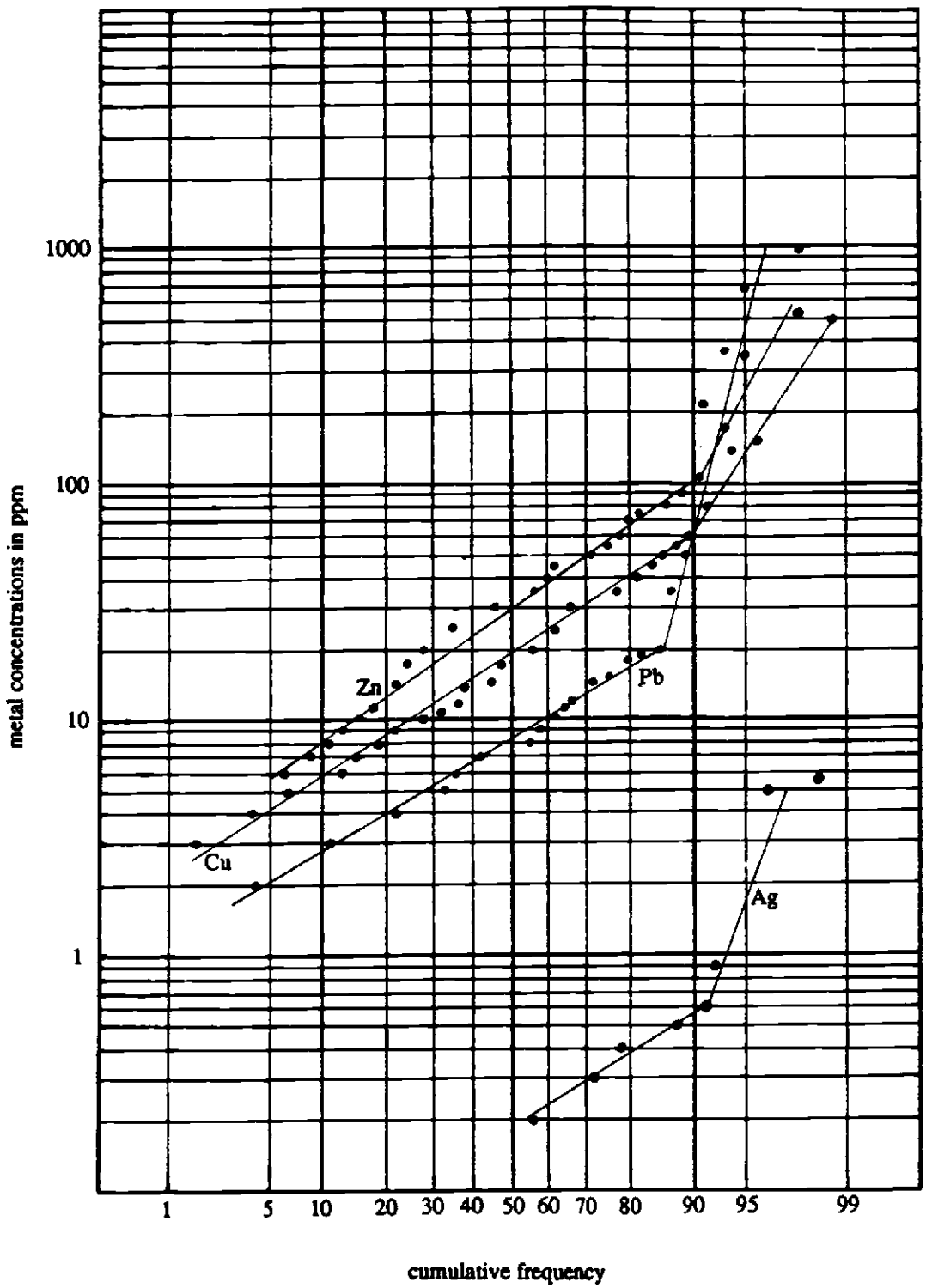

Figure 27- Cumulative frequency distributions of Cu, Pb, Zn, and Ag in the study area.

The spatial distributions of Cu, Pb, Zn, Mo, Ag, and Au are shown in Figures 28, 29, 30, 31, 32, and 33 respectively. Although concentrations of the metals are distributed without an obvious pattern, it is apparent that Sections 31 and 36 contain the highest proportion of anomalously high samples of gold (up to 580 ppb), silver (up to 5.5 ppm), and copper (up to 495 ppm).

Correlation coefficients among the metals were determined using the Statview program for the MacIntosh, as presented in Table 24. Strong correlations are observed between Mo and Ag, and Cu and Zn, whereas Pb has an antipathetic relationship with both Cu and Zn.

Table 24- Correlation matrix for metallic elements from the study area.

	Ag	Cu	Mo	Pb	Zn
Ag	1				
Cu	.62	1			
Mo	.871	.242	1		
Pb	.467	.014	.498	1	
Zn	.559	.752	.249	.115	1

Data for Cu, Pb, and Zn are plotted on a ternary diagram in Figure 34. This diagram shows that Pb and Zn mineralization in the study area is associated with vein-type deposition, except for one Cu anomaly that may be related to porphyry-type deposition. Comparison of this diagram to those presented by Power (1984) for other mining districts of the Western Cascades shows that the North Santiam, Detroit Dam, and the districts to the north in Washington are enriched in copper relative to the Yellowbottom-Boulder Creek area, whereas those districts to the south (Bohemia and Blue River) contain more zinc. This geographic change in the distribution of metals may be related to the depth to which each

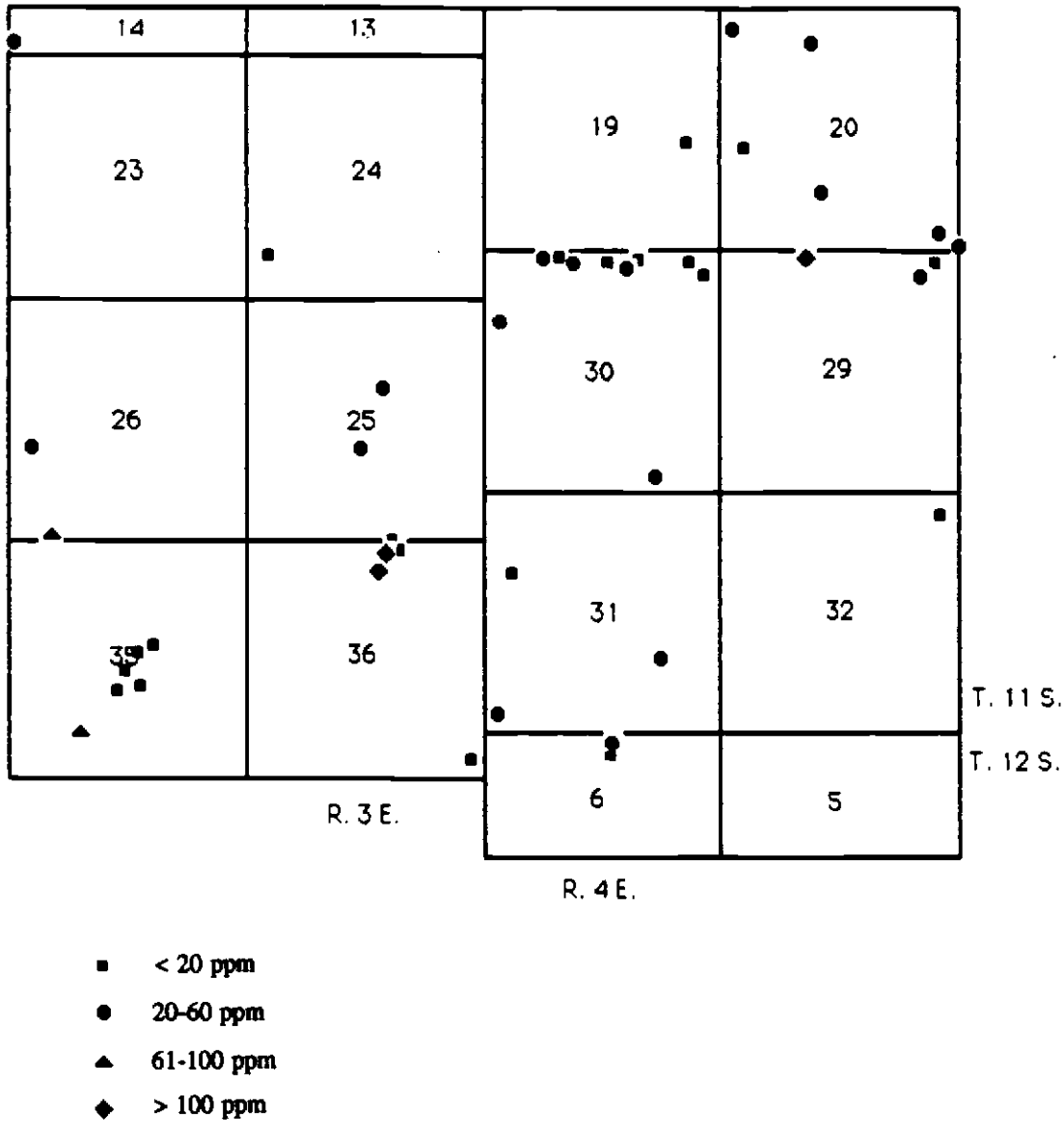

Figure 28- Distribution of copper values in rock-chip samples.

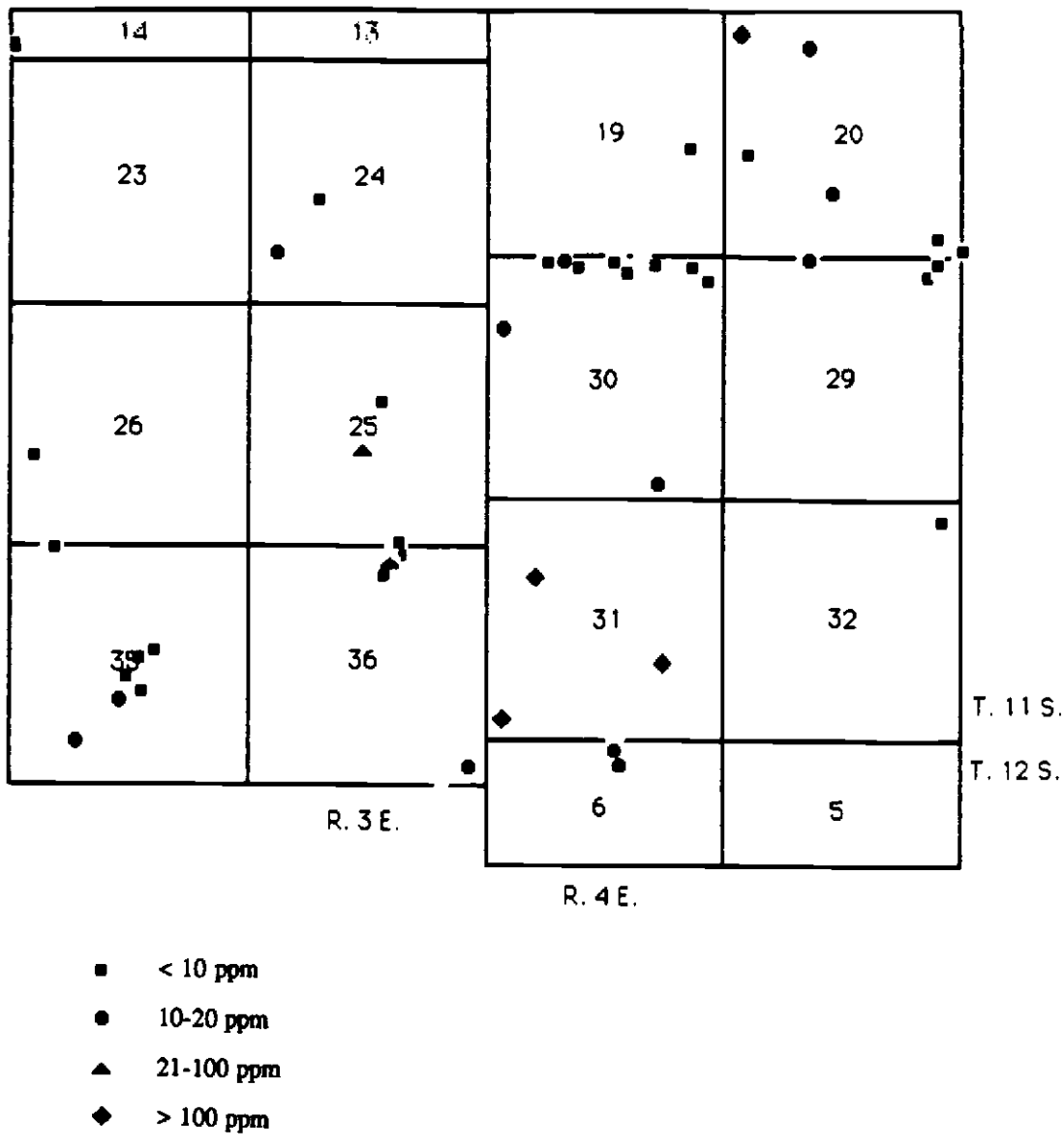

Figure 29- Distribution of lead values in rock-chip samples.

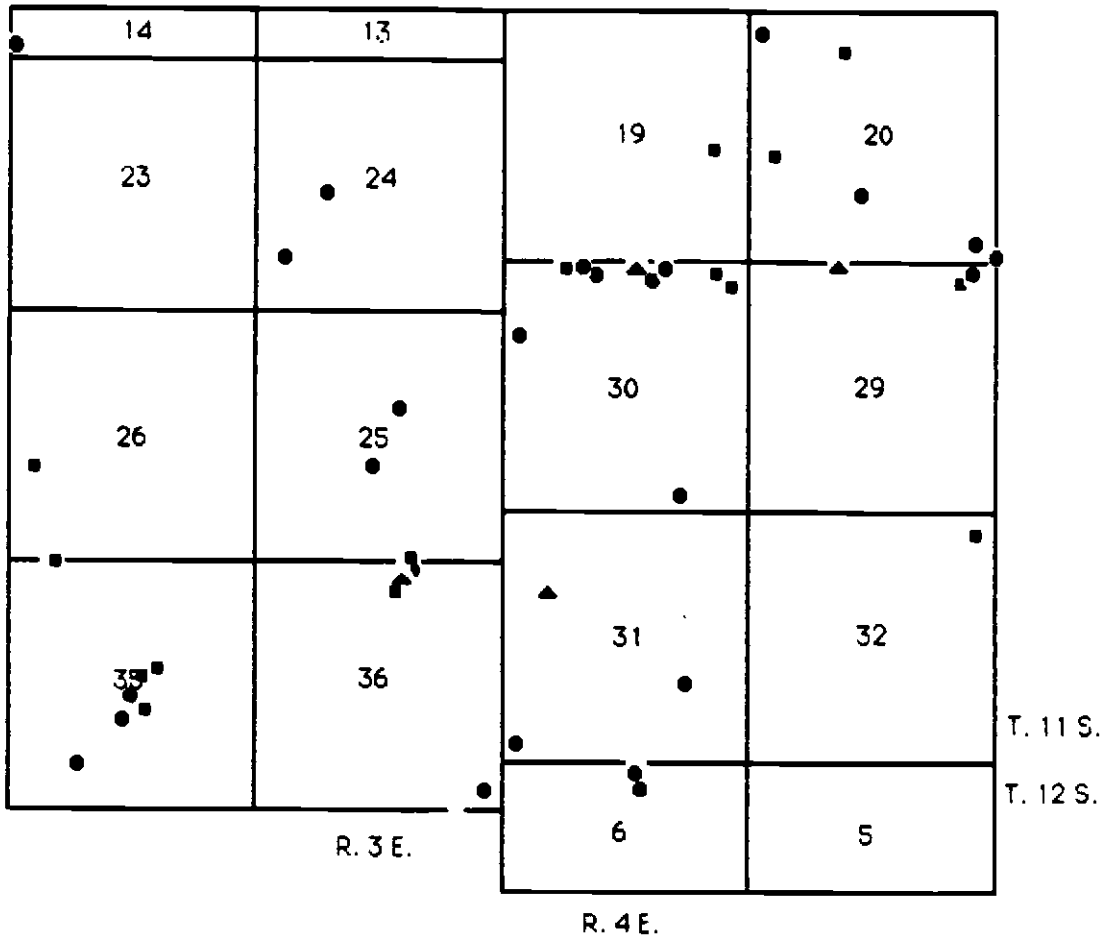

Figure 30- Distribution of zinc values in rock-chip samples.

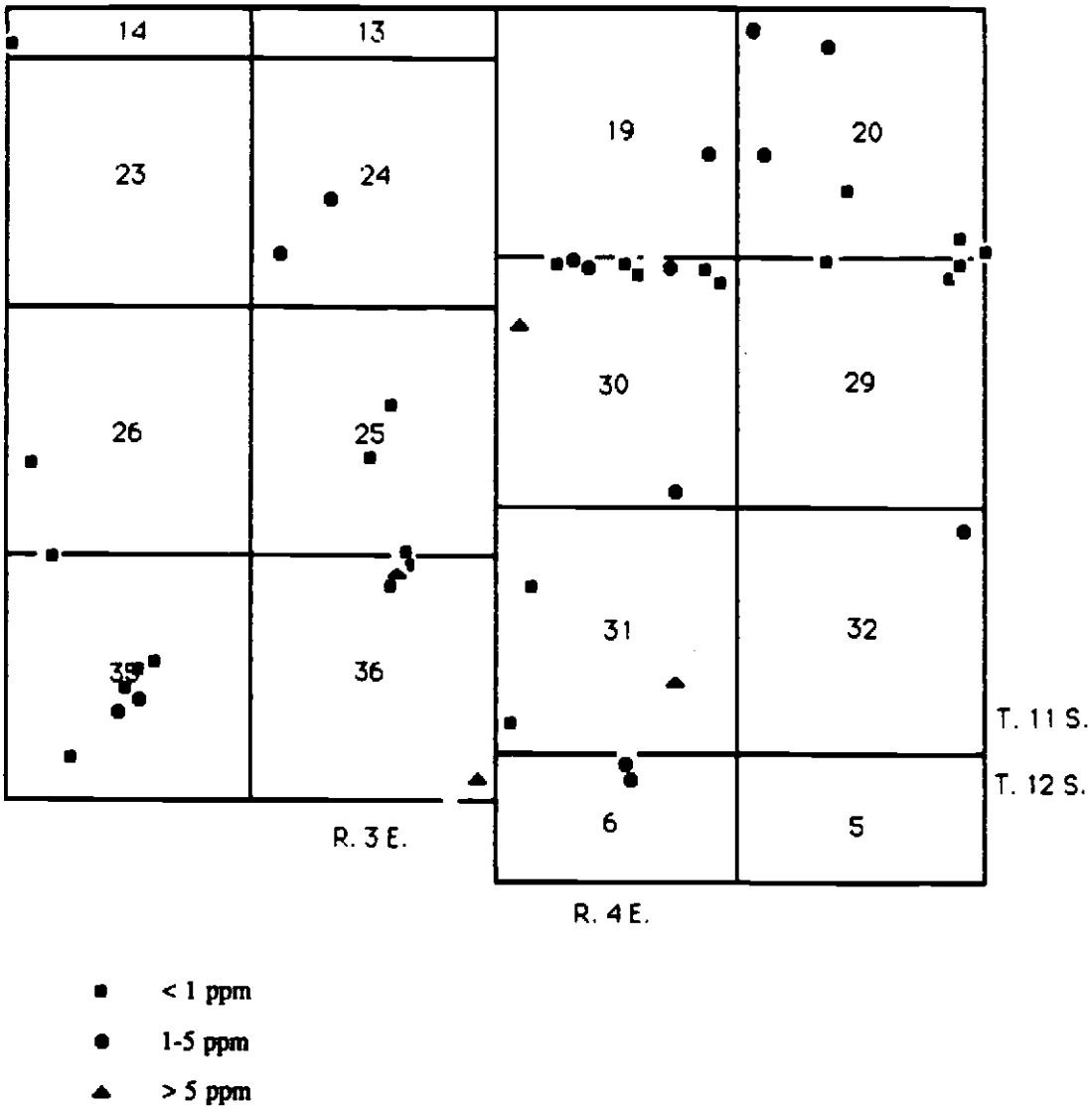

Figure 31 - Distribution of molybdenum values in rock-chip samples.

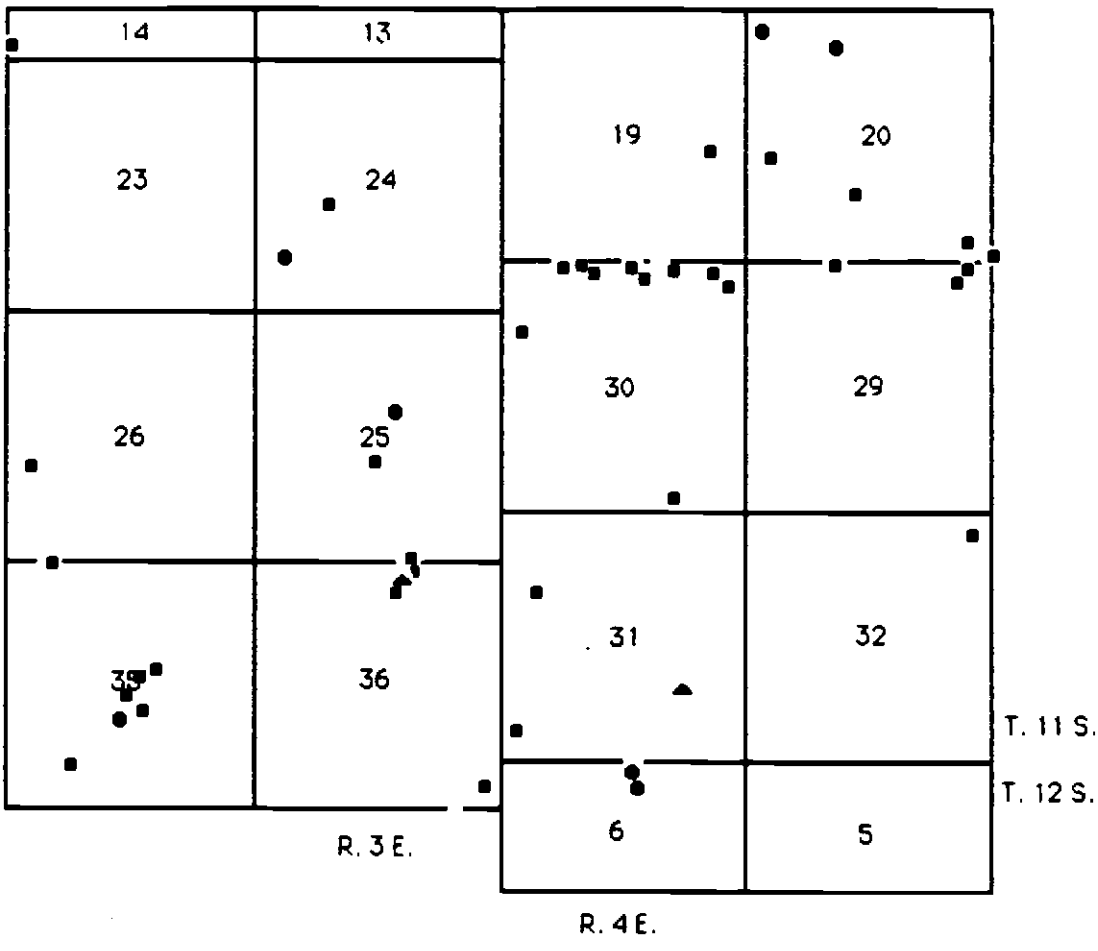

Figure 32- Distribution of silver values in rock-chip samples.

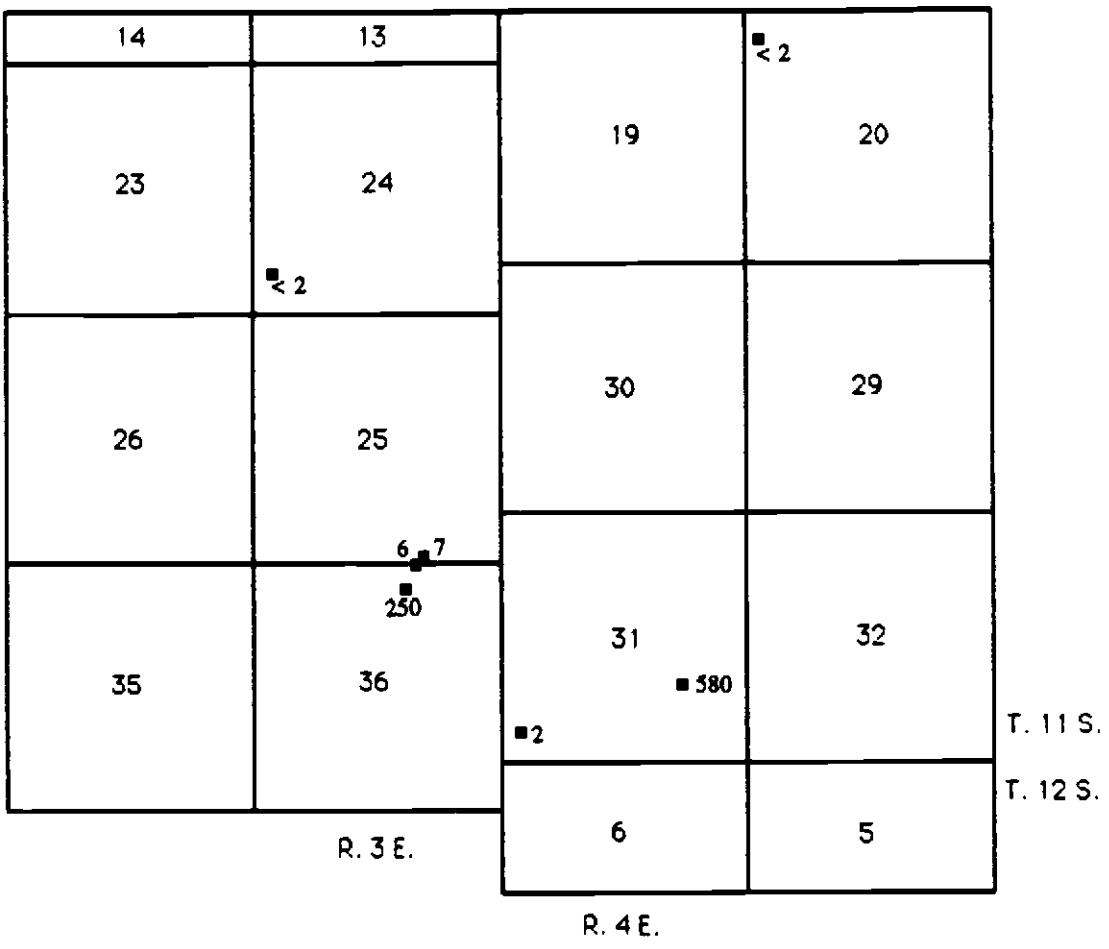

Figure 33- Distribution of gold values in rock-chip samples, indicated in ppb for each sample.

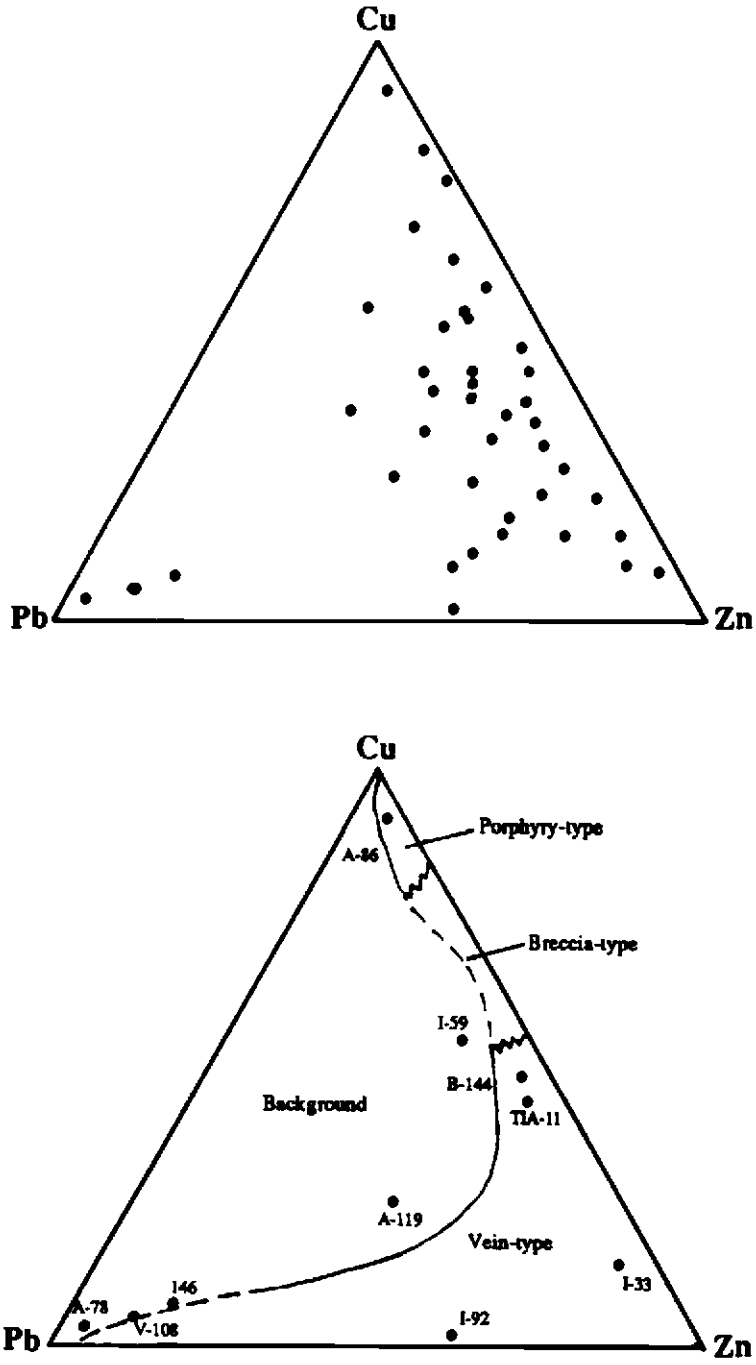

Figure 34- Cu-Pb-Zn ternary diagrams for all samples (top) and mineralized samples (bottom) from the Yellowbottom-Boulder Creek area. Mineral deposit domains are those of Field et al. (1987).

district has been eroded: those to the north expose deeper levels of the hydrothermal system (John Curless, Oregon State University M.S. Thesis in progress; Power, 1984).

Trace-metal data provided by Orvana Resources Corporation reveal similar trends to those obtained from Chemical and Mineralogical Services. A twelve-sample set was collected from the shatter zones in Sections 31 and 36 (Appendix B- samples 10005-10016). These data show that the shatter zones are deficient in Cu, but enriched in Pb, Zn, Mo, Ag, and Au. A single sample of ore-grade material assayed 11,420 ppb Au and 21 ppm Ag. The data also suggest that Sb and As cannot be used as indicator elements in this area, as both show erratic correlations with Au and Ag anomalies.

Deposition of Sulfides

The processes of hydrothermal alteration and ore deposition are closely linked (Creasy, 1966; Meyer and Hemley, 1967; Rose and Burt, 1979). Alteration minerals in the Yellowbottom-Boulder Creek area are commonly accompanied by disseminated pyrite, especially in areas of intense propylitic and argillic-phyllic alteration. The distribution of disseminated pyrite in the study area is shown in Figure 35. This pyrite is usually in cubes up to 2 mm in diameter, although pyritohedrons are also present in lesser quantities. One breccia pipe, intersected by the Boulder Creek road near the eastern boundary of Section 36, contains numerous pyritohedrons up to 1 cm in diameter. Pyrite also occurs as

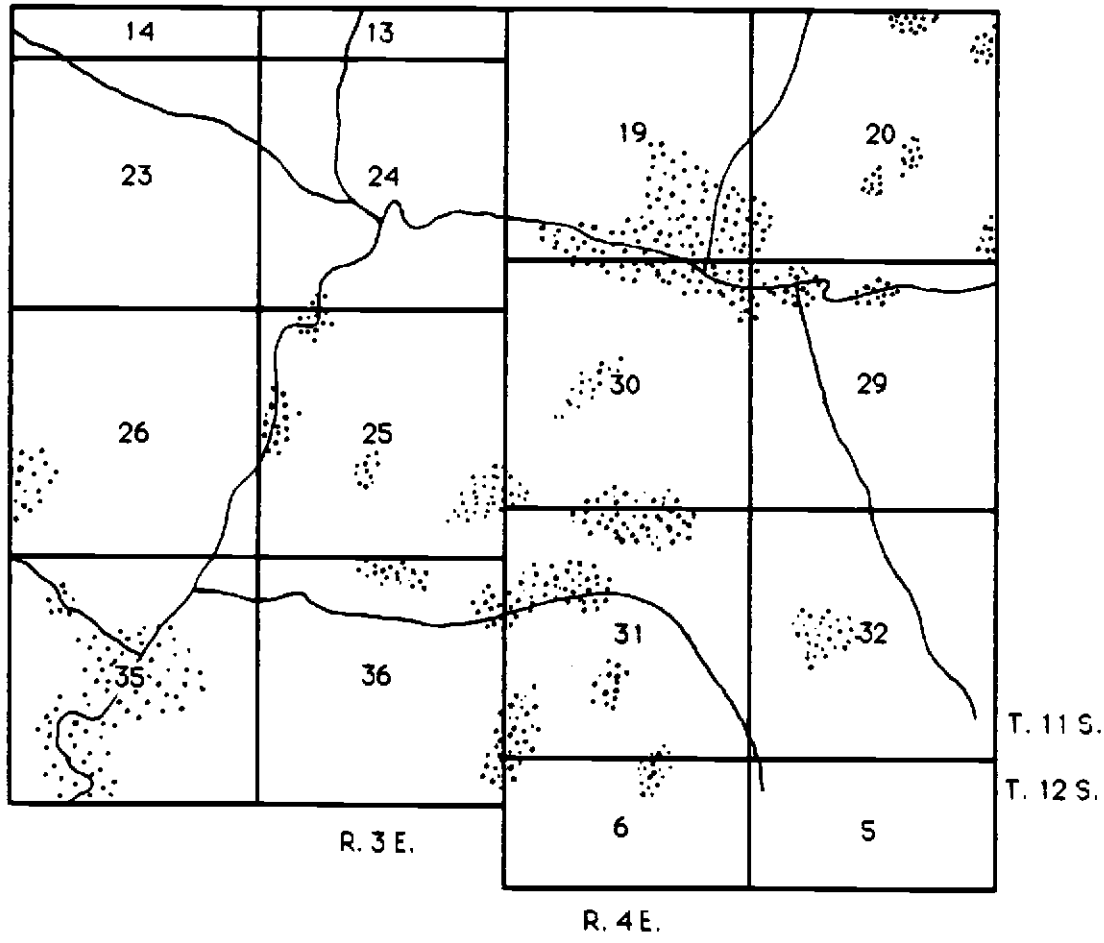

Figure 35- Distribution of disseminated pyrite in rocks of the Yellowbottom-Boulder Creek area.

finely divided crusts coating fractures, and as what appears to be immiscible sulfide droplets in a tonalite intrusion.

Galena and sphalerite are sparingly present in the Yellowbottom-Boulder Creek study area. These sulfides were deposited in veinlets with calcite and quartz (sample 148, not analyzed) that cut the volcaniclastic host rock exposed at the north end of the cluster of shatter zones in the southwest corner of Section 31. Concentrations of Pb are anomalous in wall rocks surrounding these veins (sample 146, 370 ppm); however, Zn content (70 ppm) is within the range of background values. Disseminated lead and zinc sulfides also may be present in other rocks of the immediate area, as anomalous values of these metals were identified by geochemical analyses provided by Orvana Resources Corporation (Appendix B, samples 10005-10016). Galena is present in a localized area of argillic-phyllic alteration near the northwest corner of Section 20 (sample A-78). Although not observed, the presence of galena and (or) sphalerite is also suggested by anomalous concentrations of Pb and (or) Zn in several other samples from the area (Appendix B, samples I-92, V-108, B-144, and 149)

Other sulfides reported from the Quartzville district include marcasite, chalcopyrite, stibnite, and bornite (Munts, 1978). Chalcopyrite has been reported from the tourmaline-breccia zone at Yellowstone Creek (Gray, 1977; Munts, 1978), but was not observed by myself at that location or elsewhere in the Yellowbottom-Boulder Creek area. Copper analyses for most samples from the area are largely within the range of background values, including most samples from breccia pipes and shatter zones. Exceptions are represented by two samples collected from the breccia zone in the northern part of Section 36 (B-86, 160 ppm; B-144, 495 ppm).

Copper sulfides, if originally present, may have been removed by supergene leaching of the rocks during weathering.

Sulfur-Isotope and Fluid-Inclusion Data

Concentrates of galena and sphalerite were prepared from the sulfide-quartz veins in the shatter zone of Section 31 (sample 148). These samples were crushed, mixed with CuO, and then heated to 1025° C under vacuum to convert the sulfide-sulfur to SO_2 gas. The gas samples were then sent to Global Geochemical Corporation for measurement by mass spectrometer. Relative abundances of sulfur isotopes were determined from $^{34}S/^{32}S$ ratios. The results are expressed as deviations from a standard, and reported as del ^{34}S values in per mil ($^{0}/_{00}$). The standard for sulfur is meteoritic troilite, which by definition has the value 0 $^{0}/_{00}$.

Stable isotopes of an element may be fractionated between two or more coexisting phases as a result of mass-dependent differences in chemical and physical behavior (Field and Fifarek, 1986, and references cited therein). This partitioning is independent of pressure, and varies inversely with temperature. These relationships, together with appropriate experimental studies, form the basis for the application of sulfur isotopes to geothermometry. In addition, several criteria must be met by the materials used for the analysis. The minerals must have formed simultaneously and at isotopic equilibrium, and this equilibrium must be subsequently preserved (Field and Fifarek, 1986).

Stable-isotope abundances may also be used to determine or speculate on the source of an element. Del values for ^{34}S near 0 $^{0}/_{00}$, and thus similar to that of meteoritic sulfur, are commonly interpreted to represent a magmatic source of sulfur (Ohmoto and Rye, 1979; Field and Fifarek, 1986).

The del ^{34}S values obtained from analyses of veinlet sulfides in sample 148 are + 0.3^{5} $^{0}/_{00}$ for sphalerite and - 3.5^{9} $^{0}/_{00}$ for galena, as listed in Table 25. The grouping of these values near 0 $^{0}/_{00}$ suggests a magmatic

Table 25- Sulfur isotope data

Sample #	sample description	mineral	del ^{34}S $^{0}/_{00}$
148	qtz-carb.-sulfide vein	sphalerite	+ 0.3^{5}
148	qtz-carb.-sulfide vein	galena	- 3.5^{9}
T-53	tourmaline breccia	pyrite	+ 1.0^{3}
151	tonalite intrusion	pyrite	- 1.1^{9}

source for the sulfur in this part of the Quartzville hydrothermal system. These data were also used to calculate a temperature of deposition for the sulfides by use of the technique given in Field and Fifarek (1986), and the fractionation equations for sphalerite-H_2S and galena-H_2S presented by Ohmoto and Rye (1979). The temperature calculated by this method is 157° C, which compares reasonably well with other temperatures (155-260° C) obtained by fluid-inclusion homogenization studies of quartz and calcite from this vein , as performed by KRTA Limited of Newmarket, New Zealand, and presented in the section that follows.

Samples of disseminated pyrite from the tourmaline-breccia zone in Section 35 (sample T-53) and the tonalite intrusion along Boulder Creek (sample 151) were also analyzed. Values obtained are + 1.0^{3} $^{0}/_{00}$ for the

former and -1.1 $^{9}/_{00}$ for the latter. These values are also suggestive of a magmatic source for the sulfur.

Fluid inclusions are considered to represent samples of hydrothermal fluids that have been trapped by crystallization of the host phase (Roedder, 1979). Type-1 inclusions contain a vapor bubble which forms by the exsolution of gas (generally H_2O or CO_2) from the fluid upon cooling, and range in salinity from 0 to 18 weight-percent NaCl equivalent (Nash, 1976). The temperature at which the vapor bubble disappears (the gas returns to solution) with heating, the homogenization temperature, is interpreted to represent the minimum temperature of entrapment of the hydrothermal fluid (Roedder, 1979). The temperature at which the fluid freezes may be used to estimate the salinity of the fluid as a consequence of the relationship between salinity and freezing-point depression for alkali chlorides (Roedder, 1963).

Six fluid inclusions in quartz and one in calcite in veinlets in sample 148 were examined by KRTA Limited of Newmarket, New Zealand. Temperatures of homogenization for inclusions in quartz ranged from 155 to 260° C, with a mean of 195° C. One negative crystal inclusion in calcite gave a value of 190° C. Hydrothermally altered wall rocks of the veins contain epidote, a mineral that normally forms at temperatures of at least 240° C (Deer, Howie, and Zussman, 1966). Although it is normally difficult or impossible to determine the relative ages of closely associated hydrothermal replacement and vein mineralization on the basis of visual criteria, the temperature data suggest that epidote of the wall rocks formed at an earlier and higher-temperature prograde stage of the system than did the quartz-carbonate-sulfide assemblages of cross-cutting

veinlets. Because the fluid inclusions were judged to be too small, freezing tests were not performed on this sample and therefore the salinity of the fluids was not determined.

Two secondary fluid inclusions in phenocrysts of quartz from a porphyritic dacite dike (sample I-92) were examined by myself using the Chairmeca fluid-inclusion apparatus at Oregon State University. This dike may possibly have been the source for the hydrothermal fluids that caused the veinlet mineralization previously discussed. These inclusions yielded homogenization temperatures of 191 and 202° C. Salinity was determined for one of these inclusions to be 3.7 percent NaCl equivalent.

MINERAL-RESOURCE POTENTIAL

Mining districts of the Western Cascades have been largely ignored as exploration targets for many years. Extensive forest cover, rugged terrain, and an unfavorable political climate in Oregon have combined to limit the economic attractiveness of the subprovince. Nevertheless, deposits of base and precious metals are present. A porphyry-copper deposit has recently been identified by diamond drilling in the North Santiam district in Marion County, confirming an earlier hypothesis that the vein-type mineralization of the Western Cascades represents the "tops" of porphyry-copper deposits (Power, 1984).

Immediately east of the study area, the Quartzville District has recently been the target of a soil survey designed to explore for potential mineral deposits (Orvana Resources Corporation). This project produced a geochemical map of the center of the District, and revealed the presence of disseminated base- and precious-metal values. Base metals are contained within a widespread low-grade polymetallic geochemical assemblage of trace elements. In contrast, gold is confined to northwest-trending structures that overprint the earlier polymetallic assemblage (Ian Thomson, Orvana Resources Corporation, Jan. 1988, personal communication).

The Yellowbottom-Boulder Creek area displays several geological and geochemical features that suggest the presence of porphyry-type mineralization at depth. Most are clustered in Sections 31, 35, and 36, as shown in Figure 36. The distribution of mineralization within the study area appears to correlate with features previously found in the Quartzville

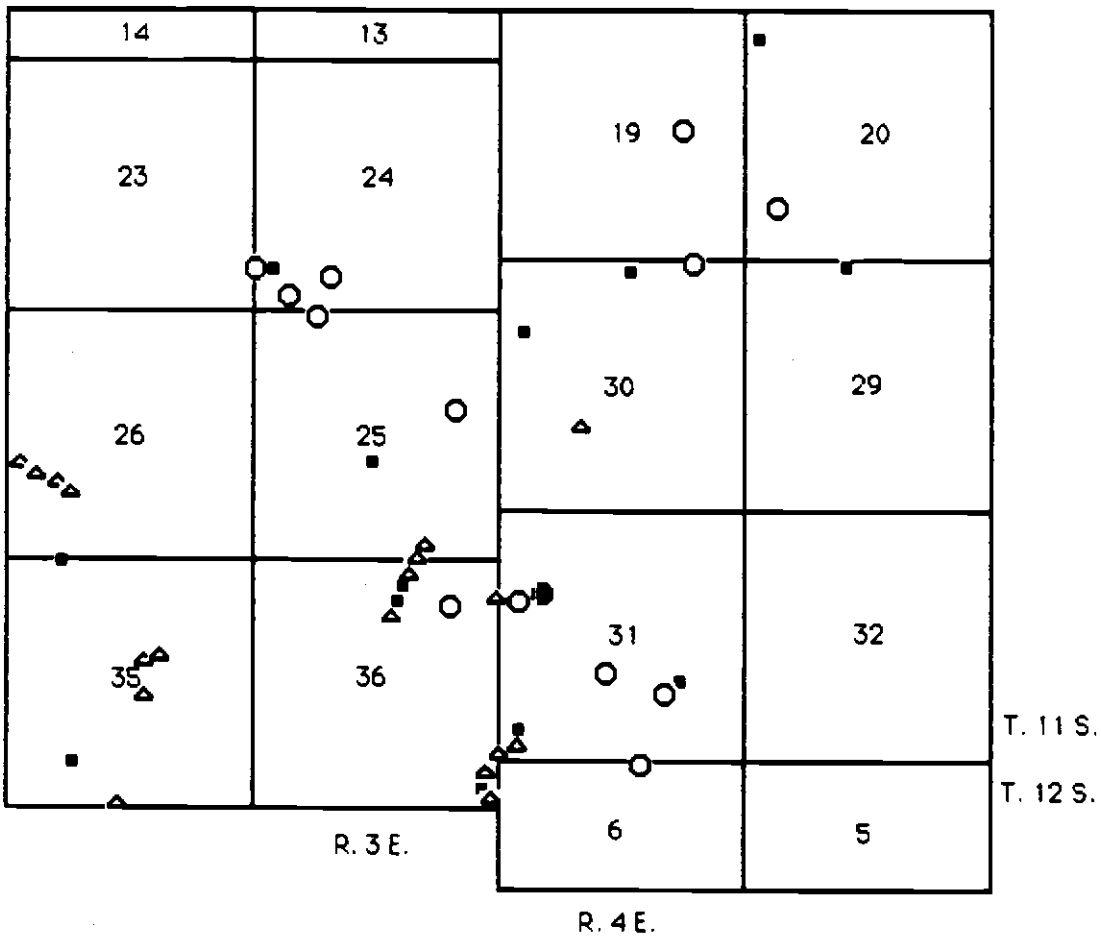

Figure 36- Summary of favorable exploration features in the Yellowbottom-Boulder Creek area.

District (Munts, 1978 and 1981) and elsewhere in the Western Cascades (Power 1984; Field et al, 1987).

Mineralization in the subprovince is present as three occurrences: porphyry copper, base-metal vein, and precious-metal vein deposits. The three may be related, as the vein deposits are thought to constitute the peripheral zones of central and deep porphyry mineralization (Power, 1984; Field et al., 1987). Features suggestive of porphyry mineralization in the Yellowbottom-Boulder Creek area include breccia pipes, propylitic and argillic-phyllic alteration, and quartz-bearing porphyritic intrusions. Gold deposition appears to be largely controlled by structure in both the Quartzville District (Munts, 1978 and 1981) and the study area, and is therefore present mostly in thin, discontinuous, precious metal-bearing veins and zones of silicification. However, porphyry-copper deposits of island-arc terranes are commonly richer in gold than their cratonic counterparts (Titley and Beane, 1981), and a recently-discovered porphyry-copper deposit in the North Santiam District contains significant gold resources (C.W. Field, June 1986, personal communication).

Accordingly, the future economic potential of the area is largely dependent on the discovery of porphyry-type mineralization, perhaps associated with by-product concentrations of gold and silver. It is recommended that a soil survey of the Boulder Creek area be undertaken to determine the distribution and extent of anomalous metal values. Problems likely to be encountered with such a survey include glacial drift, which covers portions of the Boulder Creek area, steep slopes, and recent clear-cutting which has disturbed the soil profile.

GEOLOGIC SUMMARY

The Yellowbottom-Boulder Creek area is located immediately west of the Quartzville Mining District in the Western Cascades of Oregon. This terrane is underlain by a sequence of volcanic and volcaniclastic rocks erupted from Middle Miocene to Quaternary time. Volcanic rocks are correlated with the Miocene Sardine Formation, and consist of basalt, andesite, basaltic andesite, dacite, and rhyodacite flows, pyroclastic deposits, and extensive laharic breccias. This volcanic sequence has been intruded by dikes, plugs, and small stocks of gabbroic to granitic composition that were emplaced mostly during Miocene and some possibly later in Quaternary time. Pliocene flows of olivine basalt and porphyritic andesite of early High Cascade affinity are present on the crests of Galena Ridge and Packers Divide.

Thick flows of basalt and andesite of the lower andesite unit represent the earliest volcanic activity exposed in the area. These rocks are overlain by lapilli tuffs and thin interbedded andesite and basalt flows of the lower pyroclastic unit, representative of an explosive period of volcanism. Andesite and basaltic andesite flows of the intermediate andesite unit conformably overlie this pyroclastic unit. The top part of the intermediate andesite unit is composed of a sequence of water-laid tuffs that display laminated beds and rip-up clasts. These tuffs indicate that a period of volcanic quiescence followed extrusion of the andesites and subsequent erosion led to the accumulation of volcanic detritus in a local basin of unknown extent. Unconformably overlying these epiclastic tuffs is the intermediate basalt unit, which consists of flows of basalt and dacite interbedded with volcaniclastic breccias. Renewed explosive

volcanic activity is represented by the upper pyroclastic tuff unit, composed of a sequence of ash-fall and ash-flow tuffs, that grades upward into laharic breccias of the upper pyroclastic unit. These lahars are extensive in areal distribution and apparently are not confined to channels, but rather are present as a mantle that covers the paleosurface. The collapse of volcanic crater walls and (or) failure of rain-soaked slopes on the flanks of stratovolcanoes led to formation of these lahars. Erosion of the lahars and their deposition as epiclastic sediments produced the water-laid tuffs exposed in the top part of the upper pyroclastic unit and documents a second period of quiescence during Miocene time. The emplacement of domes of rhyodacite marked the end of the Miocene volcanic activity in the area.

Volcanic rocks of Miocene age dip between 5 and 25 degrees to the southeast, presumably into the axis of the Sardine Syncline. Lineaments of a N 20-40 W orientation are numerous on aerial photographs of the area. These features end abruptly at the outcrops of flat-lying Pliocene flows that are present on Galena Ridge and Packers' Divide, and probably are Miocene in age. A few of these lineaments have been identified as faults, but field evidence for the documentation of fault movement along most of the lineaments is lacking.

Intrusive rocks include mafic plugs, several dioritic stocks, and dikes of basaltic, andesitic, dacitic, rhyodacitic, and granitic composition. Quartz-bearing porphyritic dikes are present in many parts of the study area, and are possibly associated with hydrothermal mineralization. Most dikes are aligned N 20-40 W, presumably associated with normal faults. The age of most dikes is believed to be similar to or slightly younger than that of the volcanic rocks they intrude. However, some are

localized along fault zones and are relatively unaltered, which suggests a post-volcanic age. The largest intrusion, for which the informal name Yellowbottom Stock is proposed, is composed of quartz monzodiorite and covers approximately 1 km^2. Other small stocks and plugs range from quartz diorite to tonalite in composition.

Pliocene and Quaternary volcanic activity consisted of the eruption of highly fluid flows of diktytaxitic basalt and porphyritic andesite from vents located near the western margin of the High Cascades subprovince. These flows extended westward to the Yellowbottom-Boulder Creek area and are preserved on the crests of high ridges. A flow of trachybasalt and two cinder cones represent the latest volcanic activity in the Quartzville area.

Major-oxide analyses of representative volcanic and plutonic rocks, with the exception of samples of a mafic plug and the trachybasalt flow of Quaternary age, define crudely linear trends when plotted on Harker variation diagrams. These trends suggest that the igneous rocks of the Yellowbottom-Boulder Creek area may belong to a cogenetic sequence of magmatism. The alkali-lime (Peacock) index of volcanic samples is 58.5% silica, whereas that of the plutonic rocks is 56.5% (including the sample of a mafic plug), indicating a calc-alkaline magmatic affinity. The low concentrations of K_2O in most rocks of the area are similar to those of island-arc terranes, which suggests that the parental magmas were relatively primitive. However, normative corundum in several samples is suggestive of the assimilation of lower crustal materials rich in alumina, or the melting and incorporation of subducted sediments into the magmas.

higher percentage of alumina than the host minerals (dominantly plagioclase feldspars).

Hydrothermal alteration has modified all rocks of Miocene age exposed in the Yellowbottom-Boulder Creek area. Mineralogical changes range from the replacement of groundmass minerals by a few percent chlorite to the complete recrystallization of the host rocks to sericite, quartz, and clay minerals of the argillic-phyllic assemblage. Deposition of disseminated pyrite commonly accompanied formation of the alteration minerals. The propylitic assemblage is widespread in areal extent and is considered to be the result of the interaction of hydrothermal fluids of magmatic derivation with the host rocks, whereas the argillic-phyllic assemblage is localized along faults, breccia zones, and shear zones. This correlation of argillic-phyllic alteration with the distributions of shears, breccias, and faults is observed on Plate 2, and suggests that meteoric waters penetrating these structures may have led to the hydrolysis of host rocks subsequent to propylization. Shear zones in the Boulder Creek area are also associated with the formation of a series of mineralized shatter zones.

Concentrations of the trace metals in volcanic and plutonic rocks and their mineralized and altered equivalents generally display a depletion of base metals and an enrichment of precious metals with respect to those of average granodiorite, to Caribbean intrusions, and to rocks of the Western Cascades in general. The apparent depletion of base metals may be partly the result of the inclusion of oxidized samples in the data set. Concentrations of these trace metals, reported in ppm (threshold; range), are: Ag (0.6; < .3-21), Cu (60; 4-495), Pb (20; <3-930), Zn (90; 3-1137), Mo (< 1; <1-50), and Au (8 ppb; <2-11,420 ppb). Samples containing

highly anomalous concentrations of the metals are found mostly in the Boulder Creek area. Trends obtained from these data plotted on a Pb-Cu-Zn ternary diagram suggest that anomalies for Pb and Zn indicate vein-type mineralization, whereas those for Cu may be possibly associated with higher temperature porphyry-type mineralization.

Sulfur-isotope values obtained from a galena-sphalerite pair in a quartz-sulfide veinlet from the Boulder Creek area cover a small range centered near 0 $^{0}/_{00}$ and suggest a magmatic source of sulfur. The temperature calculated from the isotopic data for this sulfide pair is 157° C. Fluid inclusion studies of quartz in this same veinlet indicate homogenization temperatures ranging from 155 to 206° C. These data collectively suggest that mineral deposition took place in the epithermal temperature range during late-stage gradual cooling of the hydrothermal system.

The presence of quartz-bearing porphyritic intrusions, mineralized breccia pipes and shatter zones, and anomalous concentrations of base metals support the hypothesis that the Boulder Creek area may be underlain by a porphyry-type hydrothermal system at depth. Linear zones of intense silicification are possibly associated with a shallower phase of epithermal mineralization, perhaps in a hot springs-type environment. A silicified zone in the Boulder Creek area exhibits vertical (deeper to shallower) changes in alteration mineralogy (silica-hematite-limonite-jarosite to silica-pyrite), and base and precious metal content (anomalous Pb, Zn, Cu, Mo, Ag, and Au to background concentrations) over a topographic interval of approximately 500 feet. These changes in alteration assemblage and metal content, together with the apparent pipe-like morphology of this zone, suggest that it may have been a feeder

conduit that channeled fluids to a hot spring. Detailed mapping and soil-geochemistry surveys should be undertaken to evaluate further the mineral-resource potential of this area.

REFERENCES

Armentrout, J.M., 1981, Correlation and ages of Cenozoic chronostratigraphic units in Oregon and Washington, in, Armentrout, J.M., ed., Pacific Northwest Cenozoic biostratigraphy: Boulder, Colo., Geol. Soc. of America Special Paper 184, p. 137-148

Baldwin, E., 1964, Geology of Oregon: Eugene, Oregon, Univ. of Oregon Press, 2nd edition

Beeson, M.H., and Moran, M.R., 1979, Stratigraphy and structure of the Columbia River Basalt Group in the Cascade Range, Oregon, in, Hull, D.A., investigator, and Riccio, J.F., ed., 1979, Geothermal resource assessment of Mount Hood: Oregon Dept. of Geol. and Mineral Industries Open-File Report O-79-8, p. 5-77

Berg, A.B., 1961, Preliminary geologic map Quartzville-Galena Mountain mining district, Linn County, Oregon (unpublished): Burlington Northern Railroad

Bottinga, Y.A., and Weill, D.F., 1970, Densities of liquid silicate systems calculated from partial molar volumes of oxide components: Amer. Jour. Sci., v. 269, p. 169-182

Brooks, H.L., and Ramp, L., 1968, Gold and silver in Oregon: Oregon Dept. Geol. and Mineral Industries Bull. 61, 337 p.

Bryant, D.G., 1968, Intrusive breccias associated with ore, Warren (Bisbee) mining district, Arizona: Econ. Geology, v. 63, p. 1-12

Buddington, A.F., and Callaghan, Eugene., 1936, Dioritic intrusive rocks and contact metasomatism in the Cascade region of Oregon: American Jour. Sci., v 31, p. 421-449

Burnham, C.W., 1962, Facies and types of hydrothermal alteration: Econ. Geology, v. 57, p. 768-784

Burnham, C.W., 1967, Hydrothermal fluids at the magmatic stage, in, Barnes, H.L., ed., Geochemistry of hydrothermal ore deposits: New York, Holt, Rinehart, and Winston, p. 34-75

Burnham, C.W., 1979, Magmas and hydrothermal fluids, in, Barnes, H.L., ed., Geochemistry of hydrothermal ore deposits, second edition: New York, John Wiley and Sons, p. 71-136

Callaghan, Eugene, and Buddington, A.F., 1938, Metalliferous mineral deposits of the Cascade Range in Oregon: U.S.G.S. Bull. 893, 114 p.

Cox, K.G., Bell, J.D., and Pankhurst, R.J., 1979, The Interpretation of Igneous Rocks: London, George Allen and Unwin

Creasy, S.C., 1966, Hydrothermal alteration, in, Titley, S.R., and Hicks, C.L., eds., Geology of the porphyry copper deposits: Tucson, the Univ. of Arizona Press, p. 51-74

Cross, W., Iddings, J.P., Pirsson, L.V., and Washington, H.S., 1903, Quantitative classification of igneous rocks, University of Chicago Press

Curless, J.M., Geology and Mineralization in the vicinity of Rocky Top, Marion County, Oregon: M.S. Thesis in progress, Oregon State University

Deer, W.R., Howie, R.A., and Zussman, J., 1966, An introduction to rock-forming minerals: New York, John Wiley and Sons

Ewart, A., 1976, Mineralogy and chemistry of modern orogenic lavas-some statistics and implications: Earth and Planet. Sci. Letters, v. 31, p. 417-432

Ewart, A., 1979, A review of the mineralogy and chemistry of Tertiary-Recent dacitic, latitic, rhyolitic, and related salic volcanic rocks, in, Barker, F., ed., Trondhjemites, Dacites, and Related Rocks, New York, Elsevier Scientific Publishing Company, p. 13-112

Ewart, A., 1982, The mineralogy and petrology of Tertiary-Recent orogenic rocks: with special reference to the andesitic-basaltic compositional range, in, Thorpe, R.S., ed., Andesites, New York, John Wiley and Sons, p. 25-95

Field, C.W., Jones, M.B., and Bruce, W.R., 1974, Porphyry copper-molybdenum deposits of the Pacific Northwest: Am. Inst. Mining Metall. Petroleum Eng. Trans., v. 255, p. 9-22

Field, C.W., Briskey, J.A., Hendrickson, T.A., Jones, M.B., Schmuck, R.A., and Bruce, W.R., 1975, Chemical trends in Mesozoic plutons associated with porphyry-type mineralization of the Pacific Northwest: Am. Inst. Mining Metall. Petroleum Eng., preprint n. 75-L-359, 25 p.

Field, C.W., and Power, S.G., 1985, Metallization in the Western Cascades, Oregon and Southern Washington (abs.): Geol. Soc. America Abstracts with Programs for 1985 (Rocky Mountain Section), v. 17, no. 4, p. 218

Field, C.W., and Fifarek, R.H., 1986, Light stable-isotope systematics in the epithermal environment, in Berger, B.R., and Bethke, P.M., eds., Geology and geochemistry of epithermal systems: Society of Economic Geologists, Reviews in Economic Geology, v. 2, p. 99-128

Field, C.W., Power, S.G., and Curless, J.M., 1987, Magmatism and mineralisation in the Western Cascades of Oregon and Washington, U. S. A., in Proceedings of the Pacific Rim Congress 87 on the geology, structure, mineralisation, and economics of the Pacific Rim: Australasian Institute of Mining and Metallurgy, p. 811-816

Fisher, R.V., Schmincke, H.-U., 1984, Pyroclastic Rocks, Springer-Verlag, New York, 472 pp.

Gill, J.B., 1981, Orogenic andesites and plate tectonics: New York, Springer-Verlag, 390 p.

Gilmour, P., 1977, Mineralized intrusive breccias as guides to concealed porphyry copper systems: Econ. Geology, v. 72, p. 290-303

Gray, J.J., 1977, A geological field trip guide from Sweet Home to the Quartzville mining district: The Ore Bin, v. 39, n. 6, p. 93-108

Gustafson, L.B., 1978, Some major factors of porphyry copper genesis: Econ. Geology, v. 73, p. 600-607

Gustafson, L.B., and Hunt, J.P., 1975, The porphyry copper deposit at El Salvador, Chile: Econ. Geology, v. 70, p. 857-912

Hammond, P.E., 1979, A tectonic model for evolution of the Cascade Range, in Armentrout, J.M., Cole, M.R., and Terbest, H., Jr., eds., Cenozoic paleogeography of the western United States: Pacific Coast Paleogeography Symposium No. 3, Anaheim, Calif., Society of Economic Paleontologists and Mineralogists, Pacific Section, p. 219-237

Hammond, P.E., Anderson, J.L., Manning, K.J., 1980, Guide to the geology of the upper Clackamas and North Santiam Rivers area, northern Cascade Range, in Oles, K.F., Johnson, J.G., Niem, A.R., and Niem, W.A., eds., Geologic field trips in western Oregon and southwestern Washington: Oregon Dept. of Geology and Mineral Industries Bull. 101, p. 133-167

Hammond, P.E., Geyer, K.M., and Anderson, J.L., 1982, Preliminary geologic map and cross sections of the upper Clackamas and North Santiam Rivers area, northern Oregon Cascade Range: Portland, Oregon, Portland State University Dept. of Earth Sciences, scale 1:62,500

Harker, A., 1909, The natural history of igneous rocks, New York: Macmillan

Hemley, J.J., and Jones, W.R., 1964, Chemical aspects of hydrothermal alteration with emphasis on hydrogen metasomatism: Econ. Geology, v. 59, p. 538-569

Irvine, T.N., and Baragar, W.R.A., 1971, A guide to the chemical classification of the common volcanic rocks: Canadian Jour. Earth Sci., v. 8, p. 523-548

Kerr, P.F., 1977, Optical Mineralogy, Fourth Edition, New York, McGraw-Hill Book Company, 492 p.

Kesler, S.E., Jones, L.M., and Walker, R.L., 1975, Intrusive rocks associated with porphyry copper mineralization in island arc areas: Econ. Geology, v. 70, p. 515-526

KRTA Limited, March, 1988, Petrology Report: Newmarket, New Zealand, 7 p.

Lawrence, R.D., 1976, Strike-slip faulting terminates the Basin and Range province in Oregon: Geol. Soc. America Bull. v. 87, p. 846-850

Le Maitre, R. W., 1976a, Some problems of the projection of chemical data into mineralogical classifications: Contr. to Mineralogy and Petrology v. 56, p. 181-189

Le Maitre, R. W., 1976b, The chemical variability of some common igneous rocks: Jour. of Petrology, v. 17, part 4, p. 589-637

Le Maitre, R. W., 1984, A Proposal by the IUGS Subcommission on the Systematics of Igneous Rocks for a chemical classification of volcanic rocks based on the total alkali silica (TAS) diagram: Australian Jour. of Earth Sci., v. 31, p. 243-255

Lepeltier, C., 1969, A simplified treatment of geochemical data by graphical representation: Econ. Geology, v. 64, p. 538-550

Levinson, A.A., 1974, Introduction to exploration geochemistry: Mayhood, Illinois, Applied Publishing, Ltd., 614 p.

Lowell, J.D., and Guilbert, J.M., 1970, Lateral and vertical alteration-mineralization zoning in porphyry ore deposits: Econ. Geology v. 65, p. 373-408

Manson, Vincent, 1967, Geochemistry of Basalts: Major Elements, in Basalts: The Poldervaart Treatise on Rocks of Basaltic Composition, v. 1, John Wiley and Sons, p. 215-269

Mason, R.S., Gray, J.J., Vogt, B.F., 1977, Mineralization in the north-central Western Cascades: The Ore Bin, v. 39, p. 185-205

McBirney, A.R., 1968, Petrochemistry of the Cascade andesitic volcanoes: Oregon Dept. Geology and Mineral Industries Bull. 62, p. 101-107

McBirney, A.R., 1969, Andesitic and Rhyolitic Volcanism of Orogenic Belts, in P. B. Hart (Ed.), The Earth's Crust and Upper Mantle, Geophysical Monograph 13, Amer. Geophys. Union, 735 p.

McBirney, A.R., 1978, Volcanic evolution of the Cascade Range, in Ann. Rev. Earth Planet. Sci., v. 6, p. 437-456

McBirney, A.R., Sutter, J.F., Nashlund, H.R., Sutton, K.G., White, C.M., 1974, Episodic volcanism in the Cascades of Oregon: Geology, v. 3, p. 585-590

Meyer, Charles, Shea, E.P., Goddard, C.C. Jr., and staff of the Anaconda Company, 1968, Ore deposits at Butte, Montana, in, Ridge, J.D., ed., Ore deposits of the United States, 1933-1967: A. I. M. E. Graton-Sales volume, v. II, p. 1373-1416

Meyer, Charles, and Hemley, J.J., 1967, Wall rock alteration, in, Barnes, H.L., ed., Geochemistry of hydrothermal ore deposits: New York, Holt, Rinehart, and Winston, p. 166-235

Moore, J.G., and Peck, D.L., 1962, Accretionary lapilli in volcanic rocks of the western continental United States: Journal of Geology, v. 70, p. 182-194

Moore, W.J., 1978, Chemical characteristics of hydrothermal alteration at Bingham, Utah: Econ. Geology, v. 73, p. 1228-1241

Munts, S.R., 1978, Geology and mineral deposits of the Quartzville mining district, Linn County, Oregon: unpubl. M.S. thesis, University of Oregon, 213 p.

Munts, S.R., 1981, Geology and mineral deposits of the Quartzville mining district, Linn County, Oregon: Oregon Geology, v. 43, p. 18

Nash, J.T., 1976, Fluid-inclusion petrology - data from porphyry copper deposits and applications to exploration: U.S.G.S. Professional Paper 907-D, 16 p.

Nesse, W.D.,1986, Introduction to Optical Mineralogy, Oxford University Press, 325 p.

Nockolds, S.R., and Allen, R., 1953, The geochemistry of some igneous rock series: Geochim. et Cosmochim. Acta., v. 4, p. 105-192

Nockolds, S.R., 1954, Average chemical compositions of some igneous rocks: Bull. of the Geol. Soc. America, v. 65, p. 1007-1032

Norton, D.L., and Cathles, L.M., 1973, Breccia pipes, products of exsolved vapor from magmas: Econ. Geology, v. 67, p. 540-546

Ohmoto, H., and Rye, R.O., 1979, Isotopes of sulfur and carbon; in Barnes, H.L., ed., Geochemistry of Hydrothermal Ore Deposits, Second Edition, John Wiley and Sons, New York, p. 509-567

Olson, J.P., 1978, Geology and mineralization of the North Santiam mining district, Marion County, Oregon: unpubl. M.S. thesis, Oregon State University, 135 p.

Peck, D.L., Griggs, A.B., Schlickler, H.G., Wells, F.G., Dole, H.M., 1964, Geology of the Central and Northern parts of the Western Cascade Range in Oregon: U.S.G.S. Prof. Paper 449, 56 p.

Perry, V.D., 1961, The significance of mineralized breccia pipes: Amer. Inst. Mining Metall. Petroleum Eng. Trans., v. 220, p. 216-226

Power, S.G., 1984, The tops of porphyry copper deposits- mineralization and plutonism in the Western Cascades, Oregon: Unpubl. Ph.D thesis, Oregon State University, 234 p.

Power, S.G., Field, C.W., Armstrong, R.L., Harakal, J.E., 1981, K-Ar ages of plutonism and mineralization, Western Cascades, Oregon and southern Washington: Isochron/West, no. 31, p 27-29

Priest, G.R., Woller, N.M., Black, G.L.,1983, Overview of the geology of the central Oregon Cascade Range, in Oregon Dept. of Geology and Mineral Industries Special Paper 15, p. 3-28

Reynolds, D.L., 1958, Fluidization as a geologic process and its bearing on the problem of intrusive granites: Am. Jour. Sci., v. 252, p. 577-614

Roedder, Edwin, 1963, Studies of fluid inclusions - II, Freezing data and their interpretation: Econ. Geology, v. 58, p. 167-211

Roedder, Edwin, 1979, Fluid inclusions as samples of ore fluids, in, Barnes, H.L., ed., Geochemistry of hydrothermal ore deposits, second edition: New York, Wiley and Sons, p. 684-737

Rose, A.W., 1970, Zonal relations of wall rock alteration and sulfide distribution of porphyry copper deposits: Econ. Geology, v. 65, p. 920-936

Rose, A.W., and Burt, D.M., 1979, Hydrothermal alteration, in Barnes, H.L., ed., Geochemistry of hydrothermal ore deposits, second edition: New York, John Wiley and Sons, p. 173-235

Schaubs, M.P., 1978, Geology and mineral deposits of the Bohemia mining district, Lane County, Oregon: unpubl. M.S. thesis, Oregon State University, 135 p.

Schriener, A., Jr., 1978, Geology and mineralization of the north part of the Washougal mining district, Skamania County, Washington: unpubl. M.S. thesis, Oregon State University, 135 p.

Sillitoe, R.H., and Sawkins, F.J., 1971, Geologic, mineralogic, and fluid inclusion studies relating to the origin of copper-bearing tourmaline breccia pipes, Chile: Econ. Geology, v. 66, p. 1028-1041

Stowell, G.E., 1921, Report on the geology and ore deposits of the Quartzville district, Oregon: Oregon Bur. Mines and Geology (unpubl. report in the files of Oregon Dept. of Geology and Mineral Industries)

Streckeisen, A. L., 1973, Plutonic Rocks- Classification and nomenclature recommended by the IUGS Subcommission on the Systematics of Igneous Rocks: Geotimes, v. 18, n. 10, p. 26-30

Streckeisen, A. L., 1979, Classification and nomenclature of volcanic rocks, lamprophyres, carbonatites, and melitic rocks: Recommendations and suggestions by the IUGS Subcommission on the Systematics of Igneous Rocks: Geology, v. 7, p. 331-335

Sutter, J.F., 1978, K/Ar ages of Cenozoic volcanic rocks from the Oregon Cascades west of 121° 30': Isochron/West, no. 21, p. 15-21

Taylor, E.M., 1968, Roadside Geology, Santiam and McKenzie Pass highways, Oregon: in Andesite conference guide book, Oregon Dept. of Geology and Mineral Industries Bull. 62

Taylor, E.M., 1980, Volcanic and volcaniclastic rocks on the east flank of the central Oregon Cascade Range to the Deschutes River, Oregon, in Oles, K.F., Johnson, J.G., Niem, A.R., and Niem, W.A., eds., Geologic field trips in western Oregon and southwestern Washington: Oregon Dept. Geology and Mineral Industries Bull. 101, p. 1-7

Taylor, E.M., 1981, Central High Cascade roadside geology, Bend, Sisters, McKenzie Pass, and Santiam Pass, Oregon, in Johnston, D.A., and Donnelly-Nolan, J., eds., Guides to some volcanic terranes in Washington, Oregon, and northern California: U.S. Geol. Survey Circ. 838, p. 55-58

Taylor, H.P., 1971, Oxygen isotope evidence for large-scale interaction between meteoric and ground waters and Tertiary granodiorite intrusions, Western Cascade Range, Oregon: Jour. Geophys. Research, v. 75, p. 7855-7874

Thayer, T.P., 1936, Structure of the North Santiam River section of the Cascade Mountains of Oregon: Jour. of Geology, v. 44, p. 701-716

Thayer, T.P., 1939, Geology of the Salem Hills and the North Santiam River Basin, Oregon: Oregon Dept. of Geology and Mineral Industries Bulletin no.15, 40 p.

Titley, S.R., 1981, Porphyry copper: American Scientist, v. 69, p. 632-638

Titley, S.R., and Beane, R.E., 1981, Porphyry copper deposits, in, Skinner, B.J., ed., Economic Geology 75th Anniversary Volume, p. 214-269

Turekian, K.K., and Wedepohl, K.H., 1961, Distribution of the elements in some major units of the Earth's crust: Geol. Soc. America Bull., v. 72, p. 175-192

Verplanck, E.P., 1985, Temporal variations in volume and geochemistry of volcanism in the Western Cascades, Oregon: M. S. Thesis, Oregon State University, Corvallis, 115 p.

Wells, F.G., 1956, Geology of the Medford quadrangle, Oregon-California: U.S. Geol. Survey Quadrangle Map GQ-89, scale 1:96,000

Wells, F.G., and Peck, D.L., 1961, Geologic map of Oregon west of the 121st meridian: U.S. Geol. Survey Misc. Inv. Map I-325, scale 1:500,000

White, C.M., 1980a, Geology of the Breitenbush Hot Springs quadrangle, Oregon: Oregon Dept. of Geology and Mineral Industries Special Paper 9, 26 p.

White, C.M., 1980a, Geology of the Breitenbush Hot Springs quadrangle, Oregon: Oregon Dept. of Geology and Mineral Industries Special Paper 9, 26 p.

White, C.M., 1980b, Geology and geochemistry of Mt. Hood volcano: Oregon Dept. of Geology and Mineral Industries Special Paper 8, 26 p.

White, C.M., 1980c, Geology and Geochemistry of volcanic rocks in the Detroit area, Western Cascade Range, Oregon: Eugene, Oregon, University of Oregon doctoral dissertation, 178 p.

Wilkinson, J.F.G., 1986, Classification and average chemical compositions of common basalts and andesites: Journal of Petrology, v. 27, p. 31-62

Williams, H., 1969, The ancient volcanoes of Oregon: Eugene, Oregon, Univ. of Oregon Press

Wolfe, J.A., 1980, Fluidization versus phreatomagmatic explosions in breccia pipes: Econ. Geology, v. 75, p. 1105-1111

APPENDICES

Appendix A- Major oxide analyses, metal concentrations, normative mineralogy, and specific gravity of selected samples of volcanic and intrusive rocks.

	TLA-52	TLA-38	TIB-1	TIB-121	TIA-11
Major oxides (%)					
SiO_2	55.03	59.40	50.96	64.78	54.04
TiO_2	1.00	1.12	1.05	0.85	1.04
Al_2O_3	16.74	15.58	17.46	15.51	18.09
Fe_2O_3	3.00	2.09	2.77	2.36	3.03
FeO	3.43	4.12	4.67	1.90	3.96
MnO	0.11	0.12	0.13	0.16	0.13
MgO	3.22	2.13	4.72	1.40	3.40
CaO	6.91	5.12	9.59	1.58	7.58
BaO	0.03	0.06	0.06	0.09	0.03
Na_2O	3.33	3.64	2.99	4.06	3.98
K_2O	0.15	1.75	1.48	3.32	0.75
P_2O_5	0.35	0.39	0.41	0.35	0.39
LOI	4.40	2.64	1.68	2.54	3.16
TOTAL	97.70	98.16	97.97	98.90	99.58
Metals (ppm)					
Cu	7	25	40	12	145
Mo	1	1	< 1	6	< 1
Pb	7	8	5	19	18
Zn	35	50	20	50	175
Ag	0.4	< 0.3	< 0.3	0.4	0.5
normative mineralogy (%)					
quartz	16.89	17.82	2.64	24.69	7.84
corundum	--	--	--	3.33	--
orthoclase	0.95	10.84	9.09	20.38	4.60
albite	30.21	32.18	26.29	35.68	34.94
anorthite	32.47	22.05	31.02	5.77	30.38
diopside	1.46	1.55	12.59	--	4.82
hypersthene	10.44	9.21	11.14	4.07	9.88
magnetite	4.66	3.17	4.17	3.55	4.56
ilmenite	2.04	2.23	2.07	1.68	2.05
apatite	0.89	0.97	1.01	0.86	0.96
S. G.	2.71	2.59	2.81	2.58	2.62

Appendix A- continued

	Q-27	Q-66	I-14	I-18	I-29
Major oxides (%)					
SiO_2	48.10	61.59	61.45	74.68	51.37
TiO_2	1.47	0.73	0.80	0.11	0.86
Al_2O_3	13.81	15.77	15.11	11.57	15.68
Fe_2O_3	5.35	3.16	2.48	1.22	2.82
FeO	2.02	2.03	2.45	0.22	3.47
MnO	0.11	0.11	0.08	0.03	0.13
MgO	9.40	2.55	2.65	0.14	4.07
CaO	9.93	5.02	4.46	1.32	4.93
BaO	0.36	0.07	0.08	0.10	0.09
Na_2O	2.79	3.76	3.88	0.40	4.62
K_2O	2.79	2.13	2.46	7.13	2.63
P_2O_5	1.12	0.29	0.29	0.13	0.30
LOI	0.93	1.71	1.57	1.21	4.89
TOTAL	98.18	98.92	97.76	98.26	95.86
Metals (ppm)					
Cu	20	35	12	9	30
Mo	< 1	< 1	1	< 1	< 1
Pb	6	8	4	5	13
Zn	30	50	30	9	35
Ag	< 0.3	< 0.3	< 0.3	< 0.3	< 0.3
normative mineralogy (%)					
quartz	--	18.99	17.67	43.72	--
corundum	--	--	--	1.14	--
orthoclase	17.02	12.96	15.13	43.47	17.10
albite	21.59	32.75	34.16	3.49	43.02
anorthite	17.46	20.44	17.22	5.88	15.71
diopside	20.11	2.53	3.04	--	7.22
hypersthene	--	5.48	6.76	0.36	7.42
magnetite	2.69	4.72	3.74	0.50	4.50
ilmenite	2.88	1.43	1.58	0.22	1.80
apatite	2.74	0.71	0.71	0.32	0.78
nepheline	1.50	--	--	--	--
olivine	10.40	--	--	--	2.46
hematite	3.66	--	--	0.91	--
S.G.	2.38	2.64	2.65	2.45	2.55

Appendix A- continued

	I-33	I-42	I-59	I-111
Major oxides (%)				
SiO_2	59.56	55.98	50.24	73.45
TiO_2	1.40	0.91	1.18	0.23
Al_2O_3	15.42	15.59	19.20	12.89
Fe_2O_3	2.88	2.47	4.23	2.51
FeO	4.38	4.03	5.54	0.19
MnO	0.13	0.12	0.20	0.01
MgO	1.99	3.92	3.42	0.16
CaO	2.63	7.56	10.10	0.40
BaO	0.08	0.05	0.02	0.12
Na_2O	5.11	2.88	2.68	3.25
K_2O	1.21	3.30	0.44	3.74
P_2O_5	0.50	0.40	0.31	0.16
LOI	2.63	1.93	1.21	2.32
TOTAL	97.92	99.14	98.77	99.43
Metals (ppm)				
Cu	20	35	80	50
Mo	< 1	< 1	< 1	1
Pb	8	7	16	15
Zn	110	25	55	75
Ag	0.3	0.3	< 0.3	< 0.3
normative mineralogy (%)				
quartz	17.20	7.27	6.89	40.81
corundum	2.22	--	--	3.25
orthoclase	7.51	20.07	2.67	22.79
albite	45.41	25.08	23.25	28.35
anorthite	10.28	20.44	40.04	0.97
diopside	--	12.46	7.53	--
hypersthene	8.98	8.24	10.30	0.41
magnetite	4.39	3.69	6.29	--
ilmenite	2.79	1.78	2.30	0.44
apatite	1.24	0.98	0.75	0.39
hematite	--	--	--	2.59
S. G.	2.41	2.67	2.79	2.29

Appendix A- continued

	A-35	TLA-39	T-53
Major oxides (%)			
SiO_2	65.12	56.64	48.06
TiO_2	0.83	0.84	0.98
Al_2O_3	15.98	17.25	16.63
Fe_2O_3	3.81	3.72	11.12
FeO	0.59	2.30	1.47
MnO	0.04	0.10	0.02
MgO	2.26	3.46	2.19
CaO	0.23	6.52	3.02
BaO	0.15	0.03	0.01
Na_2O	0.27	3.22	4.39
K_2O	4.04	0.60	1.95
P_2O_5	0.21	0.33	0.34
LOI	4.90	2.90	8.81
TOTAL	98.43	97.91	98.99
Metals (ppm)			
Cu	10	10	18
Mo	< 1	1	< 1
Pb	3	12	9
Zn	35	35	15
Ag	< 0.3	< 0.3	0.3
normative mineralogy (%)			
quartz	47.99	18.33	6.97
corundum	12.04	0.25	2.91
orthoclase	25.57	3.73	12.78
albite	2.45	28.69	41.20
anorthite	--	31.79	14.15
diopside	--	--	--
hypersthene	6.03	9.07	6.05
magnetite	--	5.58	2.18
ilmenite	1.43	1.68	2.06
apatite	0.53	0.82	0.89
hematite	4.08	0.06	10.83
rutile	0.14	--	--
S. G.	2.42	2.69	2.68

Appendix B- Summary of metal concentrations for samples of volcanic and intrusive rocks, their altered equivalents, and breccia zones. Values in parentheses are from Silver Valley Laboratories; other values from Chemical and Mineralogical Services.

Metals (ppm; gold in ppb)	A-48	A-49	A-54	A-62	A-71
silver	.3	< .3 (.2)	< .3	< .3	< .3
copper	14	6 (23)	10	25	60
lead	5	< 3 (22)	3	4	< 3
zinc	15	6 (107)	7	8	12
molybdenum	2	1 (4)	1	< 1	< 1
arsenic		(0)		(40)	
antimony		(3)		(12)	
nickel		(22)		(16)	
bismuth		(12)		(0)	
cobalt		(4)		(43)	
barium		(55)		(186)	
potassium		(606)		(5760)	
gold		(16)		(12)	

Metals (ppm; gold in ppb)	B-86	B-23	B-85	I-57	T-56
silver	< .3 (.3)	< .3	.6 (.3)	.3	< .3
copper	160 (257)	8	45 (34)	6	4
lead	5 (43)	3	4 (9)	5	4
zinc	10 (67)	90	30 (94)	55	3
molybdenum	< 1 (8)	< 1	< 1 (4)	< 1	< 1
arsenic	(976)		(17)		
antimony	(56)		(11)		
nickel	(15)		(34)		
bismuth	(53)		(0)		
cobalt	(10)		(26)		
barium	(9)		(455)		
potassium	(284)		(17324)		
gold	(279)		(32)		

Appendix B- continued

Metals (ppm; gold in ppb)	TLP-15	I-80	I-92	TIB-24	A-78
silver	.3	<.3	<.3	<.3	.9
copper	8	20	11	30	35
lead	8	16	215	8	930
zinc	18	25	350	50	35
molybdenum	<1	<1	<1	<1	1
arsenic					
antimony					
nickel					
bismuth					
cobalt					
barium					
potassium					
gold					<2

Metals (ppm; gold in ppb)	J-143	R-104	R-123	TLA-55	V-108
silver	<.3	.6 (.1)	.5	<.3	5.5
copper	15	6 (12)	35	5	40
lead	10	15 (1)	10	18	680
zinc	45	30 (78)	60	30	80
molybdenum	3	3 (3)	3	2	50
arsenic		(0)			
antimony		(1)			
nickel		(9)			
bismuth		(0)			
cobalt		(2)			
barium		(541)			
potassium		(26104)			
gold	<2	(50)			580

Appendix B- continued

Metals (ppm; gold in ppb)	A-100	A-119	B-112	B-144	I-126
silver	.3 (.2)	.5	< .3	5	.5
copper	15 (28)	25	4	495	55
lead	8 (8)	35	4	50	20
zinc	25 (122)	40	20	520	80
molybdenum	2 (6)	< 1	< 1	15	10
arsenic	(0)				
antimony	(6)				
nickel	(17)				
bismuth	(0)				
cobalt	(2)				
barium	(677)				
potassium	(29080)				
gold	(31)			250	

Metals (ppm; gold in ppb)	146	B-112a	T-53	I-105	A-118
silver	.4	< .3	.3 (.3)	(.3)	(.2)
copper	35	15	18 (20)	(13)	(346)
lead	370	7	9 (31)	(4)	(0)
zinc	70	6	15 (119)	(140)	(50)
molybdenum	< 1	< 1	< 1 (3)	(4)	(4)
arsenic			(8)	(0)	(0)
antimony			(12)	(5)	(8)
nickel			(16)	(13)	(7)
bismuth			(0)	(0)	(0)
cobalt			(43)	(7)	(7)
barium			(186)	(507)	(581)
potassium			(5760)	(18040)	(21176)
gold	2		(12)	(40)	(45)

Appendix B- continued

Metals (ppm; gold in ppb)	A-138	149	10005	10006	10007
silver	(.1)	(3.4)	(1.4)	(21)	(.4)
copper	(15)	(148)	(11)	(9)	(8)
lead	(21)	(917)	(20)	(19)	(0)
zinc	(67)	(263)	(192)	(74)	(59)
molybdenum	(6)	(4)	(6)	(8)	(13)
arsenic	(7)	(57)	(31)	(0)	(42)
antimony	(11)	(8)	(8)	(14)	(8)
nickel	(12)	(18)	(4)	(72)	(36)
bismuth	(0)	(0)	(0)	(0)	(0)
cobalt	(6)	(7)	(10)	(11)	(10)
barium	(223)	(319)	(649)	(555)	(889)
potassium	(343)	(13838)	(41153)	(34381)	(30738)
gold	(60)	(66)	(67)	(11420)	(15)

Metals (ppm; gold in ppb)	10008	10009	10010	10011	10012
silver	(1.3)	(.7)	(.3)	(.2)	(.2)
copper	(11)	(22)	(10)	(13)	(13)
lead	(5)	(9)	(0)	(14)	(11)
zinc	(113)	(93)	(85)	(90)	(129)
molybdenum	(9)	(7)	(7)	(2)	(8)
arsenic	(34)	(0)	(19)	(0)	(15)
antimony	(9)	(15)	(11)	(3)	(10)
nickel	(37)	(38)	(36)	(26)	(32)
bismuth	(0)	(0)	(0)	(0)	(0)
cobalt	(10)	(11)	(12)	(11)	(13)
barium	(675)	(508)	(437)	(853)	(516)
potassium	(34505)	(28018)	(19375)	(23617)	(20276)
gold	(257)	(50)	(30)	(73)	(<10)

Appendix B- continued

Metals (ppm; gold in ppb)	10013	10014	10015	10016
silver	(1.2)	(2.7)	(1.1)	(4.6)
copper	(15)	(20)	(19)	(24)
lead	(376)	(22)	(212)	(1137)
zinc	(485)	(112)	(99)	(207)
molybdenum	(9)	(11)	(5)	(32)
arsenic	(21)	(67)	(46)	(122)
antimony	(15)	(23)	(13)	(14)
nickel	(63)	(146)	(46)	(39)
bismuth	(0)	(0)	(0)	(0)
cobalt	(14)	(9)	(7)	(14)
barium	(422)	(163)	(161)	(322)
potassium	(21371)	(19675)	(23324)	(28703)
gold	(20)	(46)	(42)	(67)

Stream Sediment Samples:

Metals (ppm)	SS-1	SS-2	SS-3	SS-4	SS-5
silver	.3	.4	.5	<.3	<.3
copper	50	35	35	40	30
lead	13	50	13	20	5
zinc	80	160	70	100	85
molybdenum	<1	<1	<1	<1	<1